

**MODULATION OF THE HOST UBIQUITIN MACHINERY BY
LEGIONELLA PNEUMOPHILA EFFECTORS**

by

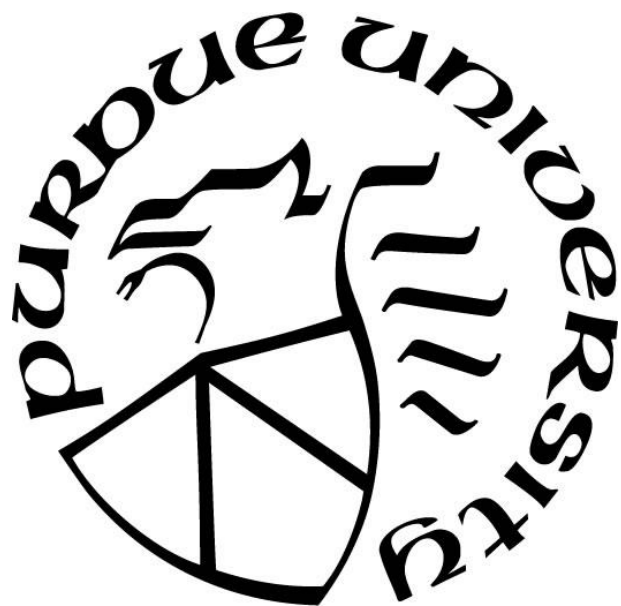
Ninghai Gan

A Dissertation

Submitted to the Faculty of Purdue University

In Partial Fulfillment of the Requirements for the degree of

Doctor of Philosophy



Department of Biological Sciences

West Lafayette, Indiana

August 2019

THE PURDUE UNIVERSITY GRADUATE SCHOOL
STATEMENT OF COMMITTEE APPROVAL

Dr. Zhao-Qing Luo, Chair
Department of Biological Sciences

Dr. Peter Hollenbeck
Department of Biological Sciences

Dr. Daoguo Zhou
Department of Biological Sciences

Dr. Daniel Suter
Department of Biological Sciences

Approved by:

Dr. Janice Evans
Head of the Graduate Program

To my family, friends and everyone I love

ACKNOWLEDGMENTS

I want to thank my supervisor Dr. Zhao-Qing Luo with my whole heart for his mentoring and support throughout my PhD study here at Purdue for 6 years. He is a real scientist who is always passionate and curious about sciences. He is knowledgeable, adventurous, and sets a wonderful role model for everybody in the lab of how to be a qualified scientist. He is extremely strict in science but gentle and kindly in life. He taught me how to think independently, how to design experiments flawlessly and how to perform experiments efficiently. During my time in the lab, I cannot remember how many times I got criticized by him, because of the apparent mistakes I made. I was also asked to come to his office to write scientific documents together with him side by side, because of my terrible writing skills and poor vocabulary. At the time now, when I am writing this thesis, I feel extremely grateful to all of his advices, which I did not understand at the beginning, because of his strictness. The best way to describe his spirits in mentoring students is to quote the old Chinese motto: the strict teacher can lead the outstanding student to the best one. I was studying plants during my undergraduate time, and I did not know much about bacteria and infectious diseases. I encountered numerous difficulties at my early time in the lab, and I even failed my preliminary exam twice. The idea of giving up and quit came to my mind for several times. It was him who always helped me out of my depression and encouraged me to continue my exploration of science. It is not hard to imagine how much efforts he put on me to tutor and shape me from nobody to a not so bad young scientist. He has a high expectation on all of his mentees. No matter where I go and what I do in the future, I will always remember what he lessoned me and keep up with the good work, and not to fail his expectation.

I also want to thank my committee members Dr. Peter Hollenbeck, Dr. Daoguo Zhou and Dr. Daniel Suter for their insightful suggestions and critical comments on my thesis projects, as well as their help in my application process of a post-doc position. I want to thank Dr. Ernesto Nakayasu at Pacific Northwest National Laboratory for his help in mass spectrometry analyses, which is critical for every single project of mine. I thank Dr. Songying Ouyang, Dr. Hongxin Guan and Dr. Xiangkai Zhen at Fujian Normal University for helpful discussion and collaboration on my projects. I would also like to thank Dr. Chittaranjan Das and Mr. Kedar Puvar from the Department of Chemistry for reagents and valuable suggestions.

I would also like to express my most sincere gratitude to my former labmates Dr. Jiazhang Qiu, Dr. Yao Liu and Dr. Wenhan Zhu for their support and help inside and outside the lab. I want to thank Mr Victor Roman, Miss Alix McCloskey for enduring me who is always annoying for so many years in the lab, I enjoy and appreciate the happy time we spent together. Finally, I also want to thank Dr. Canhua Lu, Mr. Jiayi Sun, Dr. Jiaqi Fu and Miss Kayla Perri for help and being excellent labmates.

Finally, I especially want to thank my parents, my grandparents, my sister and my entire family for their encouragement and support, which allow me to pursue my dream, even though they do not understand what I am exactly studying. And my cats Dan, Hank and Hartman for their accompany.

TABLE OF CONTENTS

LIST OF FIGURES	9
NOTE	11
ABSTRACT	12
CHAPTER 1. INTRODUCTION	13
<i>Legionella pneumophila</i>	13
Ubiquitination	18
The Ubiquitin conjugating enzyme 2N (UBE2N)	22
<i>Legionella pneumophila</i> and its exploitation of the host ubiquitin system	23
CHAPTER 2. LEGIONELLA PNEUMOPHILA INHIBITS IMMUNE SIGNALLING VIA MAVC-MEDIATED TRANSGLUTAMINASE-INDUCED UBIQUITINATION OF UBE2N	29
Abstract	29
Introduction.....	29
Results.....	31
Modification of UBE2N by a ubiquitin mutant that cannot be used by the canonical ubiquitination machinery	31
UBE2N is modified by the Dot/Icm effector MavC(Lpg2147) during <i>L. pneumophila</i> infection	33
MavC induces UBE2N ubiquitination by a mechanism that does not require the host ubiquitination machinery	37
MavC is a transglutaminase that catalyzes crosslinking between ubiquitin and UBE2N. ...	41
MavC possesses deamidation activity against ubiquitin.....	46
Transglutamination is the dominant activity of MavC in reactions containing UBE2N and ubiquitin	48
Ubiquitination of UBE2N by MavC abolished its E2 activity	51
MavC dampens the NF-κB pathway in the early phase of <i>L. pneumophila</i> infection.....	51
Discussion.....	58
CHAPTER 3. LEGIONELLA PNEUMOPHILA REGULATES THE ACTIVITY OF THE E2 UBIQUITIN CONJUGATING ENZYME UBE2N BY DEAMIDASE MEDIATED DEUBIQUITINATION	62

Abstract	62
Introduction.....	62
Results.....	64
MvcA interferes with the modification of UBE2N induced by MavC	64
MvcA deubiquitinates the UBE2N-Ub product from MavC transglutaminase activity	71
MvcA does not cleave Gly ₇₆ -Lys isopeptide bonds in canonical ubiquitination.....	73
Lpg2149 inhibits the deubiquitinase activity of MvcA	75
Deubiquitination by MvcA is more efficient than its ubiquitin deamidase activity	77
Crystal structure of MvcA bound to UBE2N-Ub	79
MvcA restores the activity of UBE2N and allows NF-κB activation.....	88
Discussion	92
CHAPTER 4. OVERALL DISCUSSION	95
CHAPTER 5. MATERIALS AND METHODS	99
Media, bacteria strains, plasmid constructions and cell lines	99
Purification of proteins for biochemical experiments.....	99
Transfection, infection, immunoprecipitation	100
<i>In vitro</i> ubiquitination assays.....	101
K63 poly-ubiquitin chain synthesis assay.....	101
Ubiquitin cleavage assay	101
Antibodies and Immunoblotting	102
Liquid chromatography-tandem mass spectrometry analysis.....	102
<i>In vitro</i> deamidation of ubiquitin and native PAGE	104
Immunostaining	104
NF-κB luciferase reporter assay	105
Crystallization, data collection and structural determination	105
Preparation and purification of UBE2N-Ub	106
Data quantitation and statistical analyses	106
REFERENCES	107
APPENDIX.....	121

VITA	128
PUBLICATIONS.....	129

LIST OF FIGURES

Fig. 1-1 Formation of <i>L. pneumophila</i> replicative vacuoles by modulating host cellular processes.	15
<hr/>	
Fig. 1-2 Canonical ubiquitination mechanism and SdeA-catalyzed ubiquitination mechanism. .	28
<hr/>	
Fig. 2-1 The E2 ubiquitin conjugation enzyme UBE2N can be modified by the ubiquitin mutant Ub-AA.....	32
<hr/>	
Fig. 2-2 <i>L. pneumophila</i> induces a molecular weight shift in UBE2N in a process that requires the Dot/Icm effector MavC.....	35
<hr/>	
Fig. 2-3 The growth phase-dependent expression of mavC and its role in intracellular growth of <i>L. pneumophila</i> in macrophages.	36
<hr/>	
Fig. 2-4 MavC induces UBE2N ubiquitination independently of the canonical ubiquitination machinery.....	39
<hr/>	
Fig. 2-5 MavC catalyzes ubiquitination of UBE2N by transglutamination.....	43
<hr/>	
Fig. 2-6 MavC is specific for UBE2N.	44
<hr/>	
Fig. 2-7 The reactivity of ubiquitin mutants in MavC-induced ubiquitination of UBE2N.	45
<hr/>	
Fig. 2-8 MavC displays a ubiquitin-specific deamidation activity.	47
<hr/>	
Fig. 2-9 Characteristics of MavC as transglutaminase and ubiquitin deamidase.	49
<hr/>	
Fig. 2-10 Analysis of ubiquitin deamidation in cells by parallel-reaction monitoring (PRM) mass spectrometry.....	50
<hr/>	
Fig. 2-11 Effects of MavC on UBE2N activity and on NF- κ B activation during <i>L. pneumophila</i> infection.	53
<hr/>	
Fig. 2-12 MavC Inhibits NF κ B activation induced by different signals.....	54
<hr/>	
Fig. 2-13 Effects of MavC on NF- κ B activation in cells overexpressing various relevant proteins.	55
<hr/>	
Fig. 2-14 Ectopic expression of MavC inhibited p65 nuclear translocation.....	56
<hr/>	
Fig. 2-15 MavC inhibits nuclear translocation of p65 during <i>L. pneumophila</i> infection.	57
<hr/>	
Fig. 2-16 A diagram of the NF- κ B activation pathways inhibited by MavC.	61
<hr/>	
Fig. 3-1 Genetic organization of mavC, mvcA and lpg2149 in the genome of <i>L. pneumophila</i> strain Philadelphia 1 and the activity of MvcA against ubiquitin and several E2 enzymes.	67
<hr/>	
Fig. 3-2 MvcA interferes with UBE2N modification induced by MavC.	68
<hr/>	
Fig. 3-3 Comparison of the reactivity of antibodies for MavC and MvcA and their cross-reactivity.	700

Fig. 3-4 MvcA cleaves the isopeptide crosslink between UBE2N and ubiquitin in UBE2N-Ub.	72
Fig. 3-5 The activity of MvcA against peptide bonds formed by several different mechanisms.	74
Fig. 3-6 The expression pattern of Lpg2149 in <i>L. pneumophila</i> and its inhibition of MvcA activity.	76
Fig. 3-7 The deamidase activity of MvcA in biochemical reactions and in cells infected with <i>L. pneumophila</i> .	78
Fig. 3-8 Structural analysis of the mechanism of substrate recognition and catalysis by MvcA.	83
Fig. 3-9 Binding of the substrate UBE2N-Ub induces conformational changes in MvcA.	85
Fig. 3-10 The insertion domain of MvcA is essential for its deubiquitinase activity but not ubiquitin deamidase activity.	86
Fig. 3-11 Interactions between MvcA and the ubiquitin portion of UBE2N-Ub.	87
Fig. 3-12 MvcA counteracts the effects of MavC during <i>L. pneumophila</i> infection.	90

NOTE

Chapters 1, 2 and 3 of the dissertation contain content of the following published unit:

1. Gan N, Nakayasu ES, Hollenbeck PJ, Luo ZQ. *Legionella pneumophila* inhibits immune signalling via MavC-mediated transglutaminase-induced ubiquitination of UBE2N. *Nat Microbiol.* 2019 Jan;4(1):134-143

Chapters 1, 2 and 3 of the dissertation contain content of the following unpublished unit:

1. Gan N, Guan H, Huang Y, Yu T, Nakayasu ES, Puvar K, Das C, Wang D, Ouyang S, Luo ZQ. *Legionella pneumophila* regulates the activity of the E2 ubiquitin conjugating enzyme UBE2N by deamidase-mediated deubiquitination (Under review).

ABSTRACT

Author: Gan, Ninghai. PhD

Institution: Purdue University

Degree Received: August 2019

Title: Modulation of the host ubiquitination machinery by *Legionella pneumophila* effectors.

Major Professor: Zhao-Qing Luo

The bacterial pathogen *Legionella pneumophila* modulates host immunity using effectors translocated by its Dot/Icm transporter to facilitate its intracellular replication. A number of these effectors employ diverse mechanisms to interfere with protein ubiquitination, a post-translational modification essential for immunity. Here, we have found that *L. pneumophila* induces monoubiquitination of the E2 enzyme UBE2N by its Dot/Icm substrate MavC(Lpg2147). Ubiquitination of UBE2N by MavC abolishes its activity in the formation of K63-linked polyubiquitin chains, which dampens NF-κB signaling in the initial phase of bacterial infection. The inhibition of UBE2N activity by MavC creates a conundrum because this E2 enzyme is important in multiple signaling pathways, including some that are important for intracellular *L. pneumophila* replication. Here we also show that the activity of UBE2N is restored by MvcA(Lpg2148), an ortholog of MavC. MvcA functions to deubiquitinate UBE2N-Ub using the same catalytic triad required for its deamidase activity. Structural analysis of the MvcA-UBE2N-Ub complex reveals a crucial role of the insertion domain in MvcA in substrate recognition. Our findings reveal that two remarkably similar proteins catalyze the forward and reverse reactions to impose temporal regulation of the activity of UBE2N during *L. pneumophila* infection.

CHAPTER 1. INTRODUCTION

Legionella pneumophila

Legionella pneumophila is a Gram-negative rod-shaped bacterium, which ubiquitously exists in aquatic environments. A broad range of water protozoa, such as amoebae are the natural hosts of *L. pneumophila*. In addition to natural aquatic environments, *L. pneumophila* also is highly adaptive in man-made water systems such as air conditioners and cooling towers. It is believed that the evolutionary pressure imposed by amoebae allows *L. pneumophila* to acquire the ability to survive and replicate in human alveolar macrophages (Escoll, Rolando et al., 2013). Indeed, the cell biological features associated with infections in amoebae and human macrophages are highly similar (Al-Quadan, Price et al., 2012) and the pathogenic elements required for establishing infections in these two types of hosts are identical (Cianciotto & Fields, 1992, Rasch, Unal et al., 2014). The first outbreak of *L. pneumophila* infection occurred in 1976 during the American Legion Convention held in Philadelphia attended by more than 2,000 veterans. During the meeting, around 200 attendees were affected, and 29 of them died (Fraser, Tsai et al., 1977). Infection by *L. pneumophila* can cause the potentially fatal Legionnaires' disease or a mild flu-like illness called Pontiac fever (Newton, Ang et al., 2010, Swanson & Hammer, 2000). *L. pneumophila* has become a major threat to human health since the first outbreak. The reported cases of Legionnaires' disease have been increasing in the past decades. According to data from the CDC, 7,500 cases of Legionnaires' disease were reported in 2017 in United States. The number is believed to be underestimated due to underdiagnosis. Children, elderly and immune-compromised populations are more susceptible to *L. pneumophila* infection. The mortality rate is about 10% (Marston, Plouffe et al., 1997). The rising infection case number and the high fatality of infected patients have drawn considerable attention of both health administrators and scientists.

L. pneumophila is an intracellular opportunistic pathogen. After being phagocytized by host cells, it remains residing within a plasma membrane-derived vacuole called Legionella Containing Vacuole (LCV) (Horwitz, 1983). Vesicles originating from the endoplasmic reticulum (ER) are important for the biogenesis of the LCV. The decoration of its surface with ER derived vesicles converts the LCV from nascent phagosome-like membranes to rough endoplasmic reticulum (ER)-like membranes, which prevents it from proceeding to the phagosome maturation process for

degradation. The maturation of LCV also requires sequential intimate interactions with other organelles such as mitochondria and ribosomes. Eventually, *L. pneumophila* egresses the vacuole and lyses the cell to start a new round of intracellular cycle by infecting a neighboring cell (**Fig. 1-1**) (Isberg, O'Connor et al., 2009).

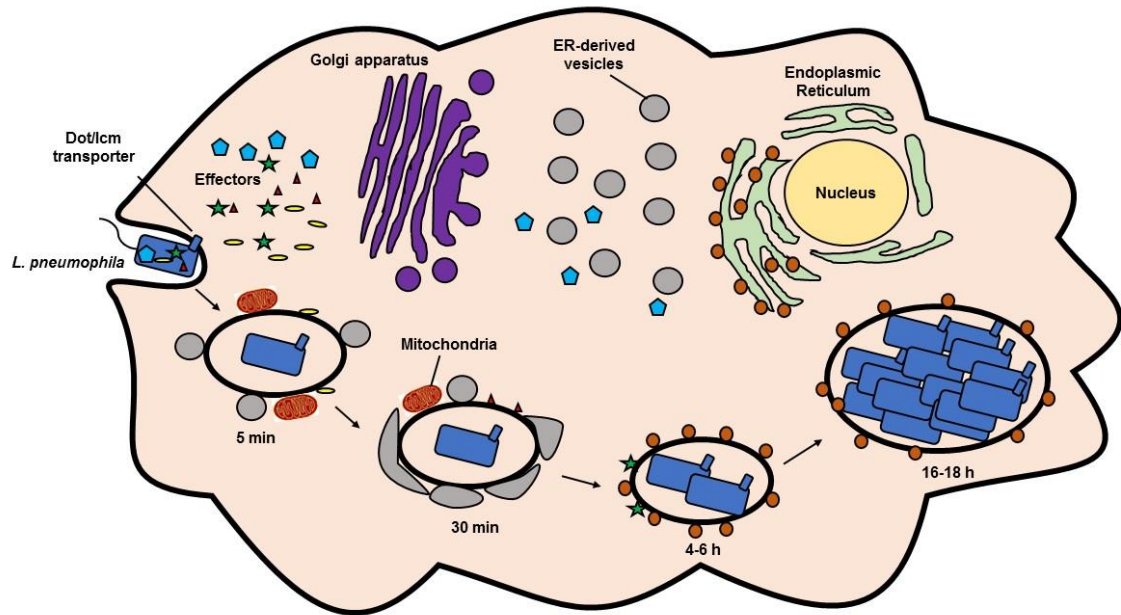


Fig. 1-1 Formation of *L. pneumophila* replicative vacuoles by modulating host cellular processes.

After being phagocytized by a host cell, the Legionella-containing vacuole (LCV) evades host endocytic pathway and recruits endosomal reticulum (ER) derived vesicles and mitochondria to its surface to convert it from the plasma-membrane-derived phagosomal membrane to membranes resembling those of the ER. At later infection stages, ribosomes are also recruited to the surface of LCV to facilitate its maturation and support the intracellular bacterial replication. *L. pneumophila* replicates to high numbers inside the vacuole and eventually lyses the cell to start a new life cycle by infecting neighboring cells.

To facilitate its intracellular replication, *L. pneumophila* utilizes the Type IVB Secretion System known as Dot/Icm (defect in organelle trafficking genes/ intracellular multiplication) system)) to deliver more than 300 effector proteins to manipulate multiple cellular activities in host cells, such as vesicle trafficking, innate immunity and protein translation (Isberg et al., 2009, Qiu & Luo, 2017b). The effector-encoding genes consist of more than 10% of *L. pneumophila* protein-coding capacity, which makes *L. pneumophila* a bacterium that possesses the largest effector arsenal among all known bacterial pathogens (O'Connor, Adepoju et al., 2011, Qiu & Luo, 2017a). *L. pneumophila* effector-encoding genes cluster in several regions on its chromosome. A genome deletion study conducted by the Isberg lab revealed that a strain lacking 31% of its effectors still replicates at levels almost comparable to wild type bacteria in mouse primary macrophages. In contrast, all large chromosomal deletions have severely impaired its ability to replicate in one or more amoebae species. These results suggest the high-level redundancy and host specificity of *L. pneumophila* effectors (O'Connor et al., 2011). The fact that *L. pneumophila* harbors the largest effector inventory offers unique opportunities to study the mechanism of bacterial interactions with hosts and to reveal the potentially diverse biochemical activities of these virulence factors.

RalF was identified as the first Dot/Icm protein substrate which functions to recruit the Arf1 small GTPase to the surface of the LCV. Bioinformatic analysis revealed that RalF contains a motif of high similarity to Sec7 domains. Sec7 domains are highly conserved in eukaryotic guanine nucleotide exchange factors (GEFs) of the Arf family small GTPases. In line with its homology to Sec7 domains, RalF is capable of stimulating the GTP-GDP exchange of Arf1 (Nagai, Kagan et al., 2002). After the discovery of RalF, the first protein substrate of the Dot/Icm secretion system, a large number of effectors were identified via the use of several effective methods, including bioinformatic analysis(Burstein, Amaro et al., 2016, Burstein, Zusman et al., 2009, Lifshitz, Burstein et al., 2013), bacteria-bacteria protein translocation (Luo & Isberg, 2004) , the use of SidC as a report (Huang, Boyd et al., 2011, Luo & Isberg, 2004), and computation based on sequences of known effectors (Chen, de Felipe et al., 2004, de Felipe, Pampou et al., 2005, Nagai et al., 2002, Pan, Luhrmann et al., 2008). These efforts led to the identification of approximately 330 effectors(Qiu & Luo, 2017b). Only about 10% of these effectors have been biochemically characterized (Qiu & Luo, 2017b), the majority of effectors are hypothetical proteins and the study of their functions is an important theme of *Legionella* pathogenesis.

Multiple important cellular activities are modulated by *L. pneumophila* effectors, including vesicle trafficking, protein translation (Belyi, Niggeweg et al., 2006, Shen, Banga et al., 2009), autophagy(Choy, Dancourt et al., 2012) and interference in metabolism of lipids involved in signaling such as phosphatidylinositol (PI) lipids. The best characterized example of the modulation of host vesicle trafficking is the hijack of small GTPases associated with the ER such as Rab1. SidM functions as a GEF for Rab1 and recruits Rab1 to the surface of LCV (Machner & Isberg, 2006, Murata, Delprato et al., 2006). In addition, SidM also is a GDI-displacement factor (GDF) that functions to dissociate Rab1 from GDI (Ingundson, Delprato et al., 2007, Machner & Isberg, 2007). LepB is a GTPase-activating protein (GAP) for Rab1, which catalyzes the conversion of GTP-Rab1 to GDP-Rab1 (Ingundson et al., 2007). Furthermore, SidM AMPylates while SidD deAMPylates Rab1, which affects the interaction between LepB and Rab1, thereby temporally controlling the activity of Rab1(Muller, Peters et al., 2010) (Neunuebel, Chen et al., 2011, Tan & Luo, 2011b). Moreover, AnkX modifies Rab1 by phosphorylcholination, Lem3 removes such phosphorylcholination (Goody, Heller et al., 2012, Oesterlin, Goody et al., 2012, Tan, Arnold et al., 2011). SidC and SdcA associate with the mono-ubiquitination of Rab1 during infection, but whether they catalyze the ubiquitination of Rab1 remains unknown (Horenkamp, Mukherjee et al., 2014). The SidE family effectors ubiquitinates Rab1 through non-canonical ubiquitination. However, the biological significance of the ubiquitination of Rab1 remains elusive (Qiu, Sheedlo et al., 2016).

Phosphatidylinositols (PIs) play key roles in membrane trafficking and cell signaling. Different organelles are decorated with different types of PIs. For instance, the plasma membrane is enriched with [PI(3,4,5)P₃], [PI(4,5)P₂] and [PI(4)P], endosomes are enriched with [PI(3)P], and the Golgi apparatus is enriched with [PI(4)P] (Di Paolo & De Camilli, 2006). Given their importance, PIs are subject to interaction and modulation with several *L. pneumophila* effectors. The localization of multiple effectors is directed by the binding with PIs. For example, SidC, SdcA, SidM, Lpg2603, Lpg1101 are recruited to the surface of the LCV, a region where PI4P is enriched, through their PI4P binding domains (Brombacher, Urwyler et al., 2009, Hubber, Arasaki et al., 2014, Weber, Ragaz et al., 2006). VipD is phospholipase A1, which removes PI(3)P from endosomal membrane upon binding to Rab5 or Rab22, avoiding the LCV from fusing with the endosomal compartment (Gaspar & Machner, 2014, Ku, Lee et al., 2012). LepB converts PI(3)P to PI(3,4)P₂ (Dong, Niu et al., 2016). SidF is a PI 3-phosphatase that converts PI(3,4)P₂ to PI4P

(Hsu, Zhu et al., 2012). Another PI phosphatase, SidP, dephosphorylates PI(3)P and PI(3,5)P₂ to PI and PI(5)P, respectively (Toulabi, Wu et al., 2013). LpdA functions as a phospholipase D to convert phosphatidylcholine to phosphatidic acid, the latter can be further converted to diacylglycerol by another effector LecE. LpdA and LecE localize to the LCV, their coordinated activities very likely will accumulate diacylglycerol on the LCV, but how this influences the intracellular growth of *L. pneumophila* has not been fully investigated (Viner, Chetrit et al., 2012).

Ubiquitination regulates almost every cellular activity in eukaryotic cells, including host cell immunity and cell signaling (Komander & Rape, 2012). To achieve successful intracellular bacterial replication, the manipulation of the host ubiquitination machinery is critical. Studying of effectors that modulate the host ubiquitination machinery has become one of the most intensively studied areas.

Ubiquitination

Ubiquitination is regarded as one of the most fundamental protein post-translational modifications in eukaryotes, which involves covalent conjugation of ubiquitin, a 76 amino acids protein to target proteins (Goldknopf, French et al., 1977, Komander & Rape, 2012). Proteomic studies show that far over 1,000 of the 20,000-25,000 annotated human proteins appear to regulate ubiquitination or to be modified by ubiquitin (Clague, Heride et al., 2015), which strongly supports its ubiquitous role in cell physiology. Ubiquitin was first found as a free protein by Goldstein and his colleagues in 1975 (Goldstein, Scheid et al., 1975). Later this protein was found to be conjugated to a lysine residue on histone H2A through its C-terminus (Hunt & Dayhoff, 1977). In the meantime, Hershko, Ciechanover and their colleagues discovered that a small protein, termed as APF-1 (ATP dependent proteolytic factor 1), was covalently conjugated to proteins before their degradation in cell extracts (Hershko, Ciechanover et al., 1980). Hershko and colleagues proposed that APF-1 severs as a signal for protein degradation. APF-1 was later identified to be ubiquitin (Wilkinson, Urban et al., 1980). Degradation triggered by APF-1 conjugation requires a set of three enzymes, the activation enzyme E1, the transfer enzyme E2 and the ligation enzyme E3 (Hershko, Heller et al., 1983). By the middle 1980's, it was established that ubiquitination in eukaryotes is achieved by a sequential multi-enzyme catalysis cascade as Hershko and Ciechanover propose. In this scheme, ubiquitin is activated through the formation of a thioester bond between an E1 specific cysteine residue and the carboxyl-terminal glycine residue in

ubiquitin. Then the activated ubiquitin is transferred to E2s by transthioleation, followed by the ligation of ubiquitin to a substrate protein mostly on lysine residues through the activity of E3s (Komander & Rape, 2012).

UBE1 was regarded as the sole E1 enzyme for all eukaryotes for a long time. However, a second E1 enzyme UAE6 was discovered in vertebrates and sea urchin by Finley and colleagues in 2007. UBE1 and UAE6 have distinct E2 charging preferences in *in vitro*. Unlike UBE1, UAE6 only charges ubiquitin to E2 enzymes, while UBE1 is capable of charging both ubiquitin and UBLs (Jin, Li et al., 2007). E2 enzymes are categorized into two functional groups: initiation E2s and elongation E2s (Ye & Rape, 2009). UBE2N falls into the elongation E2 group, whose members are unable to directly modify substrates. Instead, these enzymes often only catalyze the formation of free polyubiquitin chains or elongate existing ubiquitin chains on substrates. These enzymes. The ligation of free K63-linked polyubiquitin chains produced by the UBE2N complexes to protein substrates requires initiation E2s such as UBE2W which allows the attachment of a first ubiquitin molecule to the target protein (Christensen, Brzovic et al., 2007). For example, poly-ubiquitination of the E3 ligase TRIM5 α requires its initial mono-ubiquitination by UBE2W, then followed by K63-linked polyubiquitin chain conjugation (Fletcher, Christensen et al., 2015). E3 enzymes are classified into three major categories based on the catalysis mechanism and the presence of specific catalytic domains, namely the Really Interesting New Gene E3s (RINGs) family, the Homologous to E6-AP Carboxyl Terminus E3s (HECTs) family and the RING-IBR(In-Between-RINGs)-RING E3s (RBRs) family (Morreale & Walden, 2016). E3s in the RING family are the most abundant type of ligase, which function as a scaffold to orient and mediate a direct transfer of ubiquitin from charged E2 enzymes to protein substrates. In contrast, ubiquitin ligation catalyzed by HECT E3s is a two-step reaction. First, ubiquitin is transferred to its catalytic cysteine residue from an E2 enzyme before its ligation to a protein substrate. RBR E3 ligases also conduct two step reactions which is similar to HECT, however its mechanism is a hybrid of HECT and RING mechanisms (Morreale & Walden, 2016).

Ubiquitination can occur in multiple forms including mono-ubiquitination and poly-ubiquitination. One ubiquitin monomer can be conjugated to a single lysine residue (mono-ubiquitination) or several lysine residues (poly-mono-ubiquitination) of the substrate (Ashida, Kim et al., 2014). In addition, ubiquitin molecule itself has seven lysine residues Lys6, Lys11, Lys27, Lys29, Lys33, Lys48 and Lys63. Hence, one ubiquitin can be conjugated to another ubiquitin

molecule to form homotypic or heterotypic polymer chains (poly-ubiquitination). Polyubiquitin chains can form through one of the seven lysine residues. In addition, the primary methionine can also be utilized to form linear polyubiquitin chains (Komander & Rape, 2012). Different types of ubiquitin linkage usually dictate the fate of the substrate. For example, K48-linked polyubiquitin, arguably the best-characterized and the most abundant chain linkage type, usually drives modified substrates for proteasomal degradation, whereas K63-linked chain is mostly involved in signaling cascades (Komander, 2009). However, the function of different chain types is not always dedicated to one certain biological consequence. K63-linked chains have also been discovered to drive protein degradation, whereas K48-linked chains also can function nonproteolytically (Li & Ye, 2008).

In addition to modification by ubiquitin at its lysine residues, other types of post-translational modification on ubiquitin also exist. For example, phosphorylation can occur on serine, threonine or tyrosine residues. Ubiquitin contains 11 serine, threonine, and tyrosine residues, all of which have been shown to be phosphorylated in cells by mass spectrometric studies (Herhaus & Dikic, 2015, Swatek & Komander, 2016). The best characterized example is the phosphorylation of ubiquitin at Ser₆₅ by the kinase PINK1, which plays an important role in the activation of the E3 ligase Parkin, a protein involved in Parkinson's disease (Kitada, Asakawa et al., 1998, Valente, Abou-Sleiman et al., 2004). PINK1 phosphorylates at Ser₆₅ of ubiquitin and the Ubl domain of Parkin. Phosphorylated ubiquitin interacts with phosphorylated Parkin, which releases the autoinhibition effect imposed by the Ubl domain of Parkin (Gladkova, Maslen et al., 2018, Koyano, Okatsu et al., 2014, Matsuda, 2016). Ser₆₅-phosphorylated ubiquitin maintains the same efficiency to be charged to a set of several E2 enzymes, but its discharge from E2s has been accelerated (Wauer, Swatek et al., 2015). Furthermore, phosphorylated ubiquitin chains are more resistant to deubiquitinases (Dubs, see below). Thus, the accelerated discharge of ubiquitin and decelerated cleavage of polyubiquitin chains might also be potential mechanisms of Parkin activation which promotes the formation of polyubiquitin chains (Wauer et al., 2015).

Furthermore, ubiquitin has been shown to be modified by acetylation on some of its lysine residues (Herhaus & Dikic, 2015), deamidation on the Gln₄₀ residue (Cui, Yao et al., 2010), ADP-ribosylation and phosphoribosylation on the Arg₄₂ residue (Bhogaraju, Kalayil et al., 2016, Qiu et al., 2016). Deamidation on the Gln₄₀ residue blocks the synthesis of K48 linked polyubiquitin chains induced by different E3-E2 pairs, including a RING-domain E3 gp78c/Ube2g2. In addition,

overexpression of Ubiquitin_{Q40E}, the product of ubiquitin deamidation impairs TNF α -induced NF- κ B activation and leads to the accumulation of several UPS substrates (Cui et al., 2010). Both ADP-ribosylation and phosphoribosylation on the Arg₄₂ residue of ubiquitin are toxic to eukaryotic cells and interferes with the canonical ubiquitination machinery, which inhibits proteasomal degradation(Bhogaraju et al., 2016). Moreover, ubiquitin also can be modified by ubiquitin-like modifiers (UBLs), a group of small proteins shows certain structural similarity to ubiquitin. Ubiquitin can be modified by SUMO, and such hybrid SUMO and ubiquitin chains enhance the degradation of I κ B α (Seeler & Dejean, 2017). The modification of polyubiquitin chain by Nedd8 increases its resistance to Dubs and proteasomal degradation, which might be beneficial to maintain free ubiquitin pool (Singh, Zerath et al., 2012). UBLs are also modifiable by ubiquitin (Komander & Rape, 2012, Swatek & Komander, 2016). UBLs are conjugated to protein substrates by a multiple-enzyme catalysis cascade similar to that of ubiquitination. UBLs include SUMO (small ubiquitin-related modifier), NEDD8 (neural precursor cell expressed, developmentally downregulated 8), ISG15 (interferon-stimulated gene 15) and some others. Other yet unidentified post-translational modifications on ubiquitin likely exist. The ubiquitin code is complicated by different types of ubiquitination, and the crosstalk between ubiquitination and other post-translational modifications makes the ubiquitination code even more complex, which allows better fine tuning of signaling, particularly in the context of certain disease conditions (Komander, 2009, Song & Luo, 2019, Swatek & Komander, 2016).

Ubiquitination is highly dynamic, and the process is reversible, an event regulated by a group of enzymes called Dubs that recognize specific substrates and hydrolyze the isopeptide bond between ubiquitin monomers or the bond between substrate and ubiquitin (Komander, Clague et al., 2009). The cleavage of ubiquitinated protein substrates by Dubs allows substrate proteins to be restored to its unmodified status, and ubiquitin to be recycled. Besides, Dubs also function to maintain the homeostasis of free ubiquitin pool in cells, through cleaving polyubiquitin chains or facilitating ubiquitin maturation. Six structurally distinct Dub families have been described, including the ubiquitin-specific proteases (USPs), the ovarian tumor proteases (OTUs), the ubiquitin C-terminal hydrolases (UCHs), the Josephin family, the motif interacting with ubiquitin (MIU)-containing novel DUB family (MINDYs), and a family of Zn-dependent JAB1/MPN/MOV34 metalloprotease DUBs (JAMMs) (Mevissen & Komander, 2017). Except for JAMMs, all the other five families are cysteine proteases.

The number of enzymes involved in the ubiquitination machinery varies greatly in different organisms. Human genome encodes two E1s, at least 38 E2s (including E2s for UBLs) and around 600 to 1,000 E3s (Ye & Rape, 2009). In contrast, the number of those enzymes is much lower in yeast, which only harbors one E1, 11 E2s and around 60 to 100 E3s (Finley, Ulrich et al., 2012). Yeast harbors around 20 Dubs, while human is estimated to encode at least 1,000 Dubs (Mevissen & Komander, 2017).

The Ubiquitin conjugating enzyme 2N (UBE2N)

E2 enzymes are one essential component of the ubiquitination machinery, these enzymes not only act as the transition point between E1 and E3 but also function in determining the chain type and substrate specificity (Stewart, Ritterhoff et al., 2016). Lower and higher eukaryotes share a minimal subset of E2 enzymes, which are believed to fulfill the most basic cellular functions. UBE2N is one of those basic E2s, which directs primarily the synthesis of K63-linked polyubiquitin chains when it heterodimerizes with UBE2V1 or UBE2V2, a ubiquitin conjugating enzyme variant (Hofmann & Pickart, 1999). UBE2V1 and UBE2V2 resemble E2 enzymes, however lack a functional catalytic cysteine residue, which prevents it from transferring ubiquitin to a E3 ligase. It is believed that the function of UBE2V1/UBE2V2 is to orient the acceptor ubiquitin so that Lys₆₃ can attack the thioester linking between the donor ubiquitin and UBE2N (McKenna, Spyracopoulos et al., 2001). Together with E1, the UBE2N heterodimer is able to generate basal level K63-linked polyubiquitin chains but at an extremely low rate (Hofmann & Pickart, 1999). The dimerization of the RING finger domain in RING E3 ligases strongly promotes the catalytic activity of UBE2N regardless of the nature of the RING E3 (Branigan, Plechanovova et al., 2015, Yudina, Roa et al., 2015). Free K63-linked polyubiquitin chains synthesized by the UBE2N complex is involved in multiple cellular activities, including DNA damage repair, autophagy, NF-κB activation. The participation of the UBE2N complex in distinct pathways depends on its interaction with different E3s (Ye & Rape, 2009).

E2 enzymes are required in all described ubiquitination reactions except for those induced by members of the SidE family (Kotewicz, Ramabhadran et al., 2017, Qiu et al., 2016). Hence, it is very important to understand how the activity of E2 enzymes is regulated. Among the approximate 40 known E2s, only a few have been fully studied. E2 enzymes are also subject to regulation by ubiquitination or some other post translational modifications. The yeast E2 Ubc7, a homolog of

human UbcH7 undergoes self-ubiquitination and degradation by the HECT E3 Ufd4 when the level of Ubc7 exceeds its binding partner Cue1, a transmembrane protein that tethers Ubc7 to ER (Ravid & Hochstrasser, 2007). UBE2T undergoes automonoubiquitination *in vivo*, which is stimulated by the FANCL protein, leading to the inactivation of UBE2T (Machida, Machida et al., 2006). Although it is a key E2 enzyme in cells, the regulation of UBE2N is not fully appreciated. Previous study shows that STAT3 operates as a transcriptional repressor on the expression of *ube2N* by inhibiting the accrual of Ets-1, Set1 methyltransferase and trimethylation of histone H3 lysine 4 (H3K4me3) at the *ube2N* promoter (Zhang, Hu et al., 2014). UBE2N can be ISGylated by ISG15 at Lys₉₂ residue, which abolishes the conjugation of ubiquitin to its catalytic cysteine residue (Zou, Papov et al., 2005). It also has been shown that in heat shocked K562 cells, UBE2N is mono-ubiquitinated at Lys₉₂ (Takada, Hirakawa et al., 2001). The mono-ubiquitination on UBE2N later was found to be self-modification. The *in vitro* self-ubiquitination of UBE2N occurs without the participation of an E3 ligase but requires E1 and its catalytic cysteine. Self-ubiquitination of UBE2N at Lys₉₂ site is regarded as non-specific self-modification (Branigan et al., 2015). However, the existence of such modification on UBE2N at its Lys₉₂ residue in cells suggests that it may indicate some unveiled biological significance. And such neglected regulation of UBE2N potentially have some underappreciated importance in maintaining cell signaling integrity which is worth exploring.

***Legionella pneumophila* and its exploitation of the host ubiquitin system**

Ubiquitination plays pivotal roles in cells and modulates virtually every cellular process, particularly those involved in protein homeostasis, DNA repair, cell cycle regulation and immune responses. To symbiotic and pathogenic bacteria, it is essential to hijack and manipulate the host ubiquitination machinery to thwart host defenses. It has been well established that bacterial pathogens deliver virulence factors that function as ubiquitin ligases, Dubs or as enzymes that directly attack ubiquitin to hijack the host ubiquitination machinery (Zhou & Zhu, 2015). For example, Enterohemorrhagic *E. coli* EHEC translocates E3 effectors NleL and NleG to facilitate the formation of actin pedestal (Lin, Diao et al., 2011, Wu, Skarina et al., 2010). *Salmonella* Typhimurium infection can cause the formation of ubiquitinated protein aggregates or Aggresome Like Induced Structures (ALISs) around the *Salmonella* Containing Vacuole (SCV), which triggers autophagy and the elimination of *Salmonella*. However, *Salmonella* secrets the Dub SseL

to deubiquitinate ALISs to escape from autophagy (Mesquita, Thomas et al., 2012). *L. pneumophila*, the bacterium which harbors the largest effector arsenal also extensively modulates the host ubiquitination machinery. The first study of such modulation was reported in 2006 by the Isberg lab. Dorer and her colleagues found that Cdc48/p97, an AAA-ATPase which is important for ubiquitin-proteasome degradation pathway is critical for the LCV formation and bacterial intracellular replication (Dorer, Kirton et al., 2006). The decoration of LCV by ubiquitinated species was also discovered in the same study, which occurs shortly after its formation and depends on the Dot/Icm secretion system. After one decade of research, nearly 20 effectors have been found to be involved in the manipulation of the host ubiquitin network (Qiu & Luo, 2017a). Among those effectors, 7 are F-box containing proteins: LegU1 (Lpg0171), LicA (Lpg1408), Lpg1975, AnkB (Lpg2144), PpgA (Lpg2224), Lpg2525 and Lpp2486 (Only in strain Paris). Three effectors are U-box-containing proteins: LubX (Lpg2830), GobX (Lpg2455) and RavN(Lpg111) (Lin, Lucas et al., 2018). The *L. pneumophila* effectors SidC (Lpg2511) and its homolog SdcA (Lpg2510) are novel E3 ligases which do not show structural similarity to host E3 ligases (Hsu, Luo et al., 2014). In addition, Hidden Markov models (HHpred) analyses revealed that Lpg2370, MavM (Lpg2577), Lpg2498, LegA14 (Lpg2452) are structurally homologous to eukaryotic RING, HECT and SidC E3 ligases (Lin et al., 2018). Among those effectors, LegU1, AnkB, GobX, LubX, RavN, LegA14, SidC and SdcA exhibit E3 ligase activity (self-ubiquitination) when incubated with E1, E2, ubiquitin and ATP in *in vitro* reactions.

LegU1 binds and ubiquitinates the host protein HLAB-associated transcript 3 (BAT3). Furthermore, LegU1-BAT3 complex interacts with another effector Lpg2160, but does not modify Lpg2160. Neither the importance of LegU1 ubiquitinating BAT3, nor the importance of interaction between LegU1 with Lpg2160 is known (Ensminger & Isberg, 2010).

Lpp2082, the AnkB homolog in *L. pneumophila* strain Paris interacts with host ubiquitinated protein ParvB, a pro-apoptotic protein. Study shows that the overexpression of Lpp2082 triggers ParvB degradation and reduces caspase 3 activation level (Lomma, Dervins-Ravault et al., 2010).

LubX binds and ubiquitinates SidH, another *L. pneumophila* effector protein, leading to its degradation by the 26S proteasome. In addition, LubX binds the host factor Cdc2-like kinase 1 (Clk1), and is able to catalyze the ubiquitination of Clk1 in *in vitro* reactions, however such modification only modestly occurs when host cells are challenged with bacteria that overexpress LubX . It still remains elusive whether Clk1 is a *bona fide* substrate of LubX. How the intracellular

bacterial replication is modulated by the manipulation of Clk1 by LubX also awaits further investigation (Kubori, Hyakutake et al., 2008, Kubori, Shinzawa et al., 2010).

SidC and its homolog SdcA possess a phosphatidylinositol-4-phosphate (PI4P)-binding domain at their C-termini. Such PI4P binding domain directs their localization to the surface of LCV. SidC and SdcA were proposed to function as vesicle fusion tethering factor based on their activity of recruiting ER derived vesicles to LCV (Ragaz, Pietsch et al., 2008). Structural study of the N-terminus of SidC (1-542 amino acids) by the Mao group revealed that no homology was found between SidC and any other structurally known proteins. Interestingly, SidC contains a potential papain-like catalytic triad which is formed by Cys₄₆, His₄₄₄, and Asp₄₄₆ (Hsu et al., 2014). Papain-like catalytic triad involves in the catalysis of multiple biochemical reactions including ubiquitin ligation. Indeed, SidC undergoes strong self-ubiquitination once incubated with all necessary components for canonical ubiquitination. SidC thus was confirmed as a E3 ubiquitin ligase. The unique structure of SidC distinguishes it from other major E3 ligase groups. Biochemical studies showed that SidC works with multiple E2s but prefers UbcH7 to catalyze the synthesis of polyubiquitin chains. SidC displays a preference of using Lys₁₁ and Lys₃₃ from ubiquitin to form polyubiquitin chains while does not form primary Met₁-linked polyubiquitin chains (Hsu et al., 2014). The E3 activity of SidC is important for the recruitment of ER derived vesicles, and is activated by binding to PI4P through its C-terminal domain. However, the substrate of SidC and the connection between its E3 ligase activity and the recruitment of ER-derived vesicles remain unknown (Hsu et al., 2014, Luo, Wasilko et al., 2015). Interestingly, although SidC and SdcA share 72% sequence identity, they exhibit different E2 preference, which could be evolved for maximal exploitation of the host ubiquitination machinery. (Luo et al., 2015, Wasilko, Huang et al., 2018).

SidE family proteins: Members of this family SidE (Lpg0234), SdeA (Lpp2157), SdeB (Lpg2156), SdeC (Lpg2156) were found as *L. pneumophila* Dot/Icm effectors in 2004 (Luo & Isberg, 2004). SidEs are large proteins made of over 1500 amino acids and are highly similar and their function was not revealed until very recently. Ectopic expression of these proteins such as SdeA in yeast induces a strong growth defect, indicating that SdeA interferes with some key cellular activity (Havey & Roy, 2015, Jeong, Sexton et al., 2015). Deletion of genes coding for the SidE family effector caused about 100-fold defect in intracellular growth in the host *Acanthamoeba castellanii*, pointing to the importance of the SidE family in bacterial virulence

(Jeong et al., 2015). Our lab and our collaborators in the Chemistry Department identified that the N-terminus of SdeA (1-193 amino acids) functions as a canonical Dub which has a preference in cleaving Lys₆₃ linked polyubiquitin chains (Sheedlo, Qiu et al., 2015). SdeA is of 1,499 amino acids and the function of the rest of 1,300 amino acids remains mysterious. In the same year, a structural study of SidE predicts that it may play a role in nucleotide metabolism (Wong, Kozlov et al., 2015). Shortly, our lab discovered that SdeA catalyzes ubiquitination of several Rab small GTPases associated with the ER such as Rab1 and Rab33b. Ubiquitination catalyzed by SdeA remarkably differs from the classical ubiquitination mechanism: the reaction occurs independent of E1, E2 and ATP (Qiu et al., 2016). Ubiquitination of Rab proteins by SdeA is a multi-step process that starts by a mono-ADP-ribosyltransferase (mART) activity. The mART motif catalyzes the transfer of the ADP-ribosyl group from nicotinamide adenine dinucleotide (NAD) to Arg₄₂ of ubiquitin (Qiu et al., 2016). Then the ADP-ribosylated ubiquitin is cleaved by a phosphodiesterase activity encoded by another domain (PDE) within SdeA, to produce phosphoribosyl ubiquitin. Phosphoribosyl ubiquitin is further conjugated to serine residues of substrates (Bhogaraju et al., 2016, Kotewicz et al., 2017). Interestingly, the hydrolysis of NAD by SdeA aligns with the predication of nucleotide metabolism conducted by the structural study of SidE (Wong et al., 2015). The ADP-ribosylation and phospho-ribosylation of ubiquitin are two types of new post-translational modifications on ubiquitin. The ubiquitination of Rab33b and Rtn4 by SdeA does not require the C-terminal di-glycine of the ubiquitin molecule, which is completely different from the classical ubiquitination chemistry (**Fig. 1-2**) (Akturk, Wasilko et al., 2018, Dong, Mu et al., 2018, Kalayil, Bhogaraju et al., 2018). SidE family effectors recognize substrates independently of certain structural folds but rather potentially catalyze any protein carrying the accessible serine residue, suggesting additional substrate likely exists (Wang, Shi et al., 2018). In line with this discovery, small Rag GTPases are also shown to be the targets of SidE family, which impacts the mTORC1 pathway and nutrient metabolism in host cells (De Leon, Qiu et al., 2017).

The SdeA-induced toxicity in yeast can be suppressed by another *L. pneumophila* effector, SidJ, an effector that is important for optimal bacterial virulence in both amoebae and mammalian hosts (Liu & Luo, 2007), but not by its homolog SdjA, suggesting the a counteractive effect of SidJ to SdeA (Havey & Roy, 2015, Jeong et al., 2015, Qiu, Yu et al., 2017). SidJ had been shown to function as a unique Dub which specifically removes ubiquitin from SdeA mediated phosphoribosyl ubiquitination substrates (Qiu et al., 2017). However, such activity only exists in

SidJ proteins purified from *L. pneumophila* cells but not *E. coli* cells, suggesting that the Dub activity may require some *L. pneumophila*-specific factors. The activity of SidJ and its homolog SdjA awaits further investigation.

The host ubiquitin machinery is extensively manipulated by *L. pneumophila* effectors. Whether new effectors and new mechanisms exist need further investigation and such discovery would add a new layer to the study of the hijack of the host ubiquitin machinery by bacterial pathogens.

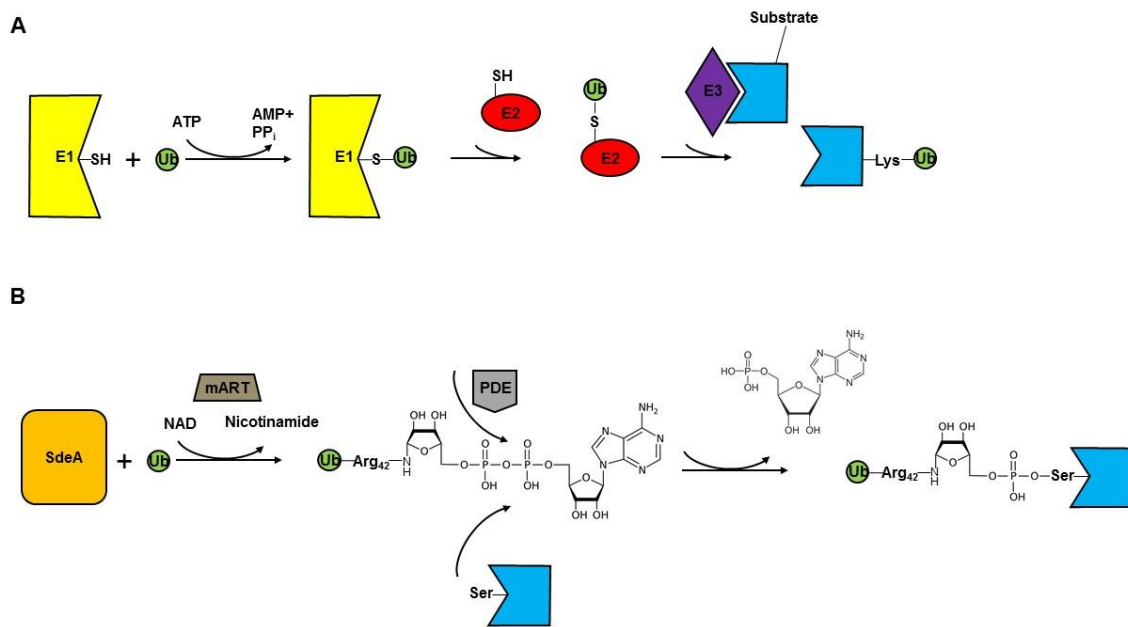


Fig 1-2 Canonical ubiquitination mechanism and SdeA-catalyzed ubiquitination mechanism.

A. In canonical ubiquitination, ubiquitin is activated by the E1 in the expense of ATP, activated ubiquitin is transferred from the catalytic cysteine residue of the E1 enzyme to the catalytic cysteine residue of E2, eventually with the help of an E3 enzymes ubiquitin is conjugated to a lysine residue on the protein substrate. **B.** In the reactions catalyzed by SdeA, ubiquitin is first activated by ADP-ribosylation at its Arg₄₂ by its mono-ADP transferase (mART) activity of SdeA. ADP-ribosylated ubiquitin is utilized by the phosphodiesterase (PDE) activity of SdeA to generate phosphoribosylated ubiquitin, concomitant with the release of AMP, phosphoribosylated ubiquitin is transferred to serine residues on a substrate protein.

CHAPTER 2. LEGIONELLA PNEUMOPHILA INHIBITS IMMUNE-SIGNALLING VIA MAVC-MEDIATED TRANSGLUTAMINASE-INDUCED UBIQUITINATION OF UBE2N

Abstract

The bacterial pathogen *Legionella pneumophila* modulates host immunity using effectors translocated by its Dot/Icm transporter to facilitate its intracellular replication. A number of these effectors employ diverse mechanisms to interfere with protein ubiquitination, a post-translational modification essential for immunity. Here, we have found that *L. pneumophila* induces monoubiquitination of the E2 enzyme UBE2N by its Dot/Icm substrate MavC (Lpg2147). We demonstrate that MavC is a transglutaminase that catalyses covalent linkage of ubiquitin to Lys⁹² and Lys⁹⁴ of UBE2N via Gln₄₀. Similar to canonical transglutaminases, MavC possess deamidase activity that targets ubiquitin at Gln₄₀. We identified Cys₇₄ as the catalytic residue for both ubiquitination and deamidation activities. Furthermore, ubiquitination of UBE2N by MavC abolishes its activity in the formation of K₆₃-type polyubiquitin chains, which dampens NF-κB signaling in the initial phase of bacterial infection. Our results reveal an unprecedented mechanism of modulating host immunity by modifying a key ubiquitination enzyme by ubiquitin transglutamination.

Introduction

Legionella pneumophila extensively modulates host cellular processes with the hundreds of effectors injected by its Dot/Icm system, which results in the biogenesis of the Legionella-containing vacuole (LCV), a phagosome that supports bacterial replication (Isberg et al., 2009). Infection by *L. pneumophila* activates the major immune regulator NF-κB by at least two mechanisms. The first is a transient Dot/Icm-independent activation, most probably by immune agonists such as flagellin and lipopolysaccharide; this activation is more apparent when macrophages are challenged with bacteria at a high multiplicity of infection (MOI) (Bartfeld, Engels et al., 2009, Losick & Isberg, 2006). The second mechanism is mediated by the Dot/Icm transporter that persists throughout much of the intracellular life cycle of the bacterium (Bartfeld et al., 2009, Losick & Isberg, 2006). NF-κB activated by the latter mechanism induces the expression of a large repertoire of genes, including those involved in cell survival, vesicle

trafficking and immunity (Abu-Zant, Jones et al., 2007, Losick & Isberg, 2006). The Dot/Icm effector LegK1 activates NF- κ B by directly phosphorylating I κ B α and other members of this inhibitor family, including p100 (Ge, Xu et al., 2009); LnaB also activates this transcriptional factor, but its mechanism of action is unknown (Losick, Haenssler et al., 2010). Cell survival genes induced by NF- κ B activation are required for productive intracellular bacterial replication (Losick & Isberg, 2006). The activation of immunity by ligands such as flagellin presumably is detrimental to the pathogen, but how *L. pneumophila* counteracts such defence remains unknown. Among other important functions, ubiquitination is essential in the regulation of immunity against infection (Jiang & Chen, 2011). Classical ubiquitination is catalysed by the action of the E1, E2 and E3 enzymes, which function coordinately to covalently attach ubiquitin to protein substrates (Hershko & Ciechanover, 1998). Interference with the host ubiquitin network is critical for the success of many microorganisms that have parasitic or symbiotic relationships with eukaryotic hosts, and such interference is often achieved by virulence factors that function as deubiquitinases, E3 ubiquitin ligases (Maculins, Fiskin et al., 2016) or as ubiquitin modification enzymes (Cui et al., 2010). More than ten Dot/Icm effectors of *L. pneumophila* function to hijack host ubiquitin signaling (Qiu & Luo, 2017b). Among these, members of the SidE effector family catalyse ubiquitination by a two-step process that completely differs from the canonical three-enzyme cascade. In the reaction catalysed by SidEs, ubiquitin is first ADP-ribosylated at Arg₄₂ to produce the reaction intermediate ADPR-Ub (Qiu et al., 2016), which is utilized by a phosphodiesterase (PDE) activity also embedded in SidEs that transfers the phosphoribosylated ubiquitin to serine residues in their substrates (Bhogaraju et al., 2016, Kotewicz et al., 2017). In our efforts to identify eukaryotic proteins capable of catalyzing ubiquitination with mechanisms similar to those used by SidEs, we found that the E2 enzyme UBE2N can be modified by a ubiquitin mutant unable to be used by the canonical ubiquitination machinery. Further studies revealed that UBE2N was monoubiquitinated during *L. pneumophila* infection by the effector MavC (Lpg2147). We also demonstrate that MavC functions as a transglutaminase that catalyzes crosslinking between ubiquitin and UBE2N, leading to the inhibition of its activity in NF- κ B activation.

Results

Modification of UBE2N by a ubiquitin mutant that cannot be used by the canonical ubiquitination machinery.

To identify potential eukaryotic enzymes capable of catalyzing ubiquitination by a mechanism similar to that of SidEs, we expressed 3xHA-Ub and 3xHA-Ub-AA (the last two glycine residues were replaced with alanine residues) in HEK293T cells. Although their number was drastically reduced compared with those modified by 3xHAUb, proteins potentially modified by 3xHA-Ub-AA were detected (**Fig. 2-1, A**). We thus performed immunoprecipitation from cells expressing 3xHA-Ub-AA with HA antibody, and proteins in gels of relevant molecular weight (Mw) were identified by mass spectrometry analysis. Among the proteins identified, the E2 enzyme UBE2N important for the formation of K₆₃-type polyubiquitin chains (Hodge, Spyracopoulos et al., 2016) was seen in multiple experiments. Subsequent experiments found UBE2N to be the only protein that can be detectably modified by 3xHA-Ub-AA in HEK293T cells (**Fig. 2-1, B**).

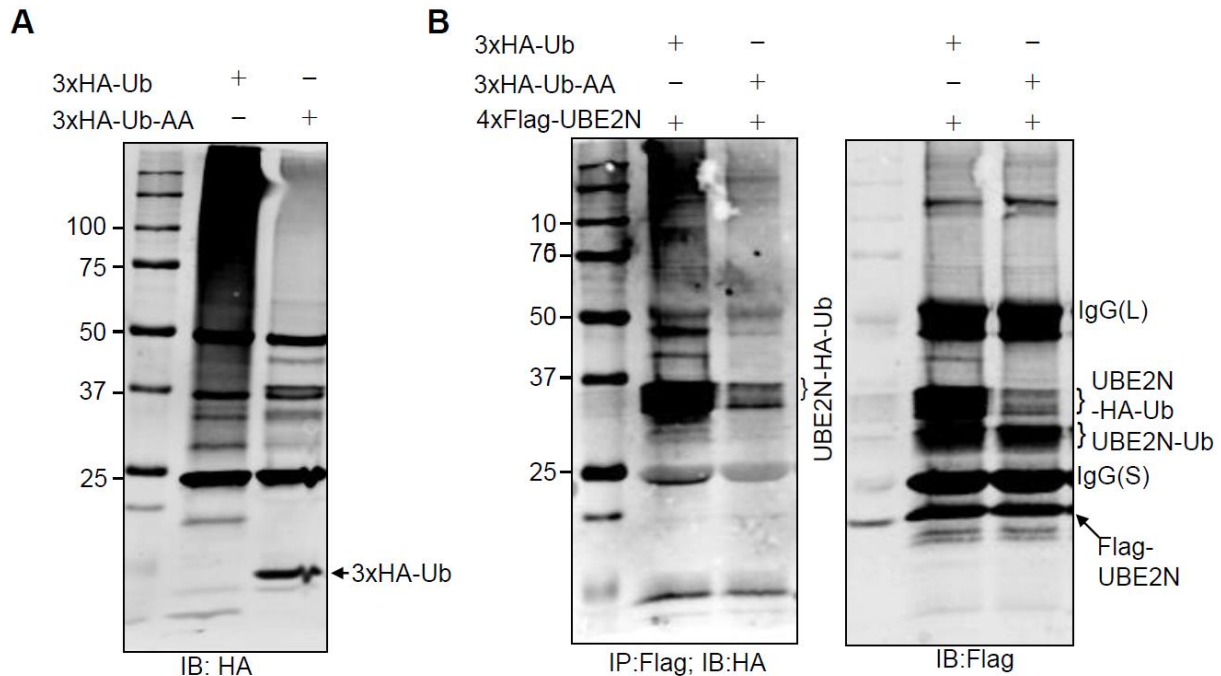


Fig. 2-1 The E2 ubiquitin conjugation enzyme UBE2N can be modified by the ubiquitin mutant Ub-AA.

A. Lysates of HEK293T cells transfected to express 3xHA tagged Ub or Ub-AA were subjected to immunoprecipitation with beads coated with an HA specific antibody and the products were probed with the HA-specific antibody. Note the presence of a few proteins between 25 and 50 kDa.

B. Lysates of HEK293T cells transfected to co-express 4xFlag-UBE2N with 3xHA-Ub or with 3xHA-Ub-AA) were subjected to immunoprecipitation with beads coated with a Flag-specific antibody, the products were probed with antibody specific for HA (left panel) or for Flag (right panel). Similar results were obtained in at least three independent experiments.

UBE2N is modified by the Dot/Icm effector MavC(Lpg2147) during *L. pneumophila* infection.

To identify the enzymes responsible for UBE2N ubiquitination with 3xHA-Ub-AA, we hypothesized that such enzymes may be induced under certain stress conditions. Clearly, the identification of such conditions would facilitate subsequent purification and characterization of the enzymes because of the potentially higher protein levels. Thus, we treated Raw264.7 cells with a variety of stresses and examined UBE2N ubiquitination. None of the tested physiochemical treatments led to a shift in Mw in UBE2N (**Fig. 2-2, A**). In these experiments, we also included samples from cells infected with two *L. pneumophila* strains. Intriguingly, we observed a Mw shift akin to monoubiquitination only in cells infected with the virulent strain (**Fig. 2-2, A**). The requirement of the Dot/Icm transporter suggests that such modification is caused by one or more of its substrates. We chose first to pursue this potential effector-induced UBE2N modification because it is technically more straightforward than identification of the mammalian proteins potentially involved in its modification.

To identify the Dot/Icm substrate(s) responsible for UBE2N modification, we took advantage of the several cluster deletion mutants of *L. pneumophila* (O'Connor et al., 2011). With the exception of strain $\Delta 5$, infection by all of other mutants caused an MW shift in UBE2N (**Fig. 2-2, B**). We thus identified the protein responsible for this modification by individually expressing effectors absent in strain $\Delta 5$ in HEK293T cells. These experiments revealed that Lpg2147 (MavC) (Huang et al., 2011) was able to cause UBE2N modification (**Fig. 2-2, C**). We thus constructed and tested strain Lp02 $\Delta mavC$ and found that infection with wildtype but not the mutant caused UBE2N modification (**Fig. 2-2, D**). Furthermore, introduction of a plasmid expressing *mavC* restored the ability of the mutant to modify UBE2N (**Fig. 2-2, D**). The level of UBE2N modification corresponds well to the expression level of MavC in bacterial strains. The relatively lower modification rates in transfected cells may be due to low transfection efficiency (**Fig. 2-2, E**). Thus, *mavC* is the only gene responsible for UBE2N modification during *L. pneumophila* infection.

In macrophages, the $\Delta mavC$ strain grew at rates indistinguishable from that of the wild-type strain (**Fig. 2-3, A**), indicating that, similar to most Dot/Icm substrates, *mavC* is not required for proficient intracellular bacterial replication in commonly used tissue culture hosts. In broth-

grown bacteria, MavC was barely detectable in the lag and early exponential growth phases (optical density at 600 nm (OD₆₀₀) of 0.05-2.2) but became highly expressed in exponential phase and continued to the post-exponential phase (OD₆₀₀ = 2.6-3.6) (**Fig. 2-3, B**), suggesting that MavC functions in the initial phase of infection.

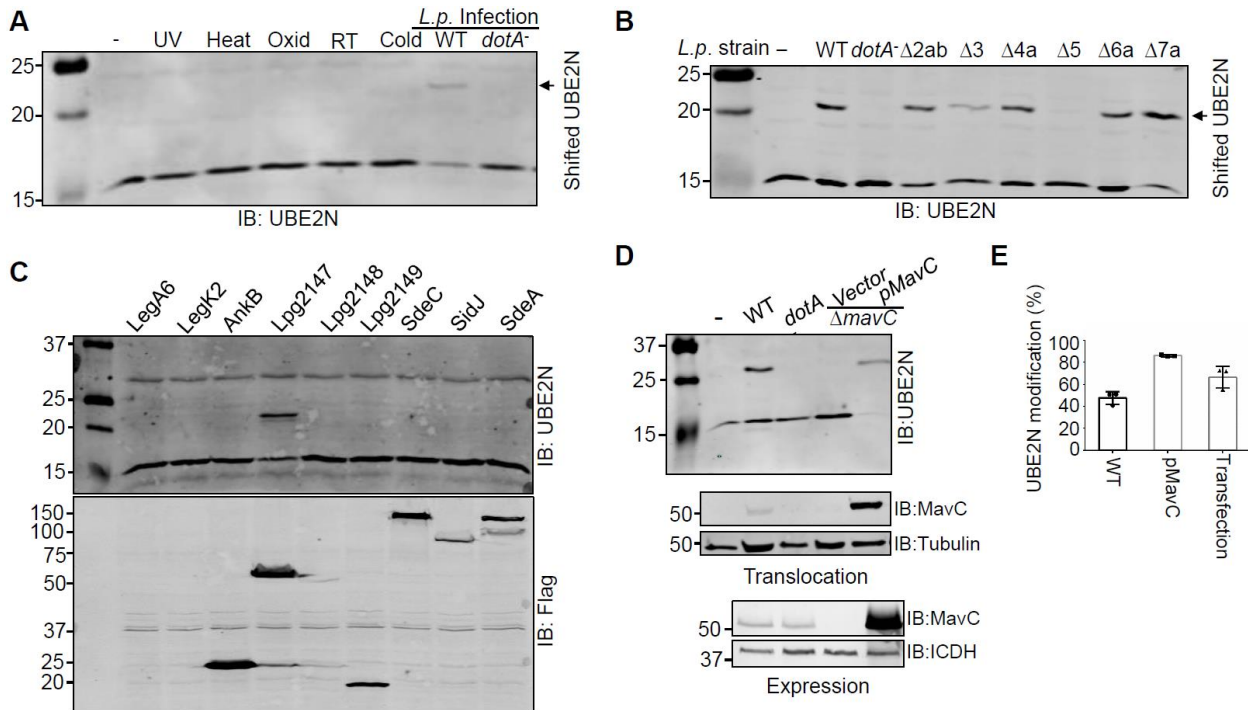


Fig. 2-2 *L. pneumophila* induces a molecular weight shift in UBE2N in a process that requires the Dot/Icm effector MavC.

A, Infection by virulent *L. pneumophila* (*L.p.*) but not several physiochemical stresses caused a Mw shift in UBE2N. Raw264.7 cells were subjected to the indicated treatments or were infected with wild-type (WT) *L. pneumophila* or its *dotA* mutant defective in the Dot/Icm type IV transporter. Total proteins resolved by SDS-PAGE were probed with a UBE2N-specific antibody. Note the detection of a protein slightly above 20 kDa in samples infected with wild-type bacteria. **B**, The gene responsible for *L. pneumophila*-induced UBE2N modification resides in the region removed from the deletion strain 5. Opsonized *L. pneumophila* were used to infect HEK293T cells transfected to express the Fc II receptor for 2 h at an MOI of 10. Total proteins separated by SDS-PAGE were probed with a UBE2N-specific antibody. Note that strain 5 cannot induce UBE2N modification. **C**, The Dot/Icm effector MavC (Lpg2147) caused UBE2N modification. A set of Dot/Icm substrates in the region missing in deletion strain 5 were individually expressed in HEK293T. The modification of UBE2N was detected by immunoblotting (top). Expression of the bacterial proteins was detected using a Flag-specific antibody (bottom). Note that expression of MavC(Lpg2147) caused UBE2N modification. **D**, MavC is the only *L. pneumophila* protein responsible for UBE2N modification. HEK293 cells infected with the indicated bacterial strains, and proteins solubilized by saponin, were probed for UBE2N (top) or for translocated MavC (middle). The expression of MavC in bacteria was also analysed (bottom). **E**, Quantitation of modified UBE2N under different experimental conditions. Blots from at least three independent experiments performed similarly were quantified by ImageJ (mean ± s.e. from three replicates). Experiments in a-d were repeated at least three times and similar results were obtained.

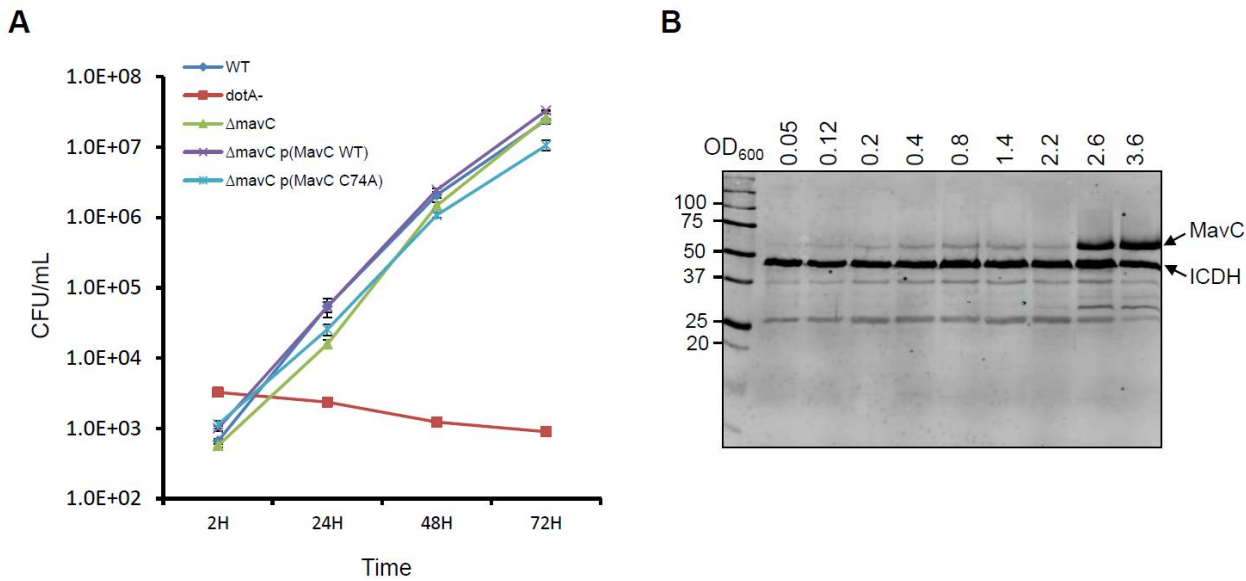


Fig.2-3 The growth phase-dependent expression of mavC and its role in intracellular growth of *L. pneumophila* in macrophages.

A. Deletion of *mavC* did not detectably affect intracellular growth of *L. pneumophila*. Raw264.7 cells were infected with the indicated bacterial strains and intracellular bacteria were determined at the indicated time points. Each strain was done in triplicate and similar results were obtained in three independent experiments. Errors were derived from three technical replicates (mean \pm s.e. from three replicates). **B.** Growth phase dependent expression of MavC. Equal amounts of cells of *L. pneumophila* strain Lp02 grown in AYE broth were withdrawn at the indicated cell density (OD_{600}) and MavC was probed. The metabolic enzyme isocitrate dehydrogenase (ICDH) was detected as loading controls. The experiments were performed independently three times with similar results.

MavC induces UBE2N ubiquitination by a mechanism that does not require the host ubiquitination machinery

Modification of UBE2N induced by MavC led to an ~10 kDa increase in its Mw, a size close to monoubiquitination (**Fig. 2-2**). To test whether it catalyzes ubiquitination, we incubated MavC, HA-Ub and 4xFlag-UBE2N with total lysates of HEK293T cells. A modified protein with a molecular weight similar to that of UBE2N-Ub was detected by HA-specific antibody (**Fig. 2-4, A**), indicating that MavC utilizes HA-Ub to modify UBE2N. Importantly, we observed indistinguishable UBE2N modification by HA-Ub in reactions containing boiled total cell lysates (**Fig. 2-4, A, rightmost lane**), suggesting that the activity of MavC may not need the host ubiquitination machinery.

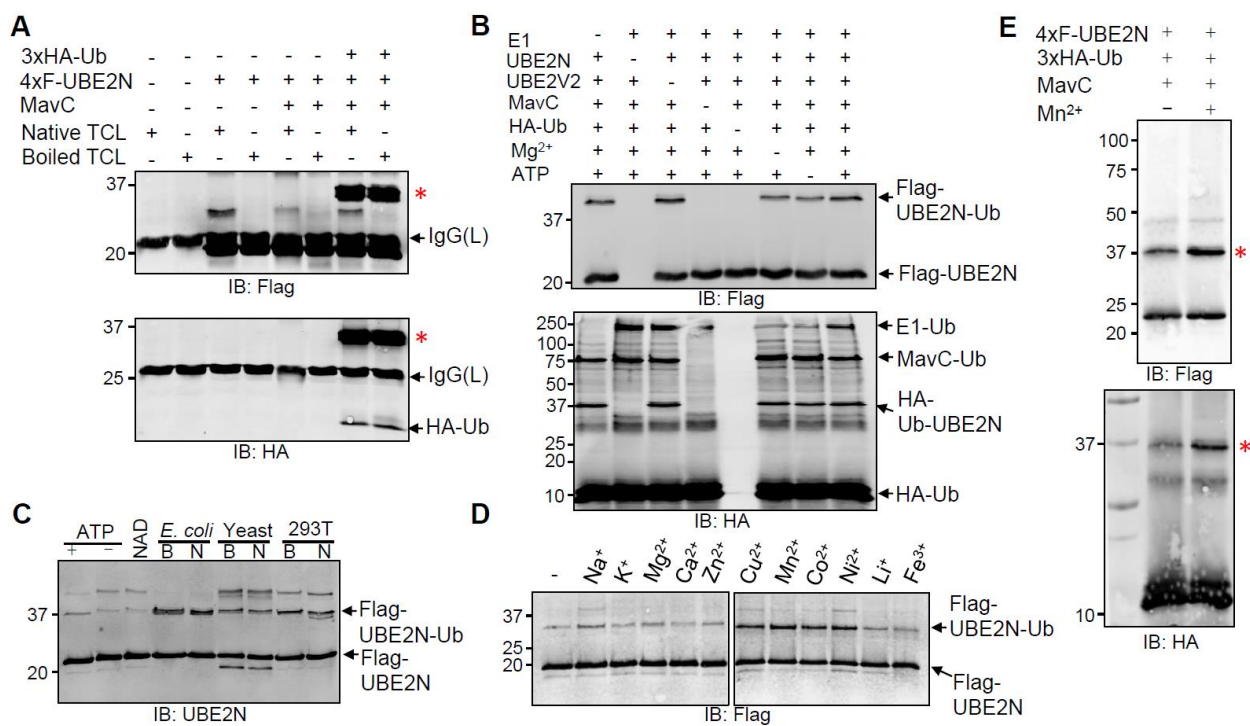
We next used biochemical assays to test the hypothesis that MavC is a ubiquitin ligase whose activity does not require components of the canonical ubiquitination reaction. To function as an E2 enzyme, UBE2N requires another protein such as UBE2V2 to form a heterodimer (Eddins, Carlile et al., 2006). In reactions that contained all the necessary components, modified UBE2N was produced (**Fig. 2-4, B, top, rightmost lane**). Unexpectedly, ubiquitination of UBE2N also occurred in reactions that did not receive the E1 enzyme (**Fig. 2-4, B, top, leftmost lane**). Such modification also occurred in reactions that did not receive Mg²⁺ or ATP (**Fig. 2-4, B, top, sixth and seventh lanes**). Importantly, self-ubiquitination occurred in MavC, again even in reactions that did not receive E1, Mg²⁺ or ATP (**Fig. 2-4, B, bottom, first, sixth and seventh lanes**). These results further suggest that MavC is capable of catalyzing ubiquitination by a mechanism that does not require components of the canonical ubiquitination machinery.

Infection with a *L. pneumophila* strain overexpressing MavC led to modification of about 80% of endogenous UBE2N (**Fig. 2-2, D**). In contrast, the rates of modification were considerably lower in reactions containing purified proteins, suggesting that MavC requires one or more cellular factors for optimal activity. The addition of ATP or NAD did not increase the modification efficiency (**Fig. 2-2, C**). Instead, lysates of prokaryotic or eukaryotic cells allowed the modification to proceed more completely and boiling treatment did not abolish such activity (**Fig. 2-2, C**). Thus, one or more heat-stable factors were required for full activity of MavC. We tested the effects of several metal ions and found that a few divalent ions including Cu²⁺, Mn²⁺, Co²⁺ and Ni²⁺ were able to enhance the activity of MavC (**Fig. 2-2, D and E**). Together, these results indicate that MavC catalyzes ubiquitination by a mechanism that does not require components of the canonical

ubiquitination machinery or even an exogenous energy source. Furthermore, its activity can be potentiated by several divalent metal ions such as Mn^{2+} and Ni^{2+} .

Fig. 2-4 MavC induces UBE2N ubiquitination independently of the canonical ubiquitination machinery.

A, MavC induces UBE2N ubiquitination. HA-Ub and Flag-UBE2N were incubated with native or boiled total cell lysates for 2 h at 37 °C. Flag-UBE2N recovered by immunoprecipitation was probed by immunoblotting with antibody specific for Flag (top) or HA (bottom). Note that UBE2N was modified by HA-Ub even in reactions containing boiled total cell lysates (eighth lane). *Modified UBE2N. **B**, MavC-induced ubiquitination of UBE2N occurred in the absence of E1, adenosine triphosphate (ATP) or Mg²⁺. A series of reactions containing the indicated components were allowed to proceed for 2 h at 37 °C. Samples resolved by SDS-PAGE were probed with Flag (top) and HA (bottom) specific antibodies, respectively. Note that ubiquitinated UBE2N was detected in samples without E1 (first lane), Mg²⁺ (sixth lane) or ATP (seventh lane). Self-ubiquitinated MavC was detected in all samples containing this protein and ubiquitin, regardless of other components required for canonical ubiquitination reaction (for example first, second, third, sixth and seventh lanes). **C**, A heat-stable compound present in cells potentiates MavC-induced UBE2N ubiquitination. ATP, nicotinamide adenine dinucleotide (NAD), boiled or native total lysates from *Escherichia coli*, yeast or HEK293T cells were added to reactions containing ubiquitin and Flag-UBE2N. Reactions were resolved by SDS-PAGE and probed with a Flag specific antibody. **D**, The activity of MavC is induced by a few divalent metal ions. The indicated metal ions were added to reactions containing ubiquitin and Flag-UBE2N at a final concentration of 5 mM. Samples resolved by SDS-PAGE after 2 h incubation at 37 °C were probed with a Flag antibody. Note that Cu²⁺, Mn²⁺, Co²⁺ or Ni²⁺ enhanced the activity of MavC. **E**, The metal ion Mn²⁺ potentiates the activity of MavC. Reactions containing the indicated components were established and the modification of UBE2N was probed by the formation of higher-molecular-weight conjugate (red *) detected with antibody specific for Flag (top) or HA (bottom). *Modified UBE2N. Experiments in **A-E** were repeated at least three times and similar results were obtained. MavC is a transglutaminase that catalyses crosslinking between ubiquitin and UBE2N.



MavC is a transglutaminase that catalyzes crosslinking between ubiquitin and UBE2N.

We analyzed the biochemical mechanism underlying MavC-mediated ubiquitination by determining the sites of ubiquitination on UBE2N and the chemical bond that links these two molecules. The protein band corresponding to modified UBE2N was analyzed by liquid chromatography-tandem mass spectrometry (LC-MS/MS) (**Fig. 2-5, A**), which led to the identification of two UBE2N peptides, -I₈₆CLDILKDK₉₄ and -D₉₃KWSPALQIR₁₀₂, which were crosslinked to the same ubiquitin fragment, -E₃₄GIPPDQQR₄₀- (**Fig. 2-5, B and C**). The fragmentation pattern and the fact that trypsin digestion did not occur at Lys₉₂ and Lys₉₄ in these UBE2N peptides suggest that the linkage is through a lysine residue. The tandem mass spectra also showed that ubiquitin is linked to the substrate through its Gln₄₀ residue (**Fig. 2-5, B and C**). By the mass difference, Gln₄₀ of ubiquitin was linked to a lysine residue in UBE2N by eliminating an ammonia molecule, leading to the formation of an N^e-(γ-glutamyl)lysine isopeptide bond between Gln₄₀ on ubiquitin and Lys₉₂ or Lys₉₄ of UBE2N (**Fig. 2-5, B and C**).

The chemical linkage that bridges ubiquitin and UBE2N resembles those formed by transglutaminases (TGases), which often catalyze transamidation between the γ-carboxamide group of a glutamine residue in one protein and the ε-amino group of a lysine residue in another protein (Lorand & Graham, 2003). The reaction catalyzed by TGases requires a Cys-His-Asp catalytic triad in which the Cys residue is involved in the formation of a γ-glutamylthioester with the Gln-containing protein (ubiquitin here) (**Fig. 2-5, D**) (Keillor, Clouthier et al., 2014). To identify the Cys residue critical for the activity of MavC, we constructed substitution mutants lacking each of its six Cys residues and examined their activity in UBE2N ubiquitination. Only mutation in Cys₇₄ abolished the ability of MavC to induce UBE2N ubiquitination (**Fig. 2-5, E**).

We confirmed the modification sites on UBE2N by testing mutants with substitutions in Lys₉₂ or Lys₉₄. Whereas incubation of the K94A mutant with MavC and ubiquitin still led to robust modification, ubiquitination of the K92A mutant was largely abolished and no modification was detected in reaction containing UBE2NK92AK94A (**Fig. 2-5, F**). Mutation in C87, the residue important for UBE2N's role as an E2 enzyme (Eddins et al., 2006), did not affect MavC-mediated modification (**Fig. 2-5, F**). Thus, the transglutamination reaction catalyzed by MavC links ubiquitin to Lys₉₂ or Lys₉₄ of UBE2N, of which Lys₉₂ is the major modification site.

We next examined the role of the catalytic cysteine in ubiquitination of UBE2N during *L. pneumophila* infection. Unlike the *ΔmavC* mutant expressing MavC, expression of MavC_{C74A} did

not cause UBE2N modification, despite the mutant protein being properly expressed and translocated into host cells (**Fig. 2-5, G**).

We also determined the ability of MavC to modify several structurally similar E2s (harboring Cys₈₇ and Lys₉₂, not necessarily at the 87th and 92th residue, respectively) (**Fig. 2-6, A**). None of these E2s, including UBE2E2, 2K and 2S, was detectably ubiquitinated by MavC in either biochemical reactions or in cells infected by *L. pneumophila* (**Fig. 2-6, B and C**). These results suggest that MavC specifically modifies UBE2N. The involvement of Gln₄₀ in the formation of the covalent bond suggests that residues important for ubiquitination catalyzed by the canonical mechanism are not required for MavC-induced UBE2N modification. Indeed, each of the lysine mutants (lacking one, more or all of the lysine residues) was active at levels comparable to wildtype ubiquitin, as was the mutant in which the last two glycine residues were replaced with alanine (**Fig. 2-7**).

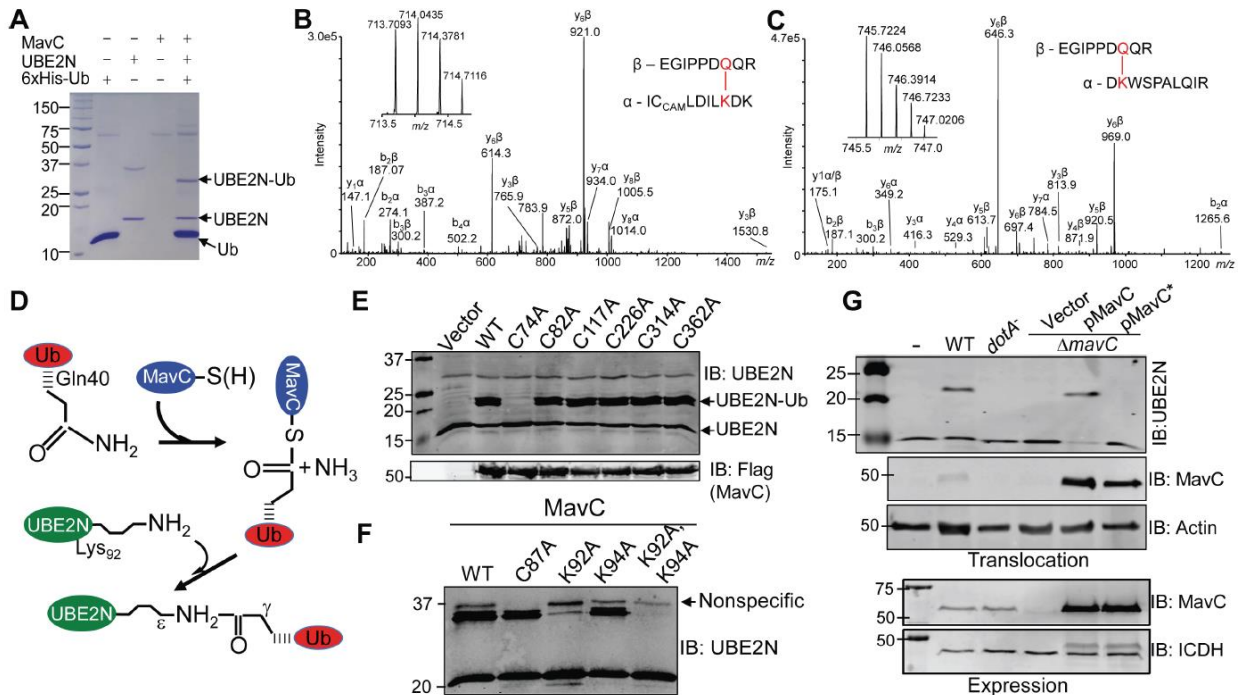


Fig. 2-5 MavC catalyzes ubiquitination of UBE2N by transglutamination.

A, MavC-induced UBE2N ubiquitination detected by Coomassie staining. Reactions containing the indicated components were allowed to proceed for 2 h and samples resolved by SDS-PAGE were detected by staining. **B,C**, MavC catalyzes the formation of an isopeptide bond between the Gln₄₀ of ubiquitin and the Lys₉₂ and Lys₉₄ of UBE2N. The ubiquitinated UBE2N shown in **A** was subjected to mass spectrometric analysis. Tandem mass spectra are shown for the ubiquitin peptide -E₃₄GIPPD**Q**QR₄₀- crosslinked with UBE2N peptide -I₈₆CLDIL**K**DK₉₄- (**B**) or -DK₉₄WSPAL**Q**IR₁₀₂- (**C**). Insets: high-resolution measurements of parent ions, which correspond to mass errors of 0.8 (**B**) and 0.4 ppm (**C**) compared to the calculated mass. CAM, carbamidomethylation. **D**, A predicted reaction scheme of MavC-mediated protein crosslinking by transglutamination. A nucleophilic Cys residue on MavC attacks Gln₄₀, a γ -glutamyl residue in ubiquitin, to form a thioester intermediate. The acylated MavC then reacts with the amine donor from the ε-lysine in UBE2N to form an intermolecular isopeptide bond. **E**, Cys₇₄ is essential for the activity of MavC. Flag-tagged MavC or its mutants harbouring mutations in each of its six Cys residues were expressed in HEK293T cells. The modification of UBE2N was probed by immunoblotting with a UBE2N-specific antibody (top). The Cys₇₄Ala mutation did not affect the expression and stability of MavC (bottom). **F**, Lys₉₂ is the major ubiquitination site in UBE2N. 4xFlag-UBE2N or its mutants were incubated with ubiquitin and MavC. The formation of Ub-UBE2N was detected by immunoblotting. Note that the UBE2N_{K92A} mutant has largely lost the ability to be modified (third lane). **G**, Cys₇₄ of MavC is essential for UBE2N ubiquitination induced by *L. pneumophila*. HEK293 cells were infected with the indicated bacterial strains for 2 h and the modification of UBE2N was probed by immunoblotting. The expression (bottom) and translocation (middle) of MavC and its mutant were probed with MavC-specific antibodies. Experiments in **A-C** and **E-G** were repeated at least three times and similar results were obtained.

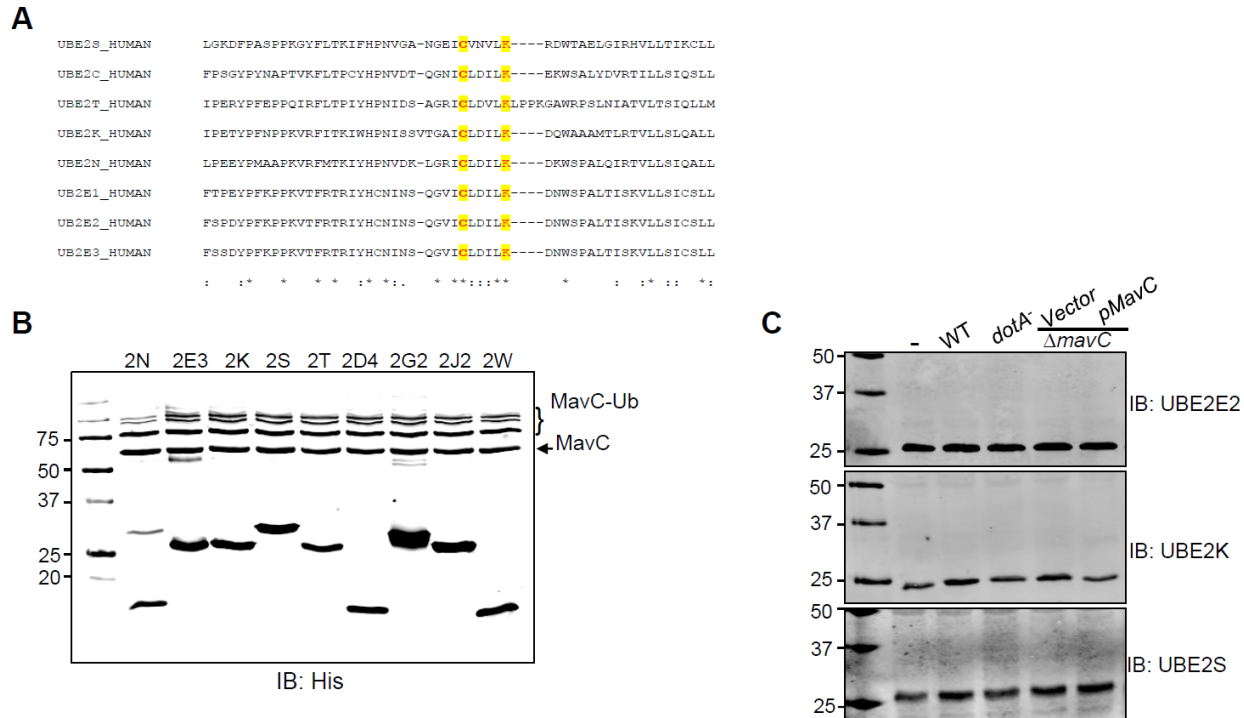


Fig. 2-6 MavC is specific for UBE2N.

A. Sequence alignment of the region harboring the active cysteine residue and the adjacent lysine residue of a series of E2 enzymes. The cysteine and lysine residues were highlighted in yellow background. **B.** The modification of a series of E2 enzymes by MavC. Reactions containing His6-tagged UBE2N or the indicated E2 enzymes were established. Ubiquitin modification was assessed by a shift in molecular weight after probing with a His6-specific antibody. **c.** Infection by *L. pneumophila* did not cause modification of three E2 enzymes similar to UBE2N in the active domain. Raw264.7 cells were infected with the indicated bacterial strains and the potential modification was probed by immunoblotting with antibodies specific for each enzyme. The experiments in **B** and **C** were performed independently three times with similar results.

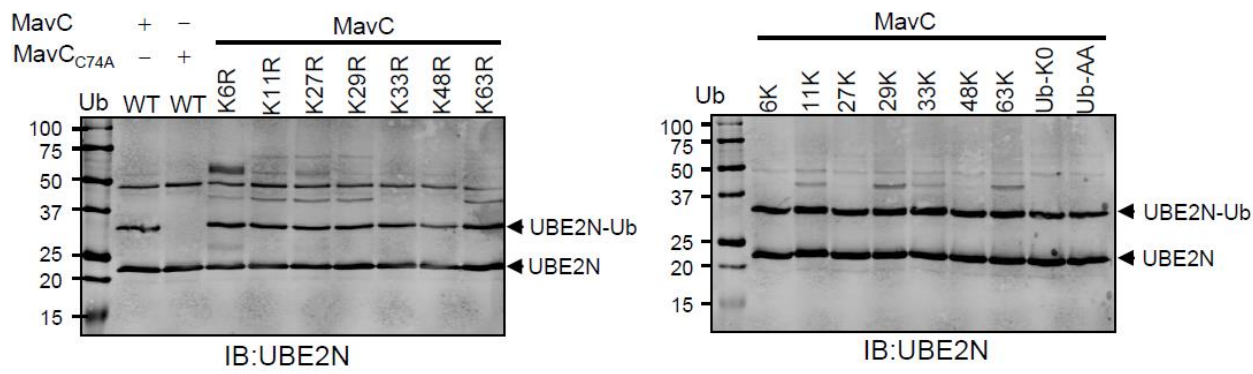


Fig. 2-7 The reactivity of ubiquitin mutants in MavC-induced ubiquitination of UBE2N.

Ubiquitin and its mutants were incubated with MavC and UBE2N in the presence of 5 mM Mn²⁺. Ub-UBE2N was detected by the formation of UBE2N species with higher molecular weight. Note that none of the mutations affected the formation of Ub-UBE2N. The symbol for single lysine ubiquitin mutants in the right panel indicates derivatives that harbor only the indicated lysine residue. For example, K6 is a mutant that contains only the 6th lysine residue. Ub-K0 is the mutant without any lysine whereas Ub-AA is the mutant in which the two glycine residues in its carboxyl were replaced with alanine. The experiments were performed independently three times with similar results.

MavC possesses deamidation activity against ubiquitin

In the absence of a suitable amine donor, the γ -glutamylthioester formed between the TGase and the substrate (ubiquitin here) can be hydrolysed to a free glutamate residue, which corresponds to a net deamidation of the substrate (Klock & Khosla, 2012). We thus examined the product of the reaction containing MavC and ubiquitin. Incubation of ubiquitin with MavC altered the mobility of ubiquitin in a way similar to the product produced by bacterial ubiquitin deamidases (Cui et al., 2010) (**Fig. 2-8, A**). Expectedly, deamidation by MavC required Cys74, a residue critical for the transglutamination activity (**Fig. 2-8, C**). Unlike Cif and CHBP (Cui et al., 2010), MavC does not detectably attack NEDD8, indicative of substrate specificity (**Fig. 2-8, A**). In mass spectrometry analysis, deamidation can be easily misassigned by automated peptide identification algorithms with the ^{13}C isotope of peptides because they differ from each other by only 0.019 Da. Yet, the high-resolution mass spectrometry analysis revealed a peak at m/z 520.7531, which is closer to the deamidated ($\delta = 1.7$ ppm) than the ^{13}C isotope ($\delta = 38.4$ ppm) mass of the ubiquitin peptide -E₃₄GIPPDQQR₄₀- (**Fig. 2-8, B**). Furthermore, only trace amounts of the unmodified peptide were detected at m/z 520.2608 in a series of reactions containing MavC and different amounts of ubiquitin. After 1 h incubation, modified ubiquitin became detectable in reactions in which the ratio between ubiquitin and MavC is 64 and the modification was almost complete when this ratio was 16 (**Fig. 2-8, C**). Thus, similar to other transglutaminases, MavC catalyzes a deamidation reaction on ubiquitin in the absence of UBE2N.

The observation that Gln40 of ubiquitin provided the side chain required for ubiquitination predicts that a mutant with a substitution mutation in this residue can no longer be used in the reaction. Indeed, UBE2N cannot be modified by ubiquitin Q40E (**Fig. 2-8, D**). Thus, similar to canonical transglutaminases from eukaryotic cells, MavC deamidates the protein that provides the glutamine residue (Eckert, Kaartinen et al., 2014).

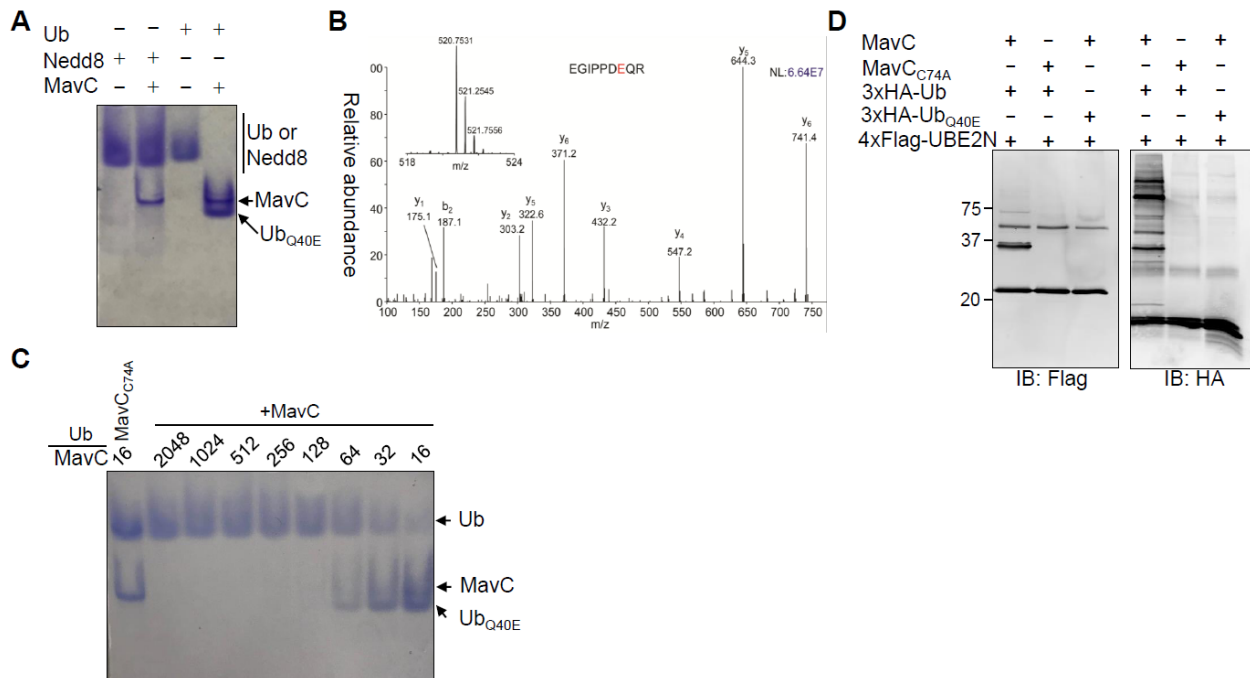


Fig. 2-8 MavC displays a ubiquitin-specific deamidation activity.

A. MavC altered the mobility of ubiquitin. Ubiquitin or NEDD8 was incubated with MavC or its MavC_{C74A} mutant and reaction products were separated in native polyacrylamide gels and the proteins were detected by Coomassie brilliant blue staining. Note that ubiquitin treated with wild type MavC migrated faster in the gel, indicating a difference in its charging status (last lane). **B.** MavC catalyzes deamidation on Gln40 of ubiquitin. Tandem mass spectrum of the ubiquitin peptide -E₃₄GIPPD**Q**QR₄₀-, which revealed deamidation on Gln40. The insert shows the high-resolution measurement of parent ion, which correspond to a mass error of 1.7 parts per million compared to the calculate mass of the deamidated peptide. **C.** Deamidation activity of MavC in reactions with different enzyme to substrate ratios. Reactions containing ubiquitin, and MavC or MavC_{C74A} mixed at the indicated molar ratios were allowed to proceed for 1 h at 37°C. Deamidated ubiquitin was detected by Coomassie staining. Note that the activity became detectable when the ratio between ubiquitin and MavC is 64. **D.** Gln40 in ubiquitin is essential for UBE2N modification. A series of reactions containing the indicated components were established in the presence of Mn²⁺. The formation of Ub-UBE2N indicated by an MW shift was detected by immunoblotting with antibodies specific for Flag (left panel) and HA (right panel). Note that ubiquitin Q40E did not react with UBE2N in reactions containing MavC. The experiments in each panel were performed independently three times with similar results.

Transglutamination is the dominant activity of MavC in reactions containing UBE2N and ubiquitin

We examined the catalytic activity of MavC through a series of reactions in which UBE2N and MavC were added at different molar ratios. Under our experimental conditions, the modification of UBE2N by MavC was still readily detectable within 1 h when the molar ratio between MavC and UBE2N was as low as 1:1,900, and approximately 50% of UBE2N was modified when the ratio was 1:120 (**Fig. 2-9, A**). To examine which activity is dominant, we established reactions in which the molar ratios of MavC to UBE2N and ubiquitin were 60 and 1,024, respectively. A portion of the reaction was withdrawn at different time points after adding MavC to analyse the extent of UBE2N modification and ubiquitin deamidation. Ubiquitinated UBE2N became detectable right after (0 min) the addition of MavC and peaked at 20 min when ~50% of the protein was modified (**Fig. 2-9, B, left**). In contrast, deamidated ubiquitin was barely detectable even after the reaction had proceeded for 2 h (**Fig. 2-9, B, right**). Deamidated ubiquitin can be detected in cells transfected to express MavC but not MavCC_{74A} (**Fig. 2-10, A and B**); it is also detectable in cells infected with a *L. pneumophila* strain overexpressing MavC but not with wild-type strain (**Fig. 2-10, C and D**), suggesting that the deamidase activity associated with MavC becomes detectable only when the protein level was artificially increased. Thus, MavC is highly active against UBE2N and transglutamination is its dominant activity.

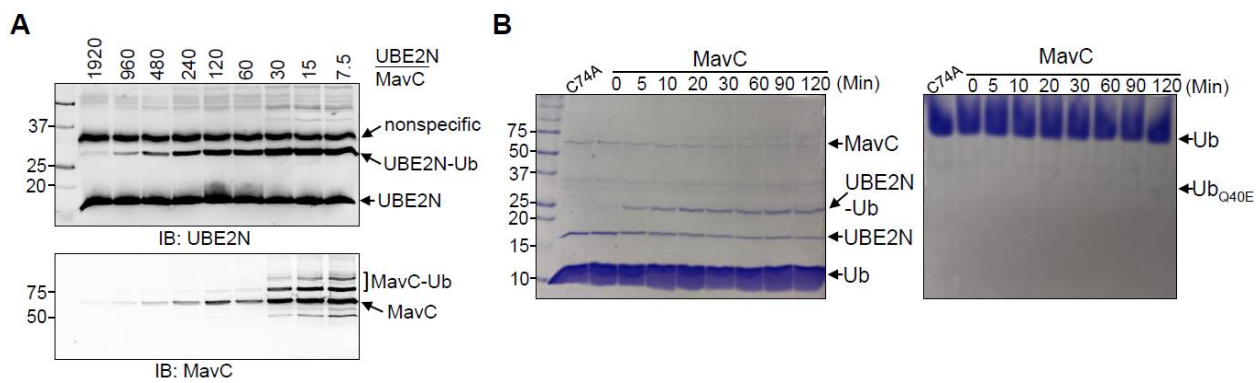


Fig. 2-9 Characteristics of MavC as transglutaminase and ubiquitin deamidase.

A, Dose-dependent modification of UBE2N by MavC. A series of reactions containing UBE2N and MavC at the indicated molar ratios were established and the reactions were allowed to proceed for 1 h before probing for the modified proteins (top). MavC was also detected (bottom). **B**, Transglutamination occurs faster than deamidation. A series of reactions with a 1:60 molar ratio for MavC and UBE2N were allowed to proceed for the indicated time durations. Modification was detected by Coomassie staining. Note that Ub-UBE2N was detectable immediately after adding MavC (0 min, left) and deamidated ubiquitin was barely detectable after 120 min incubation (right). Experiments in all panels were repeated at least three times and similar results were obtained.

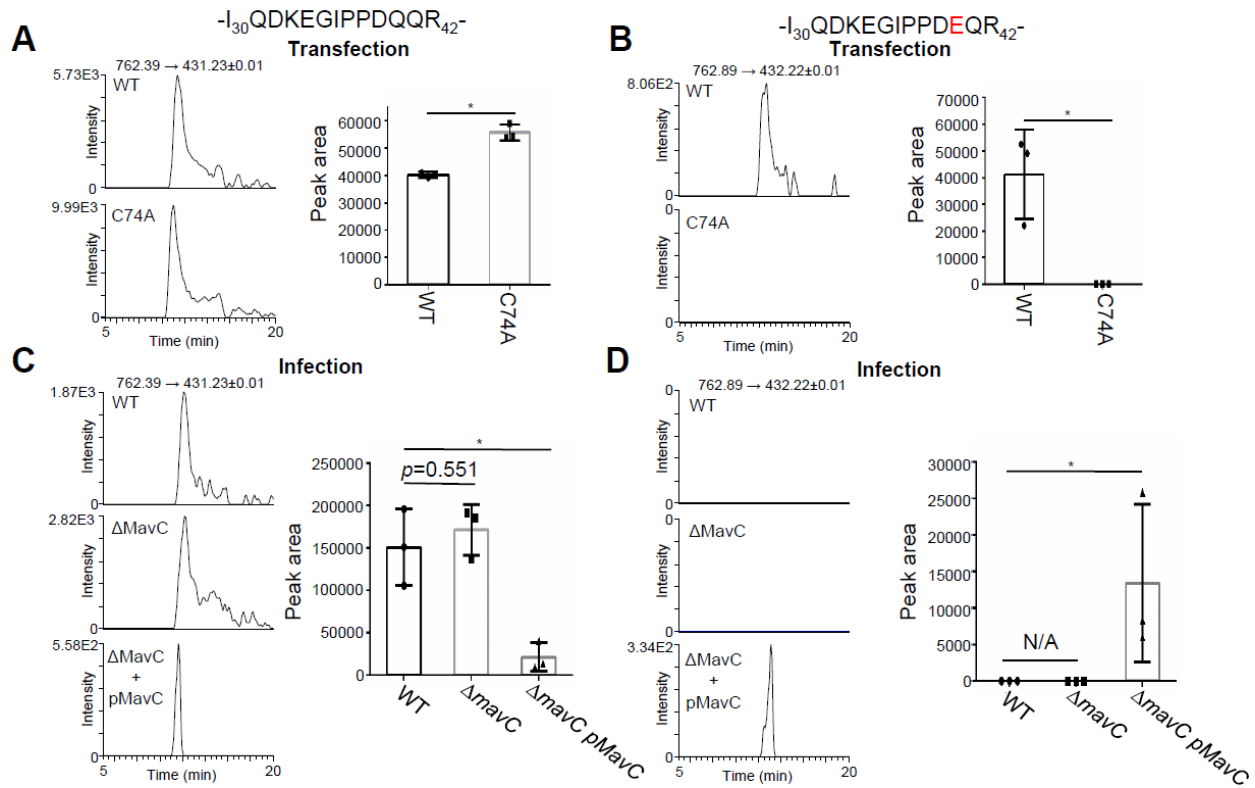


Fig. 2-10 Analysis of ubiquitin deamidation in cells by parallel-reaction monitoring (PRM) mass spectrometry.

A-B. PRM quantification of unmodified (**A**) and deamidated (**B**) ubiquitin in cells transfected with wild-type (WT) and mutant (C74A) *mavC* gene. **C-D.** PRM quantification of unmodified (**C**) and deamidated (**D**) ubiquitin in cells infected with wild-type (WT), mutant lacking the *mavC* gene ($\Delta mavC$) and complemented with a plasmid ($\Delta mavC + pMavC$). Left panels in **A** and **C** showed the extracted-ion chromatograms of unmodified peptide IQDKEGIPPDQQR (m/z 762.39) targeting fragment y3 (m/z 431.23), whereas the right panels showed the quantification of these peaks (mean \pm s.e. from three biological replicates). Left panels in **B** and **D** showed the extracted ion chromatograms of the deamidated peptide IQDKEGIPPDDEQR (m/z 762.89) targeting fragment y3 (m/z 432.22), whereas the right panels showed the quantification of these peaks (mean \pm s.e. from three biological replicates). *, p<0.05. N/A, not applicable since the values for all 3 replicates are 0, not able to calculate. Results shown are from three independent transfection or infected samples. Statistical analysis was performed with Two sided, T-test, and no adjustment was made.

Ubiquitination of UBE2N by MavC abolished its E2 activity

UBE2N forms heterodimers with proteins such as UBE2V1 and UBE2V2 to function as an E2 that catalyzes the elongation of K₆₃-type ubiquitin chains(Eddins et al., 2006), which regulate multiple cellular processes(Chen, 2005). Inclusion of MavC, but not MavC_{C74A}, in reactions containing HA-Ub, the UBE2N-UBE2V2 complex and the E3 enzyme TRAF6 drastically reduced the production of polyubiquitin chains (**Fig. 2-11, A**). The loss of E2 activity was equally apparent when purified UNE2N-Ub was used in reactions (**Fig. 2-11, B**).

MavC dampens the NF-κB pathway in the early phase of *L. pneumophila* infection.

The importance of K₆₃-type polyubiquitin chains in NF-κB activation prompted us to examine the levels of IκBα in Raw264.7 cells infected with wild-type *L. pneumophila* and the *ΔmavC* mutant. Infections by both strains caused a rapid decrease in IκBα , which, after reaching the lowest point at 30 min post-infection, began to recover. Importantly, this decrease occurred significantly faster in infections using the *ΔmavC* mutant (**Fig. 2-11, C**). The recovery of IκBα in cells infected with the mutant was also slower (**Fig. 2-11, C**). Furthermore, the decrease of cellular IκBα caused by *mavC* deletion can be restored by expressing MavC but not the C74A mutant (**Fig. 2-11, D**). Notably, IκBα in cells infected with the complementation strain overexpressing MavC accumulated at significantly higher levels than those infected with wild-type bacteria (**Fig. 2-11, D**).

In line with the above results, ectopic expression of *mavC* attenuated NF-κB activation in response to multiple distinct stimuli. The activation of NF-κB by both tumour necrosis factor-α (TNF-α) and phorbol myristate acetate (PMA) was inhibited in cells expressing MavC but not MavC_{C74A} (**Fig. 2-12, A and B**). Similarly, NF-κB activation induced by ectopic expression of Nod1, Myd88, TRAF6 and Bcl10(Liu, Fitzgerald et al., 2008, Sanada, Kim et al., 2012, Zhou, Wertz et al., 2004) was inhibited by MavC (**Fig. 2-12, C-F**).

The observation that ubiquitination of UBE2N inhibited NF-κB activation predicts that cells expressing UBE2N_{K92A} will be resistant to MavC. Indeed, NF-κB activation was not affected by MavC in cells expressing UBE2N_{K92A}(**Fig. 2-13, A**). Consistent with this observation, MavC cannot inhibit the activation induced by overexpressing p65 (**Fig. 2-13, B**). We also compared MavC to YopJ and Cif, which inhibit NF-κB activation by IKKβ acetylation and ubiquitin

deamidation, respectively(Cui et al., 2010, Mukherjee, Keitany et al., 2006). These proteins exerted similar inhibitory effects (**Fig. 2-13, C**). Yet, whereas IKK β or TAK1/TAB1 suppressed the inhibitory effects caused by MavC, neither of them suppressed the inhibition imposed by Cif (**Fig. 2-13, D and E**). Together, these results indicate that ubiquitination of UBE2N by MavC is responsible for the inhibition of NF- κ B activation.

The inhibitory effects of MavC predict that its expression will lead to the sequestration of p65 in the cytosol on stimulation. Indeed, in cells expressing MavC, TNF- α treatment did not cause p65 nuclear translocation (**Fig. 2-14**). In contrast, in cells expressing the MavCC74A mutant, TNF- α stimulation led to p65 nucleus localization in almost every cell (**Fig. 2-14**). Similarly, p65 nucleus translocation occurred in ~75% of the cells infected with strain *ΔmavC*, which was significantly higher than those infected with wild-type bacteria (**Fig. 2-15**). Notably, infections with the *ΔmavC* strain overexpressing MavC reduced nucleus translocation results indicate that MavC regulates host immunity by interfering with NF- κ B activation during *L. pneumophila* infection. of p65 to ~20% (**Fig. 2-15**), which further supports its inhibitory role in NF- κ B activation. Taken together, these results indicate that MavC regulates host immunity by interfering with NF- κ B activation during *L. pneumophila* infection.

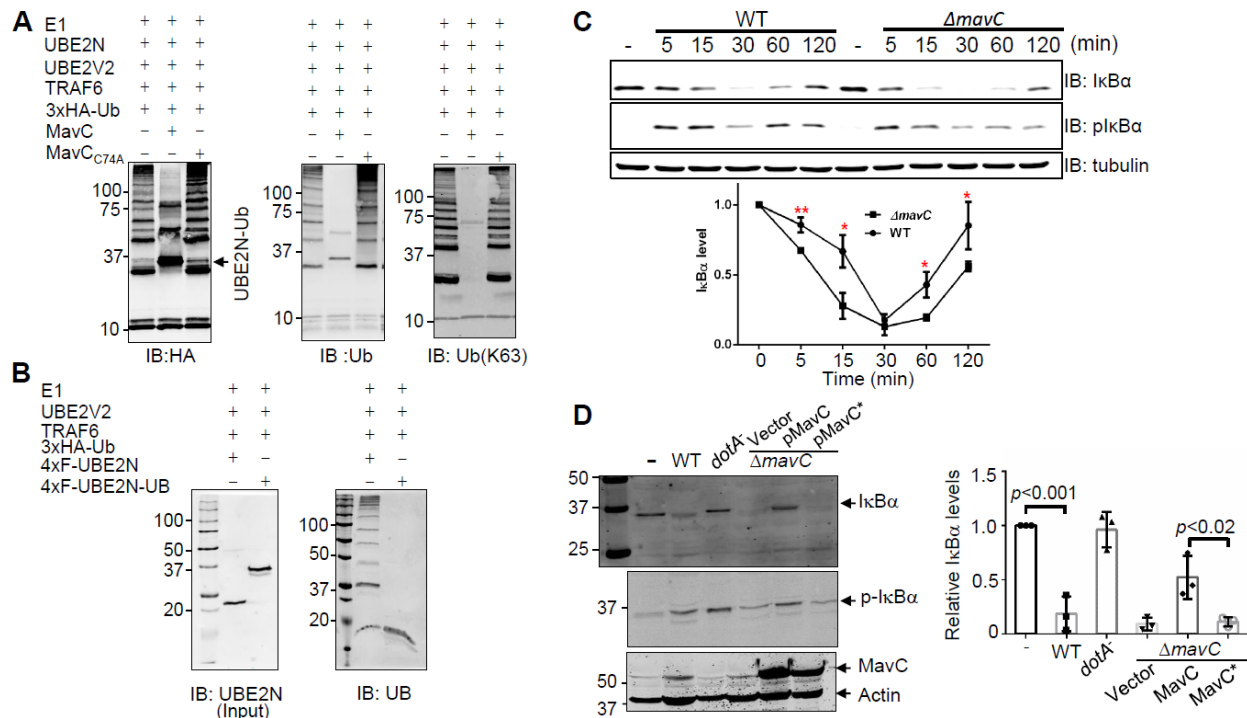


Fig. 2-11 Effects of MavC on UBE2N activity and on NF-κB activation during *L. pneumophila* infection.

A, MavC blocks the formation of K₆₃ polyubiquitin chains. Reactions containing the indicated components were allowed to proceed for 10 min at 37°C. UBE2N was preincubated with MavC or MavC_{C74A} and ubiquitin for 4 h at 37°C. Samples resolved by SDS-PAGE were probed with antibody specific for HA (left), ubiquitin (middle) or K₆₃-type linkage (right). Note that few polyubiquitin chains were detected in reactions containing MavC. **B**, Ubiquitinated UBE2N is inactive. Purified Ub-UBE2N or its native form was incubated in reactions as described in **A** and the formation of polyubiquitin chains was detected with a ubiquitin-specific antibody (right). The amount of UBE2N and Ub-UBE2N used in the reactions was also probed (left). **C**, Kinetics of IκBα level in cells infected with wild-type or the *ΔmavC* mutant of *L. pneumophila*. Raw264.7 cells infected with the indicated bacterial strains at an MOI of 5 were probed for IκBα or p IκBα . Tubulin was probed as a loading control. IκBα levels were quantitated from three independent experiments (bottom) and the values were expressed as ratios of uninfected cells set at 1.0. *P < 0.05; **P < 0.01. Note the decrease of IκBα in the first 30 min of infection occurred faster in cells infected with the MavC-deficient mutant than wild-type. **D**, Deletion of *mavC* led to reduction of IκBα in infected cells. Raw264.7 cells infected with the indicated bacterial strains for 1 h at an MOI of 10 were probed for IκBα by immunoblotting. Phosphorylated IκBα (p IκBα) and translocated MavC were also probed. Relative levels of IκBα (bottom) were the ratios between the intensity of the bands from uninfected cells and those of the indicated samples. Experiments in all panels were repeated at least three times and similar results were obtained. Quantitation shown was from three independent experiments (mean ± s.e. from three replicates). Statistical analysis used in c and d was by two-sided t-test, and no adjustment was made.

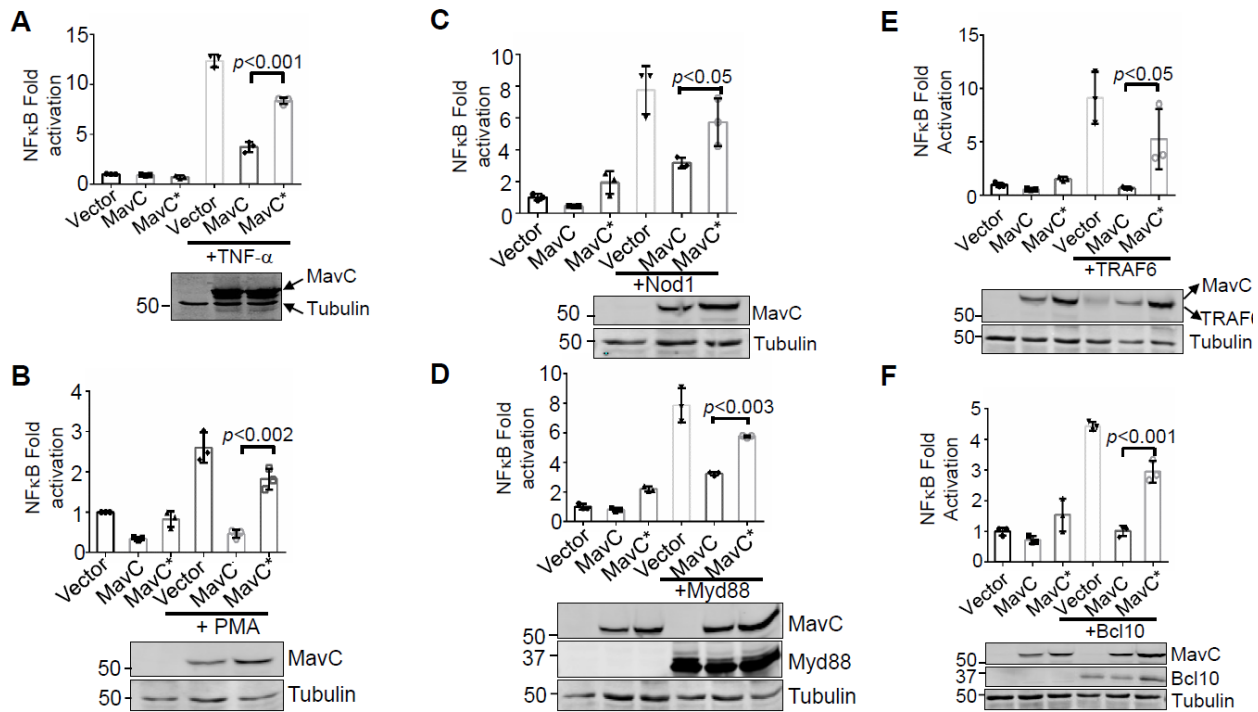


Fig. 2-12 MavC Inhibits NF-κB activation induced by different signals.

HEK293T cells were transfected with combinations of plasmids expressing a luciferase reporter responsive to NF-κB and Flag-MavC or its mutant. A plasmid expressing Renilla luciferase was co-transfected as an internal control. Transfected cells were either treated with TNF- α (**A**) or phorbol myristate acetate (PMA) (**B**) or were co-transfected to overexpress stimulator Nod1 (**C**), Myd88 (**D**), TRAF6 (**E**) or Bcl10 (**F**). NF-κB activity was determined by measuring luciferase activity. Fold activation was the ratio of luciferase activity between the indicated samples and samples received empty vector without any treatment. The expression of MavC, its mutant or the stimulator protein was probed in lysates of transfected cells and the blots shown are representatives of at least three independent experiments. Tubulin was detected as a loading control. Note that TRAF6 was also Flag-tagged and its MW is similar to that of MavC (**E**). In each case, Luciferase activity from triplicates was used to calculate the mean and s.e. values (mean \pm s.e. from three replicates), and statistical analysis was performed by Two sided, T-test, and no adjustment was made. Three independent experiments were done in triplicates with similar results.

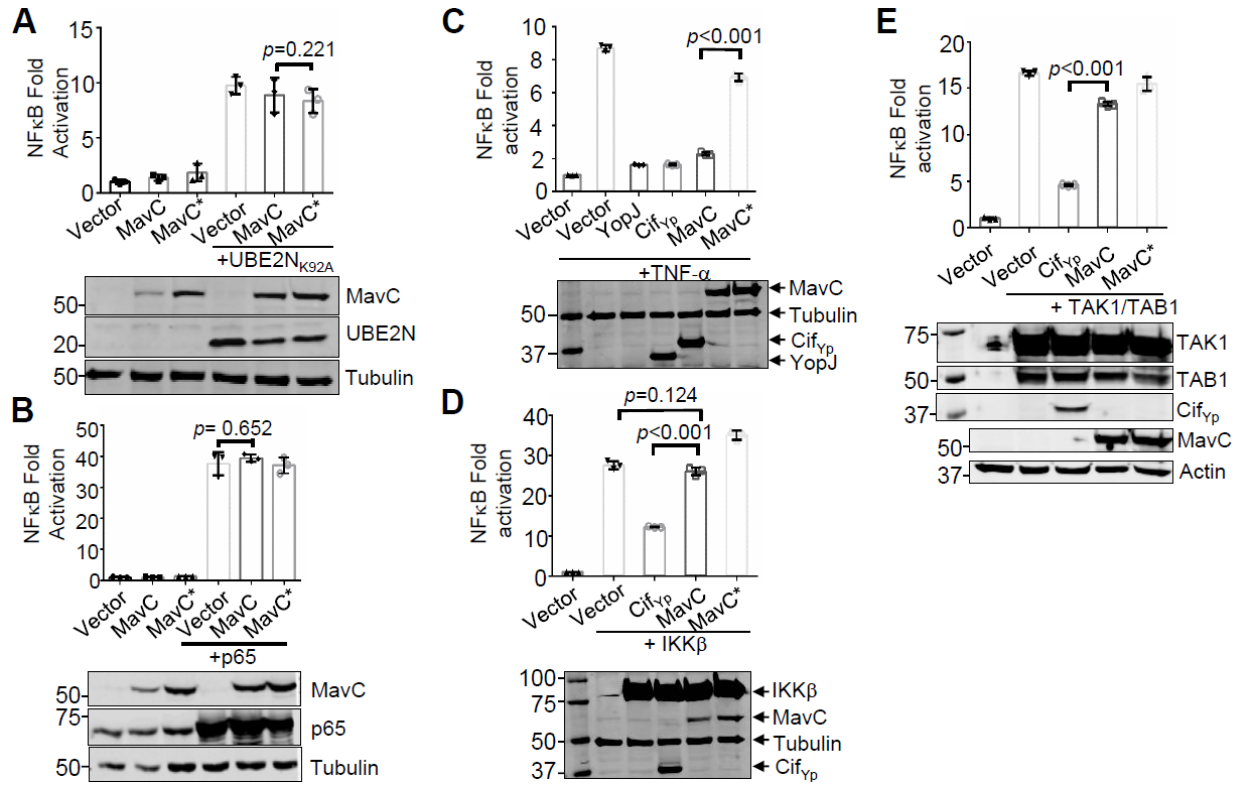


Fig. 2-13 Effects of MavC on NF-κB activation in cells overexpressing various relevant proteins.

A, UBE2N_{K92A} suppresses the inhibition caused by MavC. HEK293T cells were transfected to express UBE2N_{K92A} together with MavC or its mutant, and NF-κB activity was measured by luciferase activity. The expression of UBE2N_{K92A} and MavC was probed by immunoblotting with specific antibodies. Tubulin was detected as a loading control. **B**, MavC cannot suppress the induction of NF-κB by p65 overexpression. Cells were transfected to co-express UBE2N_{K92A} and MavC or its mutant, and NF-κB activity and protein expression were examined as described in A. **C**, The inhibitory effect of MavC in NF-κB activation is comparable to that of YopJ or Cif. Cells transfected to express the indicated proteins were treated with TNF-α, and NF-κB activity was measured by luciferase activity. **D,E**, MavC cannot inhibit NF-κB activation induced by ectopic expression of IKKβ (**D**) or TAK1/TAB1 (**E**). For NF-κB activity, in each case, similar results were obtained from at least three independent experiments carried out in triplicate (mean ± s.e. from three replicates). The immunoblots shown are one representative from at least three experiments. The expression of relevant proteins was probed by immunoblotting with specific antibodies against the protein of interest or an affinity tag, and tubulin or actin was probed as a loading control. Statistical analysis was performed by two-sided t-test, and no adjustment was made.

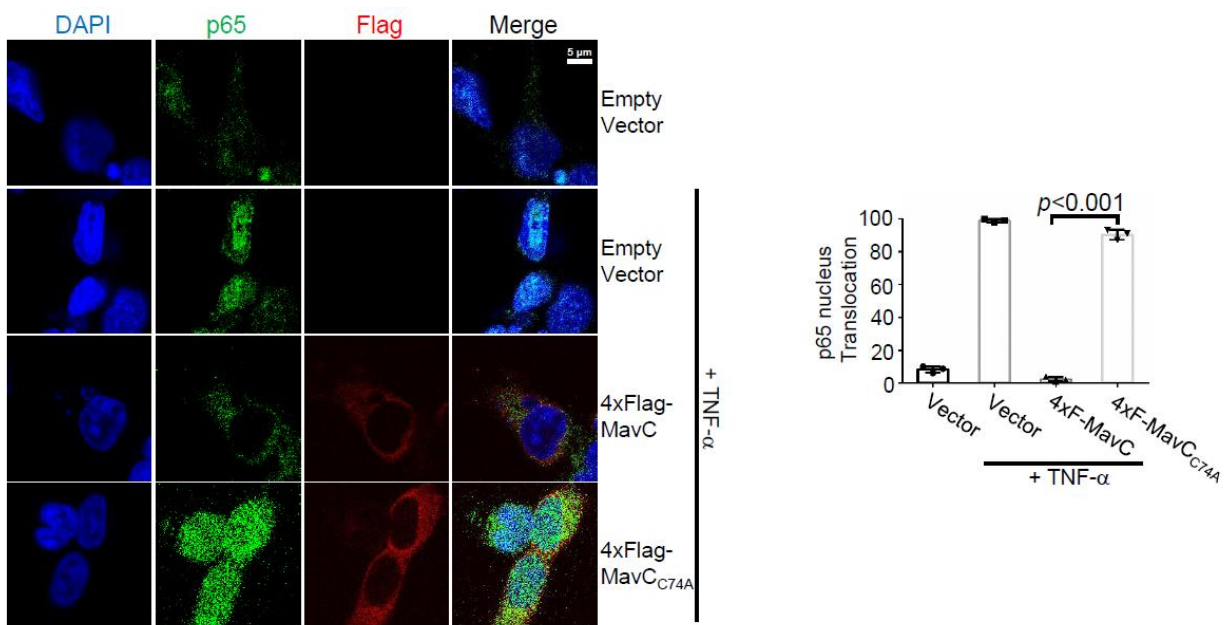


Fig. 2-14 Ectopic expression of MavC inhibited p65 nuclear translocation.

HEK293 cells transfected to express MavC or the C74A mutant were treated with 20 ng/ml TNF- α for 30 min. Fixed cells were immunostained with antibodies specific for p65 and Flag, respectively. Host nuclei were labeled with DAPI. Typical images of the samples were shown (left); nucleus localization of p65 was visually scored by examining at least 300 cells (right) (mean \pm s.e. from three biological replicates). Results shown were from three independent experiments.

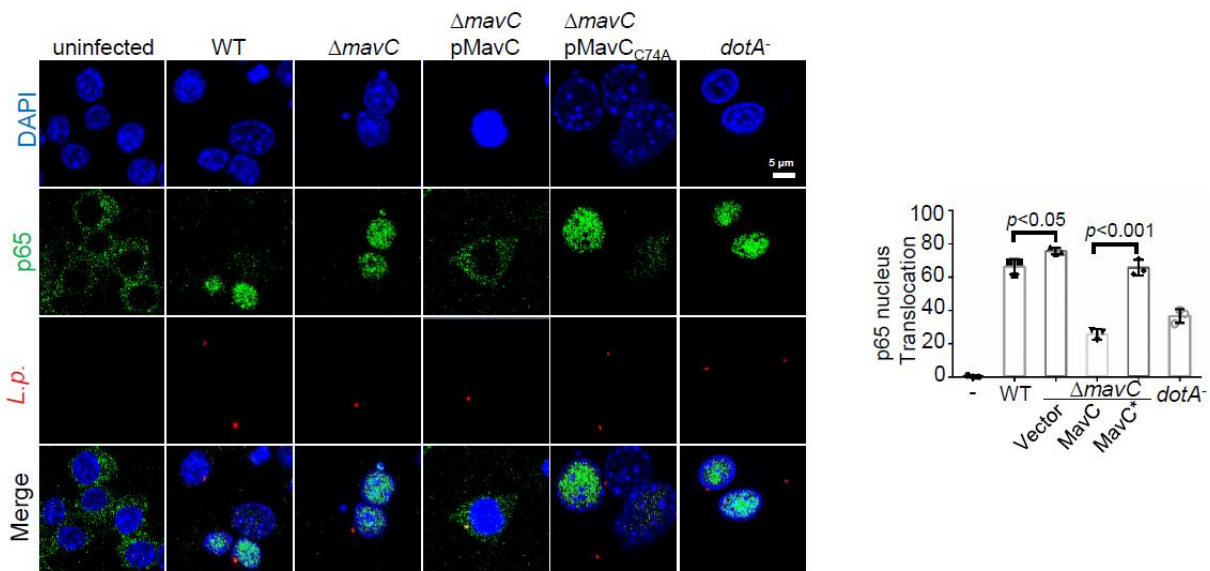


Fig. 2-15 MavC inhibits nuclear translocation of p65 during *L. pneumophila* infection.

Raw264.7 cells infected with the indicated *L. pneumophila* strains for 2 h at an MOI of 2 were immunostained with antibodies specific for p65 and the bacterium, respectively. Host nuclei were labeled with DAPI. Representative images of cells in each sample category were shown (left); nucleus localization of p65 was determined by scoring at least 300 infected cells (right) (mean \pm s.e. from three biological replicates). Results shown were from three independent experiments done in triplicate. Two sided, T-test was used to analyze the data, no adjustment was made.

Discussion

Immune cells respond to damage-associated molecular patterns (DAMPs) and pathogen associated molecular patterns (PAMPs) via various receptors, and this dictates the outcome of the interaction between a pathogen and its hosts. Pathogens have evolved various strategies to counter the host immune response to ensure successful infections. The bacterial pathogen *L. pneumophila* appears to activate the major immune regulator NF-κB in different phases of infection by mechanisms that are either independent of or dependent on its Dot/Icm transporter, which is essential for virulence(Bartfeld et al., 2009, Losick & Isberg, 2006). The activation seen after the initial phase of infection is probably attributed to Dot/Icm effectors such as LegK1 and LnaB(Ge et al., 2009, Losick et al., 2010). Whereas activation at late phases of infection is of importance in multiple respects, including the induction of genes involved in cell survival(Losick & Isberg, 2006), virulence independent activation of NF-κB is probably detrimental to bacterial colonization. At least two lines of evidence suggest that the function of MavC is to counteract the effects of NF-κB activation occurring in the early phase of infection. First, this gene is highly expressed in bacteria grown to post-exponential phase (**Fig. 2-3, B**). Second, MavC-induced reduction of NF-κB in infected cells reached the lowest level within the first 30 min after bacterial uptake (**Fig. 2-11, C**).

E2 enzymes have emerged as important players in the formation of specific ubiquitin codes by directly controlling chain type synthesis, yet our understanding of their function and regulation remains limited(Stewart et al., 2016, Ye & Rape, 2009). Interestingly, although the enzymes involved remain unknown, UBE2N has been reported to be ISGylated at Lys92, which leads to inhibition of its E2 activity(Takeuchi & Yokosawa, 2005, Zou et al., 2005). Similarly, UBE2T is automonoubiquitinated at Lys91, a modification that also inhibits its activity(Machida et al., 2006). Other E2s, such as UbcH7, have also been shown to be regulated by mechanisms such as ubiquitination, again at a lysine residue close to the active cysteine, leading to proteasome-mediated degradation(Rape & Kirschner, 2004, Ravid & Hochstrasser, 2007). Our results point to the importance of Lys92 in the activity and regulation of UBE2N, probably due to its close proximity to the catalytic Cys87 residue. The discovery of UBE2N monoubiquitination by MavC has added another layer of complexity to the regulation of E2 activity. The nature of the potential ubiquitination of UBE2N by Ub-AA observed in our initial experiments is unclear (**Fig. 2-1**), nor is the enzyme involved in such modification. Ub-AA can be linked to UBE2N via Arg42, akin to

that induced by members of the SidE family(Qiu & Luo, 2017b), or by a Gln residue by enzymes similar to MavC or other as yet uncharacterized mechanisms. Because TGases are widely present in eukaryotic cells(Lorand & Graham, 2003), it is possible that some of these enzymes also regulate cellular signaling by catalyzing ubiquitination.

Similar to established transglutaminases, MavC harbours deamidase activity that attacks ubiquitin (**Fig. 2-8**), an activity also reported by a recent study(Valleau, Quaile et al., 2018). Several lines of evidence indicate that ubiquitination of UBE2N, rather than ubiquitin deamidation by MavC, is responsible for its inhibition of the NF- κ B pathway. First, the inhibitory effects can be suppressed by co-expressing UBE2N_{K92A}, a mutant that cannot be modified by MavC (**Fig. 2-13, A**). Second, MavC cannot inhibit NF- κ B activation induced by TAK1/TAB1 or IKK β , indicating that its point of action lies upstream of these kinases, which differs from deamidases that attack ubiquitin (**Fig. 2-13, D and E**). Third, under identical reaction conditions, the transglutaminationactivity of MavC is much higher than the deamidation activity against ubiquitin (**Fig. 2-9**). Finally, whereas ubiquitination of UBE2N by MavC can be readily detected in cells infected with wild type *L. pneumophila*, deamidated ubiquitin was not detectable in such cells (**Figs. 2-2 and 2-10**). Thus, the role of ubiquitin deamidation in the function of MavC, if any, should be minor.

UBE2N is the main E2 enzyme that specifies the formation of K₆₃-type ubiquitin chains (Hodge et al., 2016, Stewart et al., 2016, Ye & Rape, 2009), and plays an important role in the activation of NF- κ B, a process that is clearly required during *L. pneumophila* infection(Abu-Zant et al., 2007, Losick & Isberg, 2006). Thus, the activity of MavC mandates the requirement of enzymes that function to reverse the modification on UBE2N. Such enzymes may be of host or bacterial origin, or both, and should serve to impose temporal regulation of UNE2N activity together with MavC. Alternatively, other yet unidentified E2 enzymes not attacked by MavC may be responsible for NF- κ B activation seen in infected cells after the initial phase of infection (Losick & Isberg, 2006). The identification of MavC as an inhibitor for NF- κ B activation reveals that *L. pneumophila* modulates the activity of this immune regulator by effectors with converse biological consequences, which is akin to the reversible regulation of other cellular events such as vesicle trafficking by effectors of opposite biochemical activities (Qiu & Luo, 2017b, Urbanus, Quaile et al., 2016). Interestingly. the *Shigella* effector OspI deamidates UBE2N to interfere with its activity (Sanada et al., 2012). Differing from the effects of MavC, which inhibits almost all known

signalling branches that activate NF-κB (**Fig. 2-16**), deamidation of UBE2N at Gln₁₀₀ by OspI only blocks its function in response to PMA via the diacylglycerol (DAG)–CBM (CARD–BCL10–MALT1) axis (Sanada et al., 2012). The targeting of UBE2N by multiple pathogens highlights its importance in immunity. Further study is required to analyse the regulation of the effects imposed by MavC and the structural basis of the mechanism of inhibition by this unique ubiquitination.

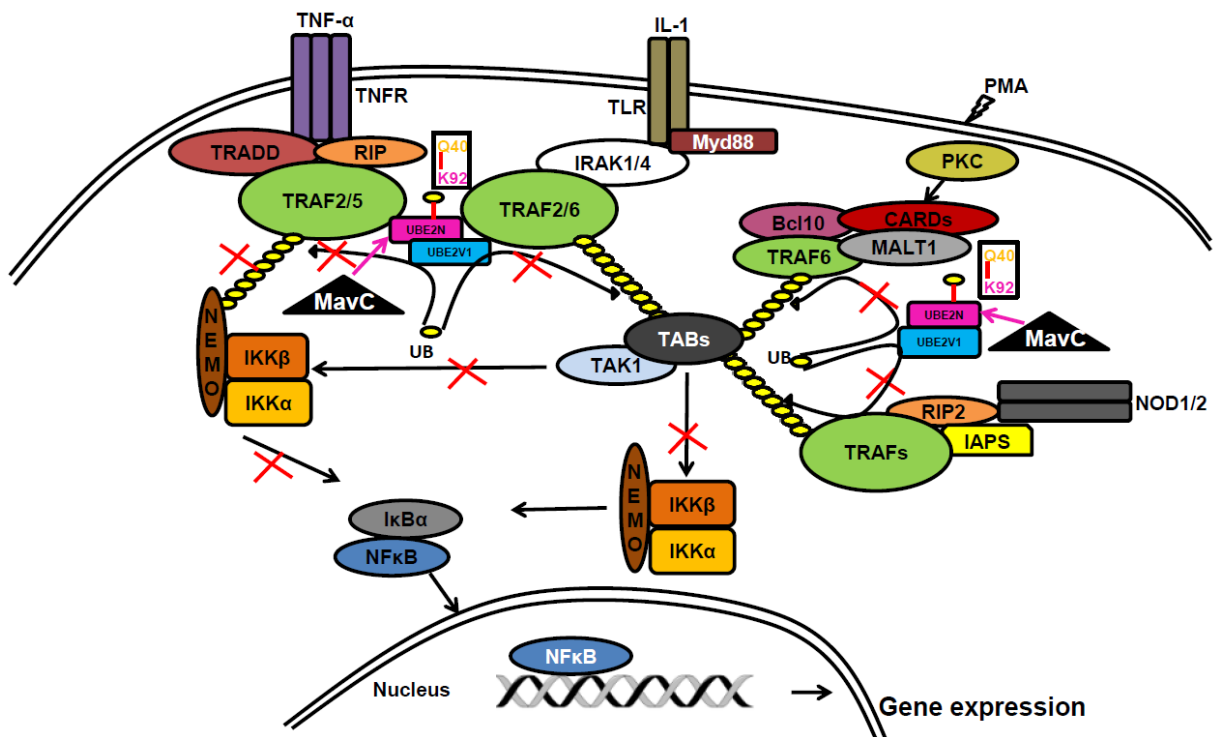


Fig. 2-16 A diagram of the NF-κB activation pathways inhibited by MavC.

The pathways induced by TNF- α , IL-1, PMA and Nod1/2 were shown. In each case, MavC (black triangle) catalyzed UBE2N ubiquitination, which blocks the synthesis of K₆₃-type polyubiquitin chains important for the activation of downstream enzymes.

CHAPTER 3. LEGIONELLA PNEUMOPHILA REGULATES THE ACTIVITY OF THE E2 UBIQUITIN CONJUGATING ENZYME UBE2N BY DEAMIDASE MEDIATED DEUBIQUITINATION

Abstract

The *Legionella pneumophila* effector MavC induces ubiquitination of the E2 ubiquitin-conjugating enzyme UBE2N by transglutamination, thereby abolishing its function in the synthesis of K₆₃-type polyubiquitin chains. The inhibition of UBE2N activity creates a conundrum because this E2 enzyme is important in multiple signaling pathways, including some that are important for intracellular *L. pneumophila* replication. Here we show that prolonged inhibition of UBE2N activity by MavC restricts intracellular bacterial replication and that the activity of UBE2N is restored by MvcA, an ortholog of MavC (50% identity) with ubiquitin deamidase activity. MvcA functions to deubiquitinate UBE2N-Ub using the same catalytic triad required for its deamidase activity. Structural analysis of the MvcA-UBE2N-Ub complex reveals a crucial role of the insertion domain in MvcA in substrate recognition. Our study establishes a deubiquitination mechanism catalyzed by a deamidase, which together with MavC, impose temporal regulation of the activity of UBE2N during *L. pneumophila* infection.

Introduction

Immune cells detect the presence of pathogens by sensing PAMPs such as flagellin, nucleic acids and lipopolysaccharide or DAMP signals resulting from alternations or damages caused by virulence factors(Diacovich & Gorvel, 2010, Kieser & Kagan, 2017, Vance, Isberg et al., 2009). The engagement of these ligands or perception of the activity of virulence factors leads to the activation of distinct signal transduction pathways and the induction of genes involved in the production of cytokines and antimicrobial agents(Diacovich & Gorvel, 2010, Kieser & Kagan, 2017, Vance et al., 2009). NF-κB is one major immune transcriptional factor that becomes activated in response to diverse stimuli including bacterial infection(Li & Verma, 2002). NF-κB activation often is achieved by the ubiquitin proteasome system-mediated degradation of IκBα, a labile protein that sequesters its components such as RelA and RelB in the cytoplasm by forming stable protein complexes(Li & Verma, 2002). Signals that cause IκBα destruction are transduced by a number of proteins with distinct enzymatic activities, including protein kinases and enzymes

involved in the formation of specific polyubiquitin chains. Among these, the E2 ubiquitin-conjugating enzyme UBE2N along with its heterodimeric partner UBE2V1 or UBE2V2 function together with such E3 enzymes as members of the TRAF (TNF receptor associated factor) family to catalyze the formation of K₆₃-type polyubiquitin chains (Deng, Wang et al., 2000), which activate the TAK1/TAB1 kinases, leading to a signaling relay that eventually phosphorylates IκB α and its subsequent ubiquitination and degradation (Deng et al., 2000). UBE2N has emerged as an important checkpoint for activation of this pathway and is subjected to precise regulation by diverse mechanisms such as posttranslational modifications, including several imposed by infectious agents (Hodge et al., 2016, Song & Luo, 2019).

In order to establish an intracellular niche permissive for multiplication, the bacterial pathogen *Legionella pneumophila* extensively manipulates host signaling with a large cohort of effector proteins (Burstein et al., 2016, Qiu & Luo, 2017a). Given the essential roles played by the ubiquitin network in immune signaling (Komander & Rape, 2012), it is not surprising that at least 10 *L. pneumophila* effectors function to modulate the host ubiquitination machinery as E3 ubiquitin ligases that coordinate with E1 and E2 enzymes from the host (Qiu & Luo, 2017a) or as deubiquitinases that remove Gly₇₆-linked ubiquitin from ubiquitinated substrates (Kubori, Kitao et al., 2018, Sheedlo et al., 2015). In addition, members of the SidE family catalyze ubiquitination by mechanisms that are unrelated to the classical three-enzyme cascade. In these reactions, ubiquitin is first activated by ADP-ribosylation via a mono-ADP-ribosyltransferase activity and is then utilized by a phosphodiesterase activity that attaches phosphoribosyl ubiquitin to serine residues of the substrate proteins (Bhogaraju et al., 2016, Kotewicz et al., 2017, Qiu et al., 2016). More recently, the *L. pneumophila* effector MavC (Lpg2147) was found to deamidate ubiquitin; it also interacts with the ubiquitin E2 conjugation enzyme UBE2N and both activities may contribute to the inhibition of NF-κB signaling (Valleau et al., 2018). Further studies demonstrated that MavC is a transglutaminase that induces UBE2N monoubiquitination by catalyzing the formation of an isopeptide bond between Gln₄₀ of ubiquitin and Lys₉₂ or, to a lesser extent, Lys₉₄ of the E2 enzyme, leading to inhibition of NF-κB activation (Gan, Nakayasu et al., 2019a). Signaling mediated by UBE2N is pivotal for multiple important cellular processes (Hodge et al., 2016, Ye & Rape, 2009), including cell survival, which is important for productive intracellular replication of *L. pneumophila* (Losick & Isberg, 2006). After entry, robust bacterial replication requires the activity of genes whose expression is dependent upon NF-κB (Losick & Isberg, 2006), which may mandate active

UBE2N in later phases of the intracellular life cycle of *L. pneumophila*. Thus, the bacterium may temporally control the activity of this E2 enzyme by reversing MavC-induced monoubiquitination. In this study we find that the activity of MavC is regulated by MvcA (Lpg2148), a protein coded by a gene adjacent to MavC. MvcA is a close homolog of MavC at both sequence and structural level; similar to MavC, MvcA exhibits deamidase activity toward ubiquitin (Valleau et al., 2018). Unexpectedly, our results indicate that MvcA also functions to remove ubiquitin from the MavC-catalyzed transglutamination product, UBE2N-Ub, at later phases of *L. pneumophila* infection. To gain structural insights into this unprecedented deubiquitination we crystallized and solved the structure of a complex of a catalytically inactive MvcA mutant in association with the UBE2N-Ub substrate. The structure provides an atomic level explanation of this unique example of the deubiquitination and deamidation executed by the same catalytic center while revealing a crucial role of the insertion domain of MvcA in its engagement of the substrate UBE2N-Ub, especially in recognition of UBE2N. Thus, the presence of the insertion domain distinguishes MvcA from canonical ubiquitin deamidases.

Results

MvcA interferes with the modification of UBE2N induced by MavC

Functional redundancy is common among *L. pneumophila* effectors, and in some cases such redundancy is achieved by the ability to code for multiple members with high level similarity to form protein families (Ghosh & O'Connor, 2017, O'Connor, Boyd et al., 2012). For example, phenotypes associated with mutants lacking the *sidE* effector family can be complemented by any of its four members (Bardill, Miller et al., 2005, Luo & Isberg, 2004). In the Philadelphia 1 strain, MavC has a homolog (50% identity and 65% similarity) encoded by its neighboring gene called *mvca* (*lpg2148*) (Valleau et al., 2018, Zhu, Banga et al., 2011)(**Fig. 3-1, A and B**). Because of the high-level similarity between these two proteins, in both primary sequence and structure and their shared deamidation activity toward ubiquitin (Valleau et al., 2018), we considered the possibility that MvcA also ubiquitinates UBE2N or one or more other E2 enzymes. When recombinant MvcA active as a ubiquitin deamidase was added to a series of reactions containing one of a panel of E2s that are similar to UBE2N, particularly in the region modified by MavC (Gan et al., 2019a, Valleau et al., 2018), modification of none of these E2 enzymes could be detected (**Fig. 3-1, C and D**). To test whether MvcA attacks UBE2N under more physiologically relevant

conditions, we examined its ability to ubiquitinate UBE2N in cells infected by *L. pneumophila* using the $\Delta mvcA$ and the $\Delta mavC\Delta mvcA$ mutants. Consistent with earlier results (Gan et al., 2019a, Valleau et al., 2018), *L. pneumophila* infection caused UBE2N modification by ubiquitin in a MavC-dependent manner. Deletion of *mvcA* did not affect the bacterium's ability to induce such modification (**Fig. 3-2, A, 5th lane**). Our antibodies for MvcA were about 5-fold less sensitive compared to those against MavC (Gan et al., 2019a), and the antibodies for these two proteins did not cross-react (**Fig. 3-3**). The MvcA antibodies were unable to detect endogenous proteins expressed in wild type bacteria (**Fig. 3-2, A, 2nd and 3rd lanes**). Expression of MvcA from a multi-copy plasmid allowed its detection in the $\Delta mavC\Delta mvcA$ mutant and in infected cells but UBE2N modification was still not detectably induced in host cells that contained detectable MvcA (**Fig. 3-2, A, 9th lane**). Unexpectedly, in cells infected with the $\Delta mvcA$ mutant overexpressing MvcA, UBE2N modification was no longer apparent. Importantly, the potential inhibition of UBE2N modification by overexpressed MvcA in strain $\Delta mvcA$ required the catalytic residue responsible for the ubiquitin deamidase activity (Valleau et al., 2018) because overexpression of the inactive MvcAC83A mutant failed to impose such suppression (**Fig. 3-2, A, 6th and 7th lanes**). In the $\Delta mvcA(pMvcA)$ strain, MavC was properly expressed and translocated into host cells (**Fig. 3-2, A, 6th and 7th lanes in the middle and lower panels**). Clearly, the lack of UBE2N modification in cells infected by this strain is not caused by disruption of MavC expression or its translocation into host cells. We further analyzed the potential interference of MvcA on MavC-induced UBE2N modification in mammalian cells by transfection. Expression of MavC alone led to almost complete modification of endogenous UBE2N. In contrast, coexpression of MvcA but not the MvcAC83A mutant defective in ubiquitin deamidation (Valleau et al., 2018) with MavC resulted in considerable accumulation of unmodified UBE2N (**Fig. 3-2, B**), further supporting the notion that MvcA interferes with the activity of MavC in a manner dependent on its catalytic cysteine used in the ubiquitin deamidase activity (Valleau et al., 2018). As expected, the canonical ubiquitin deamidase Cif from *Yersinia pseudotuberculosis* (Cui et al., 2010) did not interfere with MavC-induced UBE2N modification (**Fig. 3-2, B, 6th lane**). Consistent with results from infection and transfection experiments, addition of MvcA to reactions measuring the transglutaminase activity of MavC at a 1:1 molar ratio led to complete abrogation of UBE2N ubiquitination, and such interference required its catalytic cysteine (**Fig. 3-2, C, 3rd, 7th and 8th lanes**). Under our

experimental conditions, a substantially higher molar ratio between MavC and MvcA, close to 10:1, was needed to overcome the inhibitory effects of MvcA (**Fig. 3-2, D**).

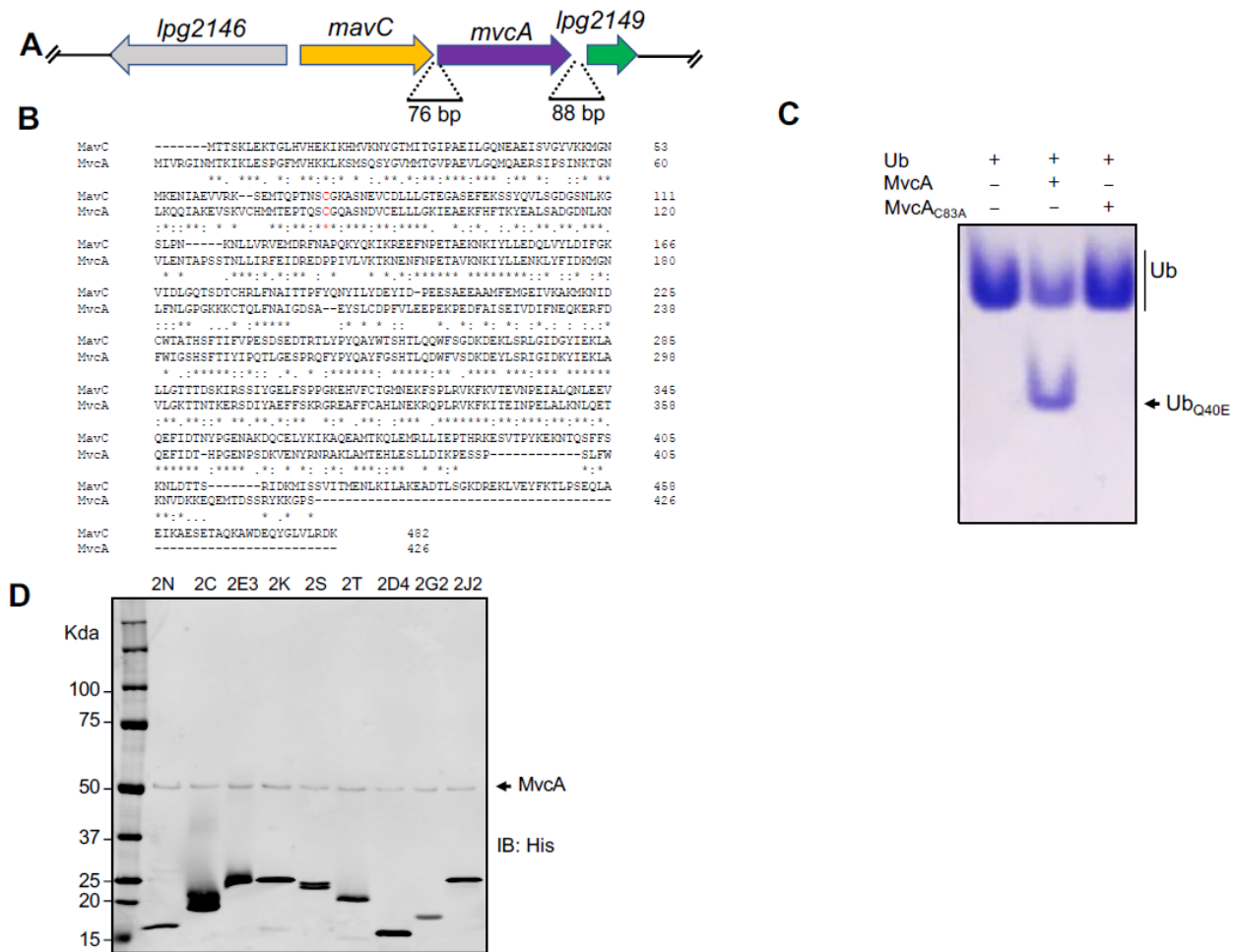
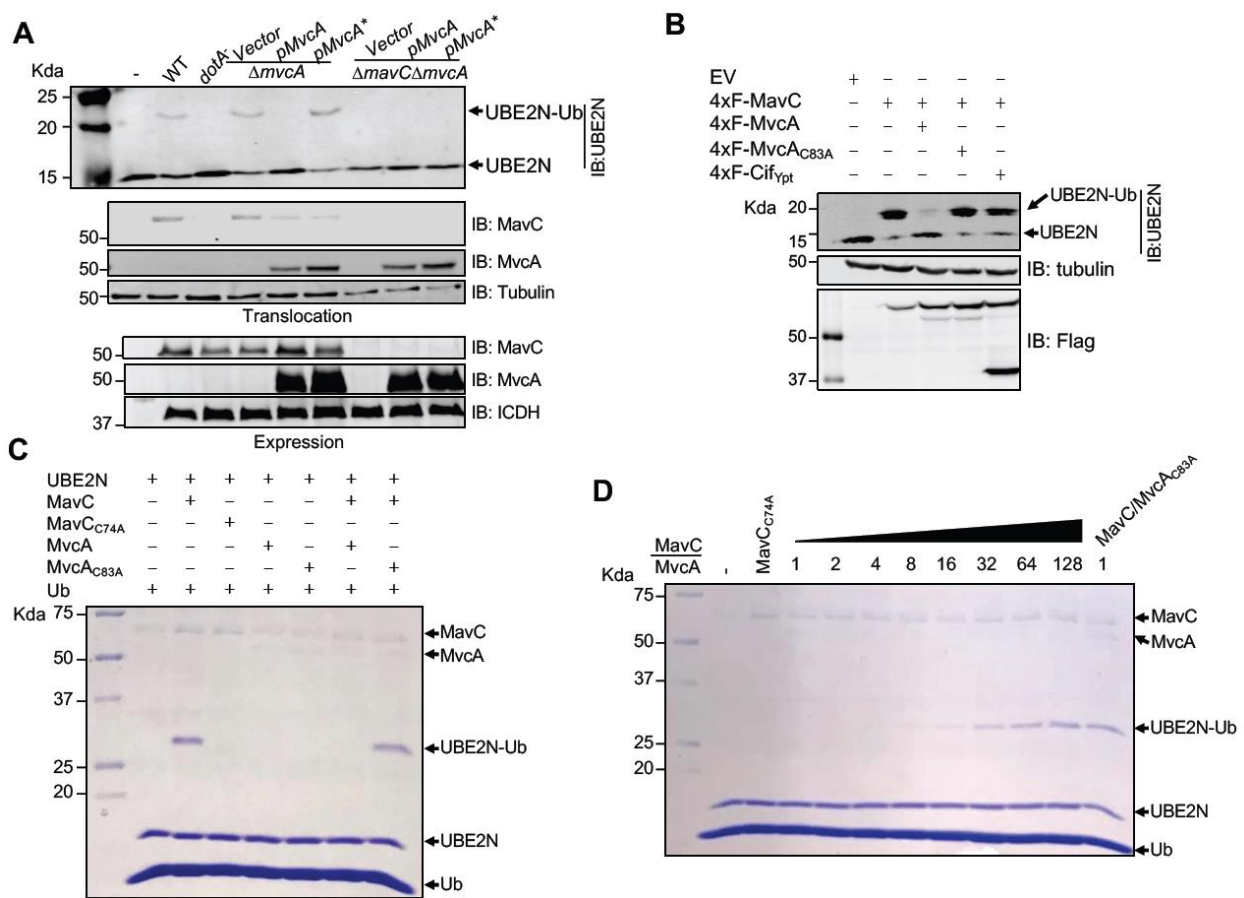


Fig. 3-1 Genetic organization of *mavC*, *mvcA* and *lpg2149* in the genome of *L. pneumophila* strain Philadelphia 1 and the activity of MvcA against ubiquitin and several E2 enzymes.

A. The organization of *mavC*, *mvcA* and *lpg2149* in the genome of *L. pneumophila* strain Philadelphia 1. Note that the 76 base pairs intergenic space between *mavC* and *mvcA* may allow them to be expressed by independent promoters. **B.** Alignment of the primary sequences of MavC and MvcA by Needleman-Wunsch Global Align. Stars indicate identical residues and colons indicate conserved amino acids. **C.** Deamidase activity of MvcA toward ubiquitin. 10 µg of ubiquitin was incubated with 1 µg MvcA and the inactive MvcAC83A mutant for 1 h at 37°C and the reaction products were separated in native-PAGE and were detected by CBB staining. **D.** The modification of several E2 enzymes by MvcA. Reactions containing His₆-tagged UBE2N or the indicated E2 enzymes were incubated with MvcA. Ubiquitination was assessed by molecular weight shift after probing with a His₆-specific antibody. None of the tested E2 enzymes were detectably modified by MvcA.

Fig.3-2 MvcA interferes with UBE2N modification induced by MavC.

A. Infection by a *L. pneumophila* strain overexpressing MvcA but not the inactive mutant MvcAC83A interferes with UBE2N modification. Raw264.7 cells were infected with the indicated bacterial strains at an MOI of 5 for 2 h. Saponin soluble proteins resolved by SDS-PAGE were probed with a UBE2N-specific antibody (top panel). MvcA*, MvcAC83A. The delivery of MavC and MvcA into infected cells was probed with antibodies specific to each of these two proteins. Note that MavC but not MvcA is detectable in cells infected with wild type bacteria (middle panels labeled as “translocation”). Tubulin was probed as a loading control. Protein levels of MavC and MvcA associated with the bacteria were similarly probed in the saponin insoluble fraction (lower panels labeled as “expression”). The bacterial metabolism enzyme isocitrate dehydrogenase (ICDH) was probed as a loading control. Note that endogenous MvcA was not detectable in bacteria grown in bacteriological medium (the middle panel of the lower portion). **B.** Coexpression of MvcA with MavC causes accumulation of unmodified UBE2N in mammalian cells. HEK293T cells were transfected with combinations of empty vector and plasmid directing the expression of MavC or MvcA. 16 h after transfection, modification of endogenous UBE2N was detected by immunoblotting (upper level). The canonical ubiquitin deamidase Cif_{Ypt} from *Yersinia pseudotuberculosis* (Ypt), which cannot modify UBE2N, was included as a control. Note that coexpression of MvcA led to accumulation of unmodified UBE2N (4th lane) in samples that expressed MavC. The expression of MavC MvcA and Cif was detected using a Flag-specific antibody (lower panel). Tubulin was probed as a loading control (lower panel). **C.** MvcA interferes with MavC-induced UBE2N ubiquitination. Reactions containing the indicated combinations of proteins were allowed to proceed for 30 min and samples resolved by SDS-PAGE were detected by Coomassie Brilliant blue (CBB) staining. Note that MvcA (inclusion of MvcA with MavC, 7th lane. Compare to MavC alone in 3rd lane) but not the MvcAC83A mutant (8th lane) abolished MavC-induced UBE2N modification. **D.** Dose-dependent modification of UBE2N by MavC and MvcA. A series of reactions containing MavC and MvcA at the indicated molar ratios were established and the reactions were allowed to proceed for 30 min. Samples resolved by SDS-PAGE were detected by CBB staining.



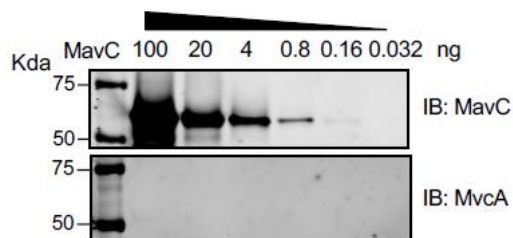
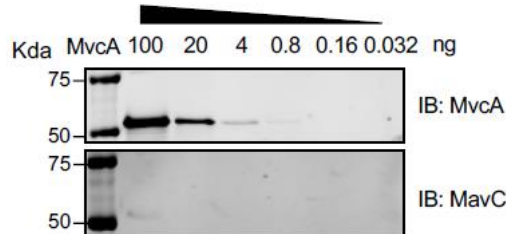
A**B**

Fig. 3-3 Comparison of the reactivity of antibodies for MavC and MvcA and their cross-reactivity.

The reactivity of antibodies against MavC and MvcA. The indicated amounts of MavC (**A**) or MvcA (**B**) were separated by SDS-PAGE, proteins transferred onto nitrocellulose membranes were detected by antibodies against MavC and MvcA respectively (**A**). Similar experiments were performed with recombinant MvcA and the detection was done with MvcA and MavC antibodies, respectively (**B**). Note that MavC antibodies can detect as little as 0.16 ng MavC whereas MvcA antibodies can detect as little as 0.8 ng of recombinant MvcA. Very little cross-reactivity was detected for either antibodies.

MvcA deubiquitinates the UBE2N-Ub product from MavC transglutaminase activity

The inhibitory effects of MvcA can be achieved by either interfering with the ubiquitin transglutaminase activity of MavC or by reversing the modification on UBE2N. To distinguish between these two possibilities, we incubated purified UBE2N-Ub with MvcA or its catalytically inactive mutant protein. In reactions receiving MvcA, two distinct proteins with molecular weights corresponding to UBE2N and Ub, respectively, were detected. This cleavage of UBE2N-Ub by MvcA required Cys₈₃, the same catalytic Cys required for its ubiquitin deamidase activity (Valleau et al., 2018) (**Fig. 3-4, A**). We explored the mechanism of cleavage by analyzing the two protein products by mass spectrometry, which revealed that UBE2N had been restored to its original form. In contrast, the ubiquitin product was in a modified form with its original Gln₄₀ having been converted into a glutamate residue (**Fig. 3-4, A**). Thus, MvcA functions as an isopeptidase that attacks the isopeptide bond between Lys₉₂ of UBE2N and Gln₄₀ of ubiquitin to generate UBE2N and Ub_{Q40E} (**Fig. 3-4, B**), which happens to be the same product that would result from the ubiquitin deamidation reaction. We further examined the activity of MvcA by testing its ability to hydrolyze UBE2N-Ub in reactions containing these two proteins at different molar ratios. Under our experimental conditions, MvcA activity was detectable in 30 min in reactions in which the molar ratio between substrate and enzyme was nearly 2000:1 (**Fig. 3-4, C**). At a ratio of only ~100:1, cleavage was readily detectable immediately after adding MvcA, and the reaction proceeded to almost completion in 10 min (**Fig. 3-4, D**). In agreement with the restoration of Lys₉₂ to its original form, UBE2N produced by MvcA from UBE2N-Ub exhibited robust E2 enzyme activity in catalyzing polyubiquitin chain synthesis (**Fig. 3-4, E**). We observed that a fraction of UBE2N-Ub was not hydrolyzed even after long duration of reaction with high amounts of MvcA (**Fig. 3-4, A, C and D**); mass spectrometric analysis of the uncleaved UBE2N-Ub protein revealed that in this molecule, ubiquitin is linked to UBE2N at Lys₉₄, as a minor site of modification induced by MavC (Gan et al., 2019a) (**Fig. 3-5, A**).

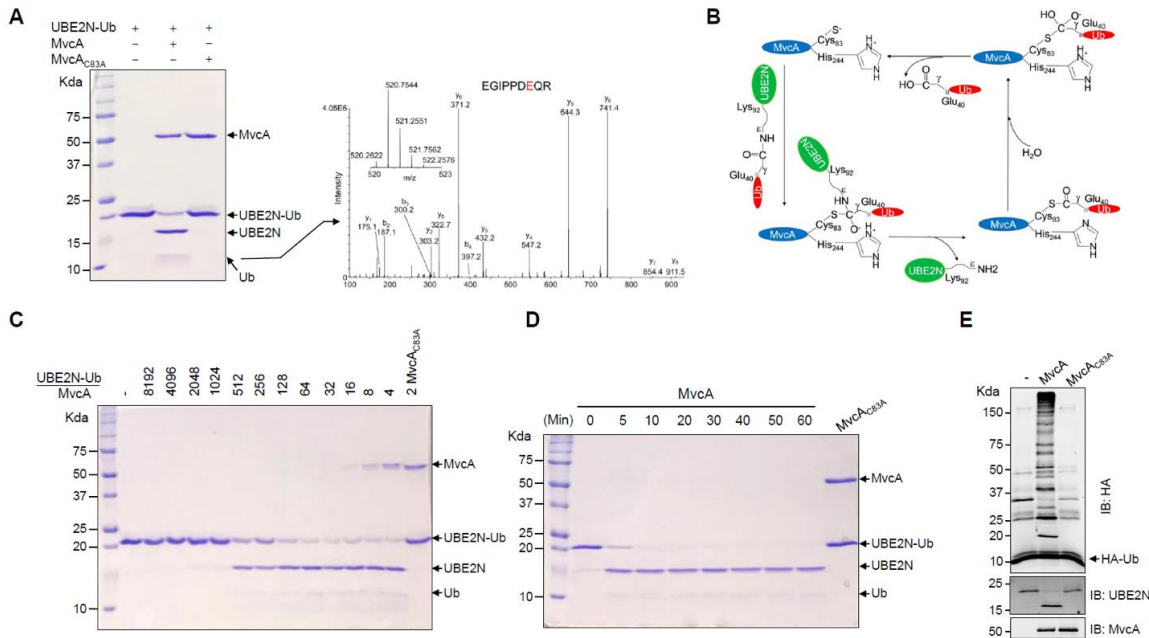


Fig. 3-4 MvcA cleaves the isopeptide crosslink between UBE2N and ubiquitin in UBE2N-Ub.

A. The hydrolytic cleavage of UBE2N-Ub by MvcA into UBE2N and ubiquitin (Q40E variant). Reactions containing the indicated proteins were allowed to proceed for 30 min and samples resolved by SDS-PAGE were detected by CBB staining (left). Mass spectrometric analysis of the protein band corresponding to ubiquitin produced by MvcA from UBE2N-Ub (right). The ubiquitin product is the Glu₄₀ variant of ubiquitin. **B.** Proposed catalytic mechanism for isopeptide bond cleavage catalyzed by MvcA. Nucleophilic attack of the isopeptide bond by the thiol from the catalytic center of MvcA leads to the release of UBE2N and formation of a thioester linked MvcA-Ub intermediate, which is further attacked by a nucleophilic water to produce UbQ40E and to regenerate the active enzyme. **C.** Dose-dependent cleavage of UBE2N-Ub by MvcA. A series of reactions containing UBE2N-Ub and MvcA at the indicated molar ratios were established and the reactions were allowed to proceed for 30 min before SDS-PAGE and CBB staining. Note that the activity was detectable in a reaction starting at the molar ratio of between UBE2N-Ub and MvcA is 2048:1. **D.** Time-dependent cleavage of UBE2N-Ub by MvcA. UBE2N-Ub was incubated with MvcA at the molar ratio of 128. Samples taken at the indicated time points were resolved by SDS-PAGE and detected by CBB staining. **E.** UBE2N produced from UBE2N-Ub via MvcA catalyzed deubiquitination is active in catalyzing the formation of polyubiquitin chains. UBE2N-Ub was preincubated with MvcA or its inactive mutant for 30 min. Then a cocktail containing E1, UBE2V2, 3xHA-ubiquitin, the E3 enzyme TRAF6 and ATP was added into reactions. Ubiquitination was allowed to proceed for 30 min. Proteins in samples resolved by SDS-PAGE were transferred onto nitrocellulose membranes and blotted with the HA specific antibody. Note the robust formation of polyubiquitin chains in the reaction receiving MvcA (middle lane).

MvcA does not cleave Gly₇₆-Lys isopeptide bonds in canonical ubiquitination

We also examined the substrate specificity of MvcA using K₄₈- and K₆₃-linked diubiquitin substrates of the eukaryotic system (bearing Gly₇₆-Lys isopeptide bonds from canonical ubiquitination). MvcA was unable to cleave either diubiquitin, which differed significantly from the canonical deubiquitinase SdeAD_{ub} from *L. pneumophila* (Sheedlo et al., 2015) which effectively hydrolyzed both substrates (**Fig. 3-5, B**). Consistently, unlike SdeAD_{ub}, MvcA was unable to remove ubiquitin from ubiquitinated proteins purified from mammalian cells to any extent detectable in our assays (**Fig. 3-5, C**). These results suggest that MvcA cannot cleave the isopeptide bond installed by the canonical ubiquitination machinery where the bond links the backbone carbonyl of the carboxyl end of Gly₇₆ of ubiquitin to target Lys residues. Instead, MvcA behaves as a deubiquitinase with selectivity for an isopeptide crosslink bond formed at an internal functional group of ubiquitin.

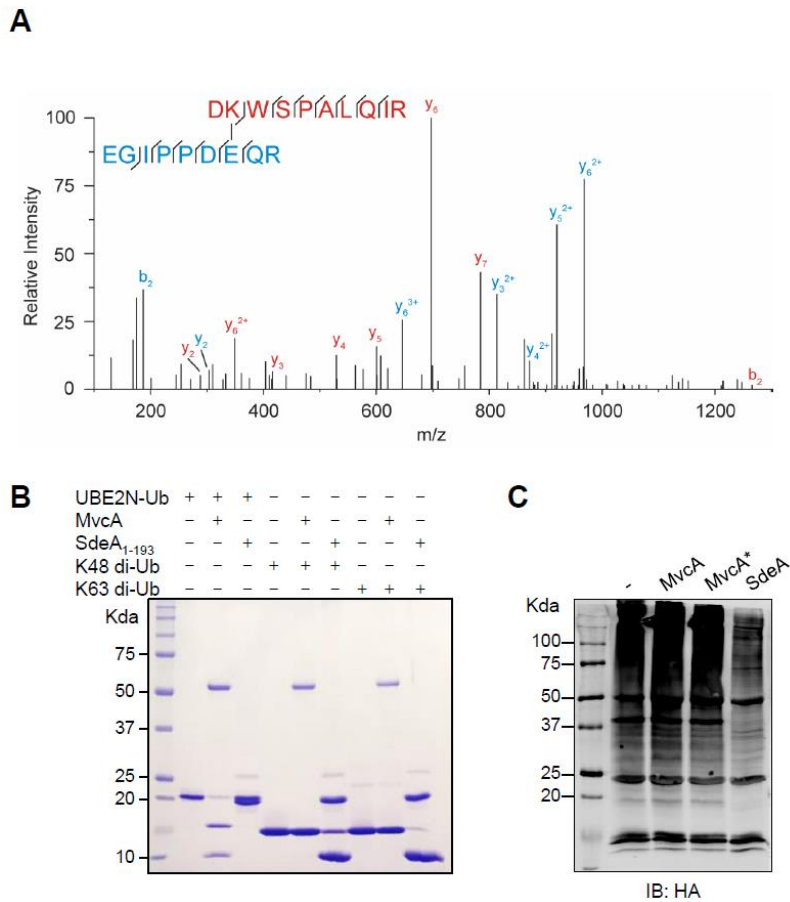


Fig. 3-5 The activity of MvcA against peptide bonds formed by several different mechanisms.

A. MvcA does not cleave ubiquitin linked to UBE2N at Lys94 via Gln40. After MvcA treatment, remaining UBE2N-Ub digested with trypsin was analyzed by mass spectrometric analysis. A conjugate in which ubiquitin linked to UBE2N at Lys94 was detected. The sequence of the diagnostic peptide bearing the isopeptide crosslink is shown. **B.** MvcA does not cleave K₄₈- or K₆₃-type diubiquitin substrates. UBE2N-Ub or two different diubiquitins were treated with MvcA at 37°C for 30 min before being resolved by SDS-PAGE and visualized by CBB staining. Note that both types of diubiquitin can be cleaved by SdeA₁₋₁₉₃, a canonical Dub from *L. pneumophila*. **C.** MvcA does not cleave isopeptide bonds formed by canonical ubiquitination. Lysates of cells transfected to produce HA-ubiquitin were immunoprecipitated with beads coated with HA-specific antibody. Beads were further incubated with MvcA, MvcA_{C83A} or full-length SdeA at 37°C for 2 h. Proteins resolved by SDS-PAGE were probed with an HA specific antibody.

Lpg2149 inhibits the deubiquitinase activity of MvcA

The ubiquitin deamidase activity of MavC and MvcA is inhibited by Lpg2149 (Valleau et al., 2018), an effector that is coded for by a gene directly downstream of *mvcA* (Zhu et al., 2011) (**Fig. 3-1, A**). Lpg2149 inhibits the ubiquitin deamidation activity of both MavC and MvcA by binding to their core domains through protein-protein interactions (Valleau et al., 2018). The binding of Lpg2149 to MavC or MvcA does not require the insertion domain, suggesting that this inhibitory protein regulates the activity of MavC and MvcA by blocking the catalytic site (Valleau et al., 2018). In agreement with this notion, addition of Lpg2149 in UBE2N-Ub deubiquitination reactions by MvcA led to inhibition of its isopeptidase activity (**Fig. 3-6, A**). The activity of MvcA was considerably inhibited in reactions in which the molar ratio between Lpg2149 and MvcA was about 10:1 and was almost completely inhibited when the ratio increased to 20:1 (**Fig. 3-6, A**). In broth-grown bacteria, the expression of *lpg2149* was only detectable in bacteria grown at the early exponential phase (**Fig. 3-6, B**), suggesting that its inhibitory effects do not occur in the early phase of *L. pneumophila* infection.

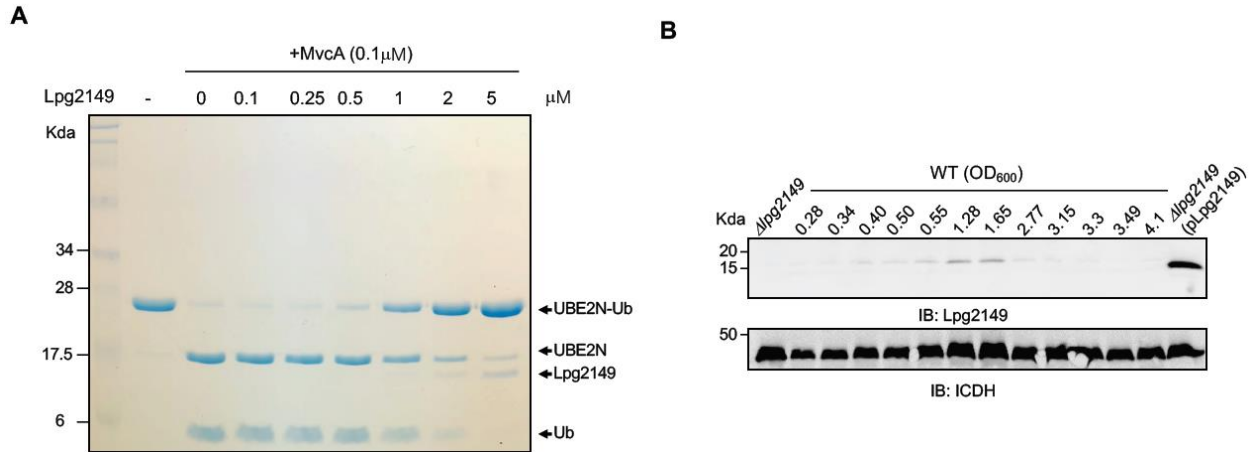


Fig. 3-6 The expression pattern of Lpg2149 in *L. pneumophila* and its inhibition of MvcA activity.

A. Lpg2149 inhibits the activity of MvcA in cleaving UBE2N-Ub. The indicated amount of His₆-Lpg2149 was added to 25 μl reactions that contain 0.12 μg MvcA and 16 μg UBE2N-Ub. Samples were separated by SDS-PAGE and detected by CBB staining after incubation at 37°C for 10 min. Please note that the amount of MvcA in this experiment was not detectable by CBB staining. Data shown was one representative experiment from three independent experiments with similar results.

B. The expression of *lpg2149* is induced in early exponential phase in broth. A 2-ml saturated culture of *L. pneumophila* was diluted into 50 ml fresh AYE broth and the new culture was incubated in a 37°C shaker. Samples were withdrawn periodically and the cell density was measured. The expression of *lpg2149* was probed with specific antibodies raised by recombinant protein (upper panel). The bacterial metabolic enzyme isocitrate dehydrogenase (ICDH) was probed as a loading control (lower panel). Cells of a mutant lacking *lpg2149* and a complementation strain sampled at early exponential growth phase were used as controls. Data shown was one representative experiment from two independent experiments with similar results.

Deubiquitination by MvcA is more efficient than its ubiquitin deamidase activity

Together with the ubiquitin deamidation activity described earlier (Valleau et al., 2018), our results indicate that MvcA has dual enzymatic activity, both requiring Cys₈₃ for catalysis. We compared the catalytic efficiency of these two activities by examining the minimal molar ratio between substrate and enzyme required for detectable activity. The activity of UBE2N-Ub cleavage was detectable when that ratio was more than 2000:1 (**Fig. 3-4, C**). In contrast, a relatively high ratio of 60:1 was required for detectable ubiquitin deamidation activity (**Fig. 3-7, A**). Consistent with these results, ubiquitin deamidation was detected in cells infected with *L. pneumophila* strains overexpressing MvcA (Valleau et al., 2018) but not in cells infected by wild type bacteria even at 6 h postinfection, a time point the protein became detectable in bacteria within host cells (**Fig. 3-7, B**). Thus, although the deubiquitinase activity may be the main function of MvcA, ubiquitin deamidation induced by MvcA likely also occurs but not at a level detectable in cells infected with wild type *L. pneumophila* (Valleau et al., 2018) (**Fig. 3-7, B**).

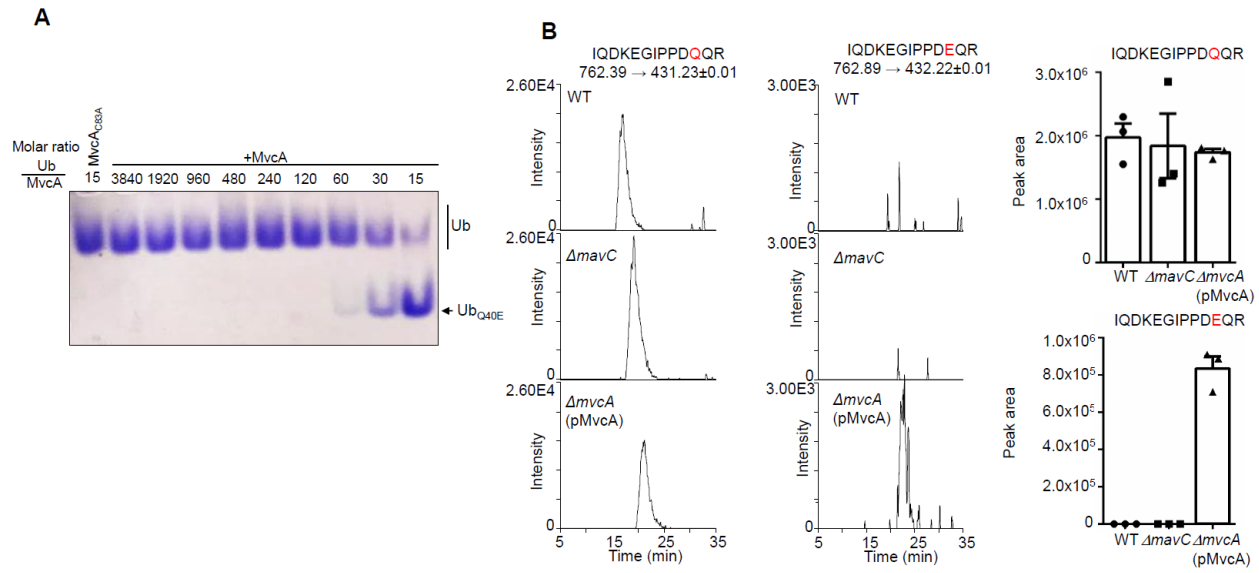


Fig. 3-7 The deamidase activity of MvcA in biochemical reactions and in cells infected with *L. pneumophila*.

A. Dose-dependent deamidation of ubiquitin by MvcA. A series of reactions containing ubiquitin and MvcA at the indicated molar ratios were established and the reactions were allowed to proceed for 1 h before native-PAGE and CBB staining. **B.** Analysis of ubiquitin deamidation in cells by parallel-reaction monitoring (PRM) mass spectrometry. U937 cells were infected with corresponding strain for 6 h at an MOI of 10. Then unmodified and deamidated ubiquitin in cells were analyzed by PRM quantification. Left panels showed the extracted-ion chromatograms of unmodified peptide IQDKEGIPPDQQR (m/z 762.39) targeting fragment y3 (m/z 431.23), and deamidated peptide IQDKEGIPPDDEQR (m/z 762.89) targeting fragment y3 (m/z 432.22), whereas the right panels showed the quantification of these peaks. Results shown are from three independent infected samples.

Crystal structure of MvcA bound to UBE2N-Ub

To understand the mechanism of UBE2N-Ub deubiquitination by MvcA, we crystallized and solved the structure of the enzyme (catalytic Cys₈₃ to Ala mutant) MvcA in complex with its UBE2N-Ub substrate, the MvcA-UBE2N-Ub (MvcAc_{83A}, UBE2N_{K94A}) complex, to a 2.45 Å resolution. During the course of this study we also crystallized and solved the structure of the apo form of the mutant enzyme (MvcAc_{83A}) to 1.94 Å, complementing the previously solved, 2.36 Å structure of MvcA (Valleau et al., 2018) (See methods for structure solution and refinement methods) (**Table. 1; PDB, 6JKY and Table. 2; PDB, 6K11**). There are two very similar looking copies of the MvcA-UBE2N-Ub complex per asymmetric unit (ASU), with root mean square deviation (rmsd) of C_α atoms over the entire complex being 0.85 Å. In the complex the substrate UBE2N-Ub is seen folding into a shape to complement a saddle shape presented by the MvcA active-site area, being straddled by the UBE2N and Ub portion of the substrate. The structure of MvcA can be described as one being comprised of a core domain flanked by the largely helical tail domain (consisting of three α-helices, two from the amino terminal portion, α2 and α3, and one from its carboxyl end, α15) (Crow, Hughes et al., 2012, Valleau et al., 2018) and the insertion domain (residues 142-239) to form an overall C-shaped structure with a cleft at the concave face presenting the catalytic center, housed by the core domain. Comparing the apo structure to that of the complex, the loops linking the tail domain and the insertion domain to the core seem to function as flexible hinges for relative motion between the domains (Crow et al., 2012, Valleau et al., 2018) (**Fig. 3-8, A**), which allow for induced-fit substrate binding. Comparing to the apo form, the cleft in the complex has become wider, which is caused by the slight outward movement of the tail region and a distinct clockwise rotation of the insertion domain to accommodate substrate binding (Valleau et al., 2018) (**Fig. 3-8, B**). The engagement of UBE2N-Ub creates a configuration in which the Lys₉₂-Glu₄₀ isopeptide bond between UBE2N and Ub is locked at the center of the Cys₈₃-His₂₄₄-Gln₂₆₅ catalytic triad (Cys₈₃ was mutated to Ala in our structure) (**Fig. 3-8, C and D**), with the C_α atom of Ala₈₃ being 3.7 Å away from the carbonyl C of the isopeptide bond. The short, 3₁₀-helical segment bearing Lys₉₂ in apo UBE2N has been stretched to an extended loop in the complex, resulting either from the formation of the isopeptide bond or the manner in which it is recognized by the enzyme, providing access of the scissile bond to the catalytic pocket of MvcA (**Fig. 3-8, C**). Several residues from both MvcA and UBE2N-Ub participate in the formation and

stabilization of the observed catalytic arrangement that seems to be poised for hydrolysis of the isopeptide bond. Among these, Glu₄₀ in ubiquitin interacts with Ser₈₂, Ala₈₃ and Phe₂₆₈ in MvcA through hydrogen bonding involving side chain and backbone atoms. The interactions of Arg₁₄₀, a residue close to the insertion domain of MvcA, with Asp₉₃ of UBE2N and Asp₃₉ of ubiquitin seem to hold the scissile isopeptide bond in a proper orientation to be attacked by the catalytic Cys of the enzyme. The involvement of Arg₁₄₀ and ubiquitin was predicted in an earlier study by modeling (Valleau et al., 2018). This reactive arrangement is further supported by hydrogen bonding interactions between Gly₂₄₂ and Ser₂₄₃ in MvcA with Asp₃₉ of ubiquitin, respectively (**Fig. 3-8, D**).

A rotation of the insertion domain of MvcA relative to the apo form facilitates its interactions with UBE2N-Ub (**Fig. 3-8, B and Fig. 3-9**). There are three contact areas between MvcA and the UBE2N portion of the substrate (A, B, and C in **Fig. 3-8, E-G**). In the contact area A, four basic residues (Arg₆, Arg₇, Lys₁₀ and Arg₁₄) from the amino terminal helix (α 1) of the UBE2N portion of the substrate forms a positively charged surface, which interfaces a region formed by the α 8 helix of MvcA and an adjacent loop presenting four negatively charged residues (Asp₂₀₈, Glu₂₁₃, Glu₂₁₄ and Glu₂₁₆) (**Fig. 3-8, E and Fig. 3-9, A and B**). In addition to electrostatics, hydrogen bonding between the interfacing residues also appears to contribute to substrate recognition in this contact area (**Fig. 3-8, E**). Contact B contributes to the recognition by bringing a hydrophobic pocket in UBE2N formed by six residues (Leu₈₈, Trp₉₅, Leu₉₉, Ile₁₀₀, Val₁₀₄ and Ile₁₀₈) into proximity of Leu₃₃₀ of MvcA, also featuring hydrogen bonds between the chains of Asn₃₃₁ of MvcA and Leu₉₁ of UBE2N (**Fig. 3-8, F**). Interactions in Contact C are mediated by two hydrogen bonds formed between Arg₃₂₂ of MvcA and the backbone atoms of Ala₁₁₄ and Pro₁₁₅ of UBE2N (**Fig. 3-8, G**). Taken together, these results reveal that the insertion domain plays an important role in MvcA's ability to recognize UBE2N-Ub, particularly its UBE2N part. Given the similarity between MvcA and canonical ubiquitin deamidases such as CHBP, we proposed that MvcA might have evolved from such CHBP-like enzymes by acquiring the insertion domain. In support of this model, deletion of this domain resulted in MvcA mutants that retained the ubiquitin deamidase activity (Valleau et al., 2018) but failed to hydrolyze UBE2N-Ub (**Fig. 3-10**).

To validate the roles of the residues predicted to be important for substrate recognition by MvcA based on the crystal structure, we created MvcA mutants with mutations in Arg₁₄₀, Asp₂₀₈, Glu₂₁₄, Glu₂₁₆, Arg₃₂₂ and Leu₃₃₀, respectively. With the exception of MvcAE_{214A}, which still effectively cleaved UBE2N-Ub, the deubiquitinase activity of other mutants has been

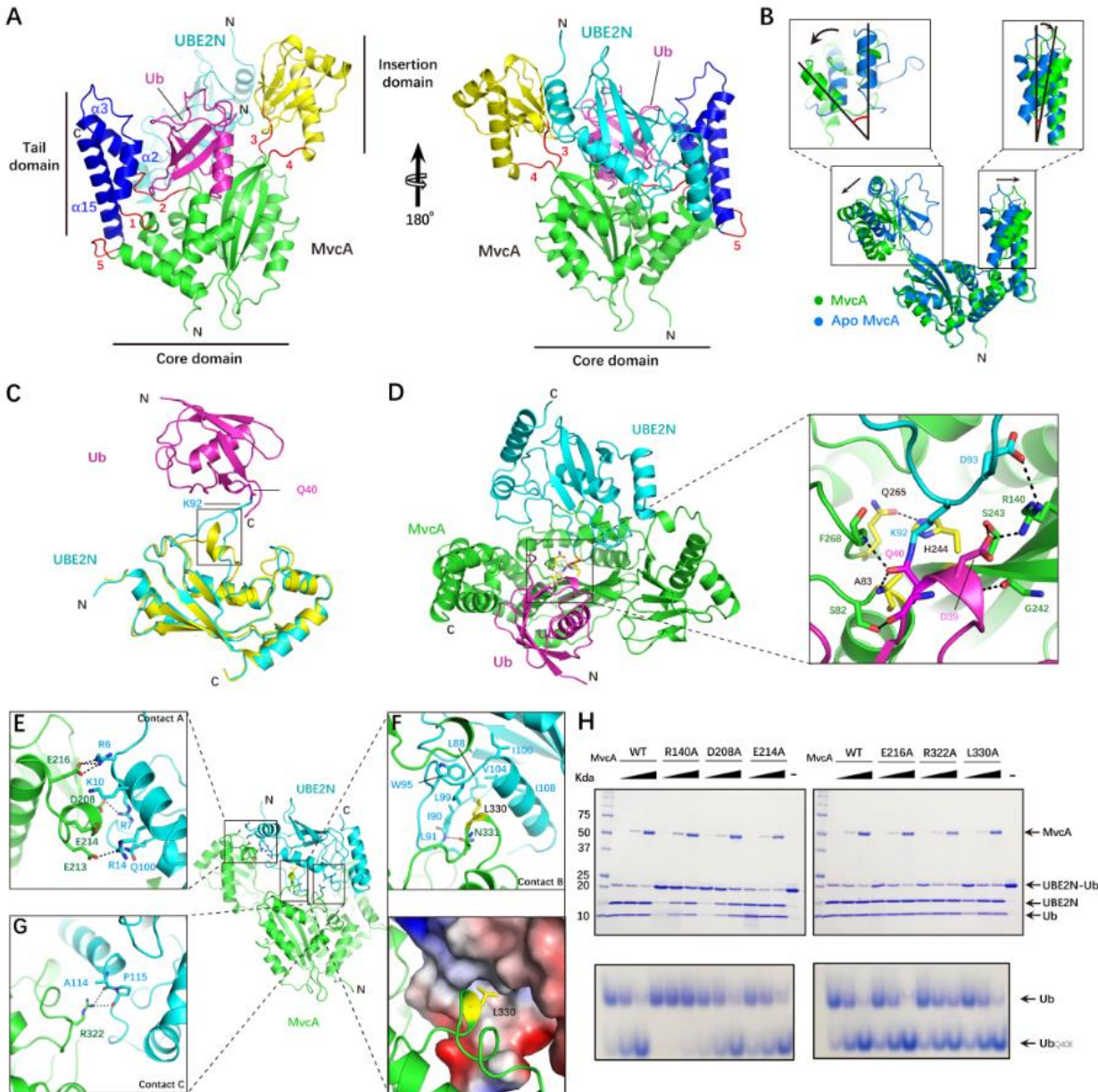
compromised (**Fig. 3-8, H**). Mutations in Arg₁₄₀ or Asp₂₀₈ severely affected the ability to remove ubiquitin from UBE2N-Ub, but only Arg₁₄₀ is critical for the ubiquitin deamidase activity, indicating that this residue is important for both activities (**Fig. 3-8, H**). In contrast, Asp₂₀₈ is one of the four residues whose side chains contribute to the formation of a negatively charged loop involved in recognizing the UBE2N portion of the substrate, which explains its minor role in ubiquitin deamidation. The defects displayed by MvcA_{E216A}, MvcA_{R322A} and MvcA_{L330A} were detectable but not severe, which is consistent with their role as one of the several residues contributing to substrate binding (**Fig. 3-8, E-G**).

Differing from MvcA, which has undergone a conformational change in the complex (**Fig. 3-8, B**), the structure of ubiquitin is almost identical to that of the free form or in complex with CHBP (C α rmsd of 0.86 Å) (Yao, Cui et al., 2009) except for the highly flexible carboxyl tail (**Fig. 3-11, A**). The combined surface area of the interface between MvcA and ubiquitin is close to 1356.6-Å², which corresponds to 6.6% and 28.1% of the total surface area of MvcA and ubiquitin, respectively. Ubiquitin is situated in the deep cleft between the core domain and the tail domain region, where it makes contacts with MvcA via hydrogen bonds and hydrophobic interactions contributed by 5 distinct contact regions (A-D and the carboxyl terminus contact) (**Fig. 3-11, B and C**). Contact A contains hydrogen bonds formed by Arg₅₀ of MvcA and backbone carbonyls of Lys₆ and Leu₆₉ of ubiquitin (**Fig. 3-11, D**). Contact B is mediated by hydrophobic interactions between the loop linking the two arms of the β-hairpin in the amino end of ubiquitin and a hydrophobic pocket of MvcA. Specifically, Leu₈, Thr₉ and Gly₁₀ in the hydrophobic loop of ubiquitin engage the hydrophobic pocket formed by Val₃₃, Thr₃₆, Val₃₈, Pro₃₉, Val₄₂, Leu₄₃, Met₄₆ and Met₇₆ of MvcA (**Fig. 3-11, E**). In Contact C, the α1 helix of ubiquitin forms four hydrogen bonds with residues of MvcA, including Gln₃₁(Ub):Glu₁₃₇(MvcA), Asp₃₂(Ub):His₁₀₄(MvcA), Glu₃₄(Ub):Asn₈₈(MvcA) and Gly₃₅(Ub):Arg₁₃₅:(MvcA) (**Fig. 3-11, F**). Interestingly, hydrogen bonding between Gln₃₁(Ub) and Glu₁₃₇(MvcA) is also important in the recognition of ubiquitin by MvcA as a deamidase (Valleau et al., 2018). Contact D contains mostly a single hydrogen-bonding interaction between Glu₂₄ of ubiquitin and Lys₁₇₇ of MvcA (**Fig. 3-11, G**). The flexible tail of ubiquitin is held by contacts with an adjacent groove of MvcA via hydrogen-bonding interactions involving mostly backbone atoms of the tail and side chain of Arg₇₂ of ubiquitin (**Fig. 3-11, H**). Inspection of a superimposed image of the apo and the complex structure reveals that certain regions on apo MvcA were occluded for ubiquitin binding (**Fig. 3-11, B**). These clashes are

removed in the complex due to an outward movement of the tail domain (indicated by the black arrow in **Fig. 3-11, B**) and the same motion of the insertion domain required for engagement of UBE2N. These observations highlight once again the induced fit nature of MvcA-substrate interaction.

Fig. 3-8 Structural analysis of the mechanism of substrate recognition and catalysis by MvcA.

A. Ribbon representation of the MvcA-UBE2N-Ub complex observed in the crystals. For MvcA, the tail domain (blue), core domain (green) and the insertion domain (yellow) of MvcA are shown. The tail domain contains three helices (α_2 , α_3 and α_{15}). The linkers between the tail domain and the core domain are termed loop 1, 2 and 5 (red) and those that connect the insertion domain and the core domain are termed loop 3 and 4 (red). Ubiquitin (Ub) is shown in magenta and UBE2N in cyan. The view on right is generated by rotating the structure shown on the left by 180 degrees around the indicated axis. **B.** The movement of the tail domain and the insertion domain in MvcA upon substrate binding. Note the shift (arrows) of the tail domain (right) and the insertion domain between Apo MvcA(marine) and MvcA in the complex (green). The left box highlights the rotation suffered by the insertion domain upon complex formation, and the right box shows the rotation observed in the tail domain. **C.** The structure of UBE2N (cyan)-Ub (magenta) in the complex. Lys₉₂ of UBE2N and Gln₄₀ of ubiquitin linked by an isopeptide bond produced from MavC catalyzed transglutamination are shown as sticks. The conformational change of the β_{10} helix of UBE2N is indicated by a box. The structure of UBE2N (PDB code: 1JAT) not conjugate to ubiquitin is shown in yellow for comparison. **D.** Key residues involved in the formation of the catalytic center from MvcA (green) and their interactions with UBE2N-Ub (UBE2N, cyan; Ub, magenta). Residues in the catalytic triad (Ala(Cys)₈₃-His₂₄₄-Q₂₆₅, yellow), Ser₂₈₂, Arg₁₄₀, Gly₂₄₂, Ser₂₄₃, and Phe₂₆₈ of MvcA, Lys₉₂ and Asp₉₃ of UBE2N, as well as Asp₃₉ and Gln₄₀ of Ub are shown in sticks. Hydrogen bonds are shown as dashed lines. **E-G.** Detailed views of UBE2N contact patches A (E), contact B (F) and contact C (G). Key residues involved in interactions between MvcA (green) and UBE2N (cyan) are labeled and shown as sticks. Leu₃₃₀ of MvcA is labeled in yellow stick in the bottom right panel, which shows it interacting with a nonpolar pocket of UBE2N (shown in electrostatic surface). Hydrogen bonds are shown as dashed lines. **H.** Mutational analysis of residues important for substrate recognition by MvcA predicted by structural analysis. For deubiquitination reactions, 0.05, 0.25 or 1.25 μ g of each mutant protein was incubated with 2.0 μ g UBE2N for 30 min in 25 μ l reactions. For ubiquitin deamidase activity, 0.25, 0.5 or 1.0 μ g of MvcA was incubated with 10 μ g of ubiquitin for 60 min in 25 μ l reactions. Proteins resolved by SDS-PAGE or native PAGE gels were detected by CBB staining. Note: except panel H, the structural work was performed by Dr. Hongxin Guan and colleagues at Fujian Normal University.



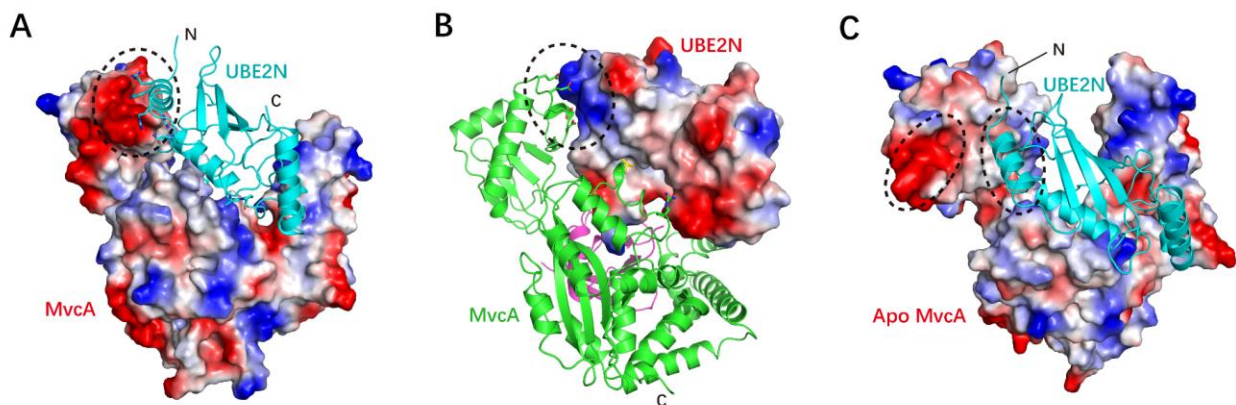


Fig. 3-9 Binding of the substrate UBE2N-Ub induces conformational changes in MvcA.

A-B. Electrostatic interactions between the insertion domain of MvcA and UBE2N. Positively charged residues of UBE2N were shown as sticks and negatively charged region of MvcA is indicated by a dashed circle. MvcA (electrostatic surface)-UBE2N (cyan ribbon) (**A**). Negatively charged residues of MvcA are shown as sticks and the positively charged region of UBE2N is indicated by a dashed circle. MvcA (green ribbon)-UBE2N (electrostatic surface)-Ub(magenta ribbon) (**B**). **C.** A docking model of Apo MvcA (electrostatic surface)-UBE2N (ribbon). Negatively charged regions of MvcA and the positively charged α 1 of UBE2N are indicated by dashed circles. Note: the structural work was performed by Dr. Hongxin Guan and colleagues at Fujian Normal University.

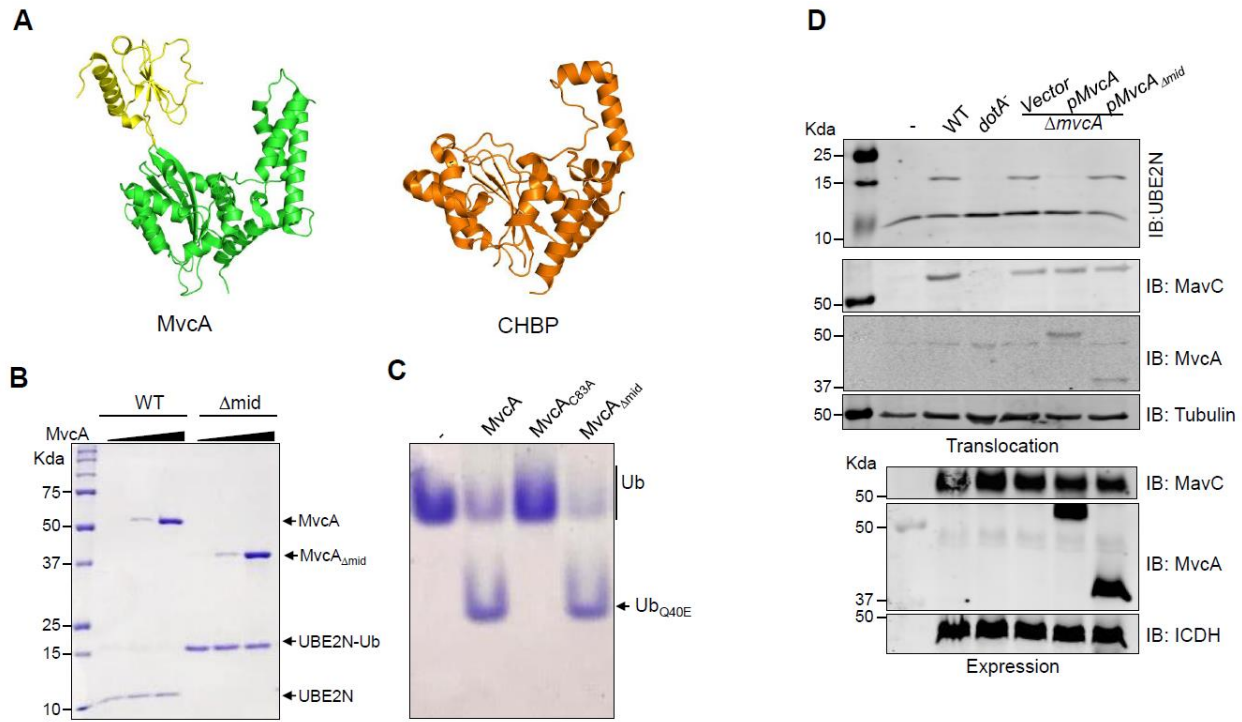


Fig. 3-10 The insertion domain of MvcA is essential for its deubiquitinase activity but not ubiquitin deamidase activity.

A. The structures of MvcA (left, PDB: 5SUJ and our own structure, PDB: 6K11) and CHBP (right, PDB: 4HCN). **B.** A MvcA mutant lacking the insertion domain has lost the ability to cleave UBE2N-Ub. Reactions containing the indicated components were allowed to proceed for 30 min before SDS-PAGE and CBB staining. **C.** A MvcA mutant lacking the insertion domain (Δmid) still deamidates ubiquitin. Ubiquitin was incubated with MvcA or the Δmid mutant and the reaction products separated by native-PAGE were detected by CBB staining. **D.** The insertion domain of MvcA is required for UBE2N-Ub cleavage during *L. pneumophila* infection. Raw 264.7 cells were infected with the indicated bacterial strains for 2 h at an MOI of 10, and the modification of UBE2N was probed by immunoblotting. The expression (lower panels) and translocation (middle panels) of MavC, MvcA and the Δmid were probed with antibodies specific for MavC and MvcA, respectively. Note that although Δmid was translocated into infected cells, it failed to abolish MavC-induced ubiquitination of UBE2N.

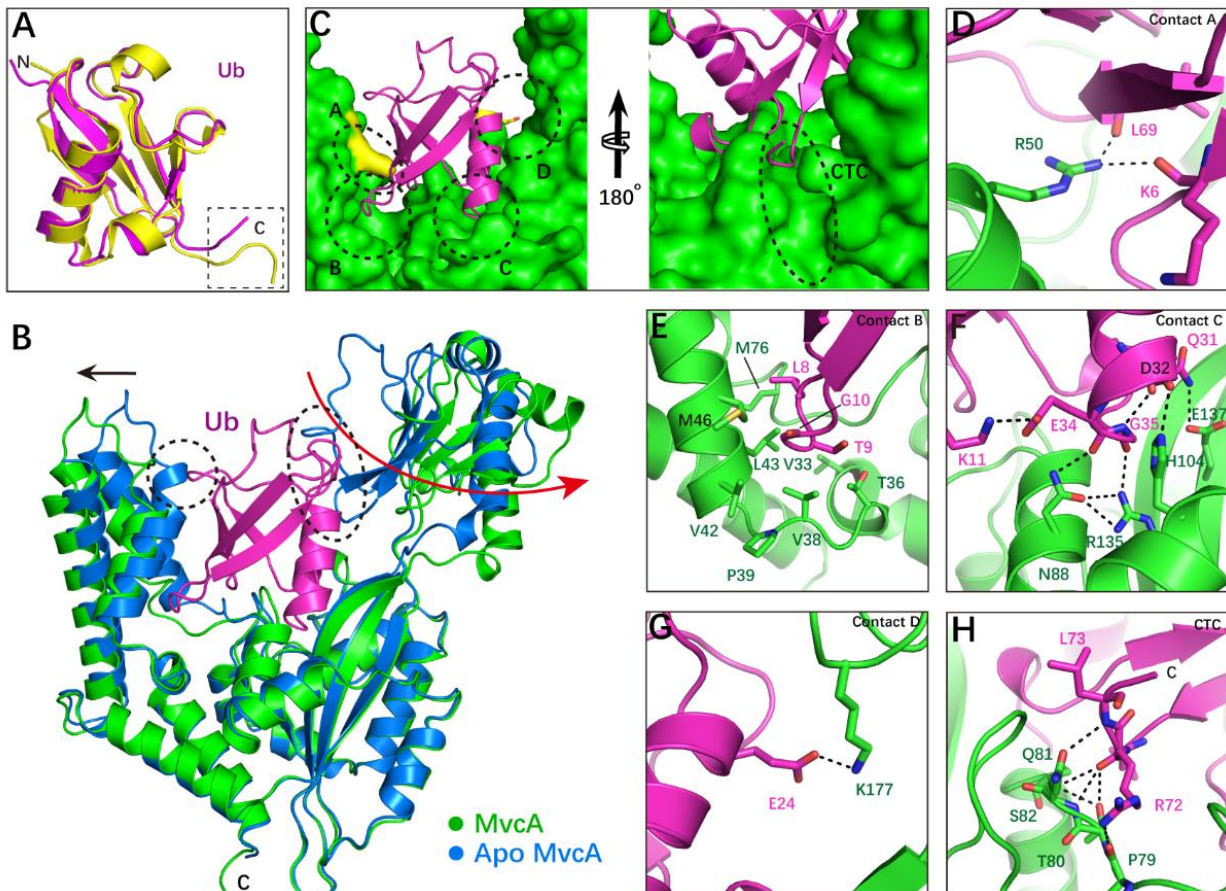


Fig. 3-11 Interactions between MvcA and the ubiquitin portion of UBE2N-Ub.

A. Structural alignment of ubiquitin (magenta) from the MvcA-UBE2N-Ub complex and Ub (yellow) from CHBP-Ub (PDB code:4HCN), the carboxyl tails are indicated by a dashed box. **B.** Overall structure of MvcA(green)-ubiquitin(magenta) from the complex in comparison with Apo MvcA (blue). The conformational changes are indicated by two arrows, the black one indicates the shift of the tail domain and the red one indicates the rotation of the insertion domain. The potential clash areas between Apo MvcA and ubiquitin are indicated by a dashed circles. **C.** The five contacting interfaces between MvcA(green surface) and ubiquitin(magenta), each is indicated by a dashed circle and a letter from A-E. The image on the right is obtained by a 180° rotation of the left structure around the indicated axis. The interaction patch involving the C-terminal tail of ubiquitin is indicated by dashed circle. CTC: carboxyl terminus contacts. **D-H.** Detailed views of contact areas A (D), contact B (E), contact C (F), contact D (G)and the carboxyl terminus contact (CTC) (H). Key residues involved in interactions between MvcA and ubiquitin are labeled and shown as sticks. The hydrogen bonds are shown as dashed lines. Note: the structural work was performed by Dr. Hongxin Guan and colleagues at Fujian Normal University.

MvcA restores the activity of UBE2N and allows NF-κB activation

UBE2N is involved in the formation of K63-type polyubiquitin chains that regulate multiple cellular processes including endocytosis, inflammatory and DNA damage response pathways (Hodge et al., 2016). Because active NF-κB is required for maximal *L. pneumophila* intracellular replication (Losick & Isberg, 2006), constitutive expression of MavC may affect virulence due to prolonged inhibition of NF-κB activation. UBE2N is positioned relatively upstream of the signaling components involved in NF-κB activation (Skaug, Jiang et al., 2009), inhibition of its activity by MavC would lead to accumulation of IκBα in cells challenged by *L. pneumophila*. Indeed, we detected higher levels of IκBα in cells infected with the strain *ΔmavCΔmvcA* overexpressing MavC compared to those harboring the empty vector or expressing the inactive MavCC_{74A} mutant (**Fig. 3-12, A**). To test the impact of extended UBE2N inhibition on intracellular bacterial replication, we infected cells ectopically expressing MavC or MavCC_{74A} with *L. pneumophila* and assessed its growth by monitoring the formation of replicative vacuoles containing multiple bacteria. Comparing to untreated cells or cells expressing MavCC_{74A}, cells expressing MavC yielded significantly more vacuoles of smaller size enclosing 1-2 bacteria (**Fig. 3-12, B**). Furthermore, in cultured macrophages, overexpression of MavC in strain *ΔmavCΔmvcA* caused approximately a 5-fold growth defect 72 h after uptake (**Fig. 3-12, C**). Thus, a timely relief of the MavC-induced inhibition of UBE2N activity is important for bacterial virulence. Indeed, in cells infected with wild type *L. pneumophila*, the level of UBE2N-Ub began to decrease at 3 h postinfection (psi) and became almost undetectable at 6 h psi. In contrast, in cells infected with strain *ΔmvcA*, UBE2N-Ub was still readily detectable at 10 h psi (**Fig. 3-12, D**). Thus, MvcA functions to modulate the activity of MavC by reversing UBE2N ubiquitination to allow NF-κB activation after the initial phase of infection.

Despite extensive efforts, we were unable to detect MvcA in broth-grown bacteria (**Fig. 3-2, A, lower panel**). Yet, in bacteria isolated from host cells, MvcA became detectable 5 h psi (**Fig. 3-12, E**), suggesting that the gene was induced several hours after bacterial uptake, which is in line with the level of UBE2N modification (**Fig. 3-12, D**). These results predict that MvcA will counteract the inhibitory effects of MavC on NF-κB activation. Indeed, in cells infected with *ΔmvcA* overexpressing MvcA, the level of IκBα quickly decreased but failed to recover, which is accompanied by more nuclear translocation of p65. In contrast, IκBα recovered 60 min psi in cells

infected with strain *ΔmvcA*(pMvcAc_{83A}), indicating the inhibition of NF-κB activity by MavC (**Fig. 3-12, F and G**).

Fig. 3-12 MvcA counteracts the effects of MavC during *L. pneumophila* infection.

A. Overexpression of MavC but not the inactive mutant MavCC_{74A} in the *ΔmavCΔmvcA* mutant background causes I κ B α accumulation in infected cells. U937 cells infected with the indicated bacterial strains at an MOI of 5 were probed for I κ B α . Tubulin was probed as a loading control.

B. Prolonged UBE2N modification by MavC restricts bacterial vacuole maturation. HEK293 cells transfected to express MavC or MavCC_{74A} were infected with wild type *L. pneumophila* expressing GFP for 12 h. The vacuole was scored and categorized by the number of bacteria it contained. Data shown were from three independent experiments, each with at least 300 vacuoles counted. *, p<0.05; **, p<0.01; n.s., not significant.

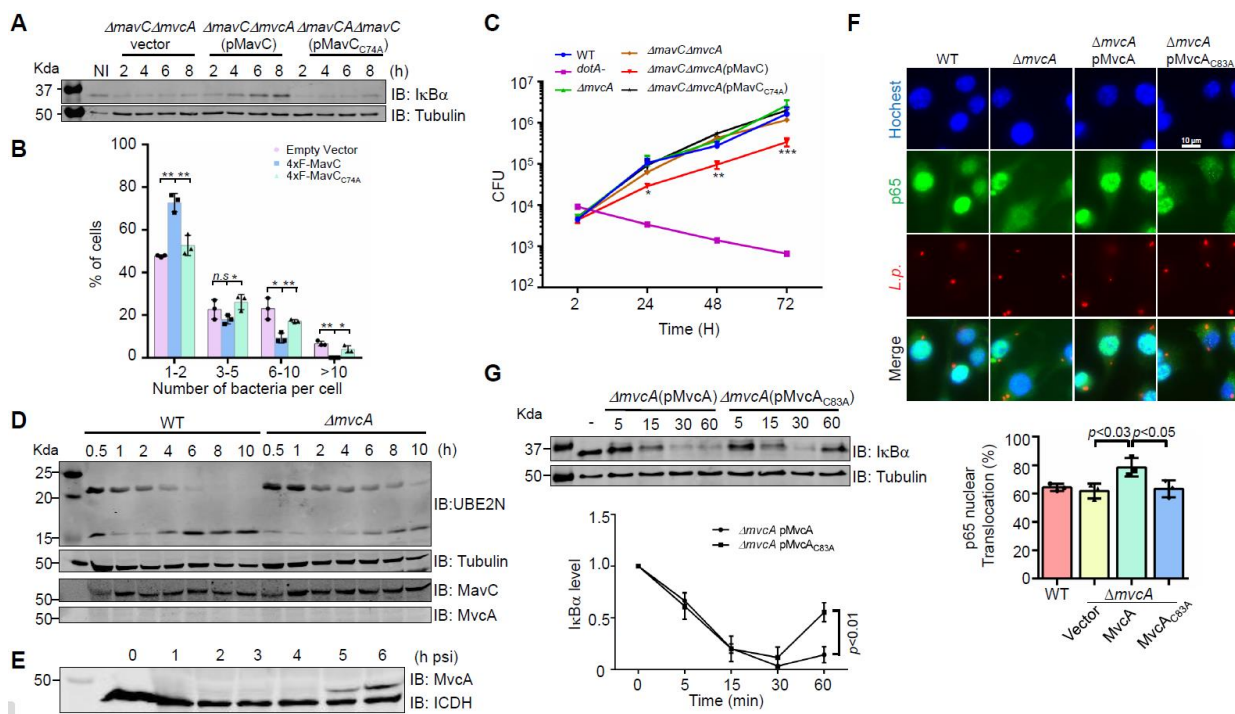
C. Overexpression of MavC but not MavCC_{74A} affects intracellular growth of the *ΔmavCΔmvcA* mutant of *L. pneumophila*. Raw264.7 cells were infected with the indicated bacterial strains and intracellular bacteria were determined at the indicated time points. Each strain was examined in triplicate and similar results were obtained in two independent experiments. *, p<0.1; **, p<0.01; ***, p<0.001(t-test by comparing p(MavC) with p(MavCC_{74A})).

D. MvcA is required for reversal of UBE2N modification during *L. pneumophila* infection. U937 cells infected with wild type or the *ΔmavcA* mutant were withdrawn at the indicated time points. Samples resolved by SDS-PAGE were probed for UBE2N, translocated MavC and MvcA. Tubulin was probed as a loading control. Note that in samples infected with the *ΔmavcA* strain, the level of UBE2N-Ub decreased at slower rates.

E. MvcA becomes detectable in intracellular bacteria several hours after uptake. U937 cells infected with wild type *L. pneumophila* at an MOI of 10 were lysed at the indicated time and recovered bacteria were probed for MvcA by immunoblotting. The bacterial isocitrate dehydrogenase (ICDH) was probed sequentially as a loading control.

F. MvcA restores the nuclear translocation of p65 inhibited by MavC during *L. pneumophila* infection. Raw264.7 cells were infected with the indicated *L. pneumophila* strains for 2 h at an MOI of 1. Fixed cells were immunostained with antibodies specific for p65 and the bacterium, respectively. Host nuclei were labeled with Hoechst. Representative images of cells in each sample category were shown (upper panels); nuclear localization of p65 was determined by scoring at least 300 infected cells (lower panel). Results shown were from three independent experiments done in triplicate.

G. Overexpression of MvcA but not its inactive mutant MvcAC_{83A} promotes I κ B α degradation during *L. pneumophila* infection. U937 cells were infected with the indicated bacterial strains at an MOI of 5. Lysates of cells infected for the indicated time were probed for I κ B α . Tubulin was probed as a loading control (upper panels). I κ B α levels at the indicated time points were evaluated by measuring the band intensity from three independent experiments (lower panel).



Discussion

The observation that the two structurally similar proteins MavC and MvcA function to regulate the activity of UBE2N with opposite biochemical effects points to the differential need of this E2 enzyme during *L. pneumophila*; it also highlights the diversity of mechanisms involved in controlling ubiquitin signaling by posttranslational modifications (Song & Luo, 2019). Given their high similarity (Cui et al., 2010, Valleau et al., 2018), MavC and MvcA likely are evolved from canonical ubiquitin deamidases such as CHBP and Cif by acquiring the insertion domain. These proteins then diverged at one point to confer opposing biochemical activities in regulating the activity of UBE2N. The acquisition of the insertion domain enables MvcA to recognize UBE2N-Ub. Although the ubiquitin portion is not the substrate of its deamidase activity, the interactions between MvcA and the ubiquitin portion of the substrate in the MvcA-UBE2N-Ub structure bear some similarity to those seen between Cif_{Bp} and ubiquitin or NEDD8 (Yao et al., 2009), which was also proposed by Savchenko and colleagues (Valleau et al., 2018). It likely that the insertion domain in MavC is also involved in recognizing UBE2N by MavC, but the mechanism of such recognition and whether and how it differs from the recognition of UBE2N-Ub by MvcA needs further investigation. Although the exact source remains unknown, the evolutionary pressure that led to the acquisition of the deubiquitinase activity of MvcA likely came from host cells in which the inhibitory effects of MavC needs to be relieved. The regulation of UBE2N activity by MavC and MvcA with opposite biochemical function extends the list of *L. pneumophila* effectors that function to regulate the activity of another effector (Qiu & Luo, 2017a, Urbanus et al., 2016). Such effectors, also called meta-effectors (Kubori et al., 2010) often function to impose spatiotemporal regulation of the activity of other effectors by potentially diverse mechanisms (Qiu & Luo, 2017a, Urbanus et al., 2016). The temporal regulation of MavC imposed by MvcA is achieved by the differential expression of the genes at different stages of the intracellular life cycle. The *mavC* and *mvca* genes are separated by 76 base pairs, which may allow independent regulation of transcription (**Fig. 3-1, A**). Yet, the mechanism underlying their differential expression awaits further investigation. With antibodies raised for MvcA, we could not detect the protein in bacterial cells grown at all the growth phases in a bacteriological medium (**Fig. 3-12, E**), which differs from an earlier study that tagged a 3xFlag epitope to the amino termini of the proteins (Valleau et al., 2018). Such discrepancy may be caused by differences in the sensitivity of the antibodies. Alternatively, the addition of the 3xFlag epitope tag to the 5-prime end of these genes may have

caused unintended consequences of altered expression pattern of the genes. Although we can detect the protein in *L. pneumophila* isolated from host cells 6 h postinfection, translocated MvcA was not detectable in infected cells at this time of infection (**Fig. 3-12, E**). Given the clear reversal of UBE2N ubiquitination by MvcA (**Fig. 3-12, E**), the inability to detect this protein at this time point may be due to the low quantity of protein delivered into host cells, degradation by host machineries such as the ubiquitin-proteasome system or a combination of these factors (Dorer et al., 2006, Kubori & Galan, 2003, Kubori et al., 2010).

The regulation of MavC activity by MvcA is further complicated by the activity of Lpg2149, which inhibits the deamidase activity of both proteins, the ubiquitination activity of MavC (Valleau et al., 2018) and the deubiquitinase activity of MvcA (**Fig. 3-6, A**). The fact that *lpg2149* was expressed at the highest level when the bacteria grew to the early exponential phase (**Fig. 3-6, B**) suggests that this protein exerts its inhibitory role when the bacteria have begun to replicate. The biological significance, the exact time and extent to which such inhibition occurs await further investigation. The genes *mavC*, *mvcA* and *lpg2149* are present only in some isolates of *L. pneumophila*, but not in other species (Burstein et al., 2016). Because isolates within the *L. pneumophila* species are responsible for most of the reported *Legionella* infection (Newton et al., 2010), it is thus tempting to speculate that these genes contribute the adaption of *Legionella* to hosts such as humans. MavC and MvcA are functionally similar to transglutaminases(TGs), some of which are known to cleave peptide bonds in biochemical reactions without any clear physiological relevance (Kiraly, Thangaraju et al., 2016, Lorand & Graham, 2003, Parameswaran, Cheng et al., 1997). MvcA is thus the first TG functional homolog with a biologically significant peptidase activity.

At first glance, the deubiquitinase reaction and ubiquitin deamidation seem to be related because both involve hydrolytic release of an amine group from the Gln side chain. However, the two reactions occur in two different contexts with distinct substrate preference, hence they are biochemically distinct: the deamidation can occur without the presence of the E2 substrate but the isopeptidase activity requires E2 binding elements in the enzyme (such as the insertion domain). The thioester intermediate can form from the ubiquitin substrate alone but its formation from the UBE2N-Ub substrate requires the presence of the UBE2N portion of the substrate. The ability of

the catalytic triad of MvcA to catalyze two different biochemical reactions is reminiscent of a number of enzymes that have dual activities catalyzed by a single motif. For example, some archaea contain an enzyme that functions as both a fructose 1,6-bisphosphate (FBP) aldolase and FBP phosphatase (Say & Fuchs, 2010). The *Chlamydia* effector ChlaDub1 utilizes the same motif to catalyze deubiquitinase and acetyltransferase activities (Pruneda, Bastidas et al., 2018). More relevant, in addition to specifically cleaving the isopeptide bond between Pup and the substrate lysine residue, the depupylose Dop from *Mycobacterium tuberculosis* deamidates the Gln residue at the carboxyl terminus of Pup, the prokaryotic ubiquitin-like protein, prior to its ligation to the substrate induced by the ligase PafA (Burns, Cerda-Maira et al., 2010, Pearce, Mintseris et al., 2008). Interestingly, Dop and PafA are structural homologs (Ozcelik, Barandun et al., 2012). More studies are needed to analyze how these enzymes achieve the high-level of reaction specificity despite seemingly similar substrate recognition features. Furthermore, as some of these enzymes function exclusively in host cells, it will be interesting to determine whether enzyme pairs with similar properties exist in eukaryotes.

CHAPTER 4. OVERALL DISCUSSION

E2 enzymes are one essential component of the canonical ubiquitination machinery. In addition to acting as the transition point between E1 and E3 enzymes, E2s function in dictating the chain type and substrate specificity (Stewart et al., 2016). A minimal of 13 E2 enzymes are shared among all eukaryotes, which are believed to fulfill the most basic cellular functions. UBE2N is one of those basic E2s, which along with its heterodimeric partners UBE2V1 and UBE2V2, function together with various E3 enzymes to specifically catalyze the formation of K63-type polyubiquitin chains (Hodge et al., 2016, Stewart et al., 2016, Ye & Rape, 2009). K63-type polyubiquitin chains are important in multiple signaling transduction cascades including the pathways in NF-κB activation (Sanada et al., 2012), DNA repair (Thorslund, Ripplinger et al., 2015), autophagy (Fiesel, Moussaud-Lamodiere et al., 2014) and vesicle trafficking (Ikeda & Dikic, 2008).

NF-κB is a major immune transcriptional factor that becomes activated in response to diverse stimuli including bacterial infections. NF-κB activation triggered by immune agonists such as flagellin and lipopolysaccharides attributes to the initiation of the bacterial clearance mechanism of host cells (Bartfeld et al., 2009). It is essential for bacterial pathogens to counteract such defense induced by NF-κB activation. Infection by *L. pneumophila* appears to cause a two-phased NF-κB activation induced by pathogen-associated molecular patterns (PAMPs) and Dot/Icm effectors, respectively (Bartfeld et al., 2009, Losick & Isberg, 2006). Here, we show that MavC functions to dampen NF-κB activation by ubiquitinating UBE2N, which appears to counteract the activation induced by PAMPs associated with the bacteria, likely sensed by members of the TLR immune receptors (Gan, Nakayasu et al., 2019b, Kieser & Kagan, 2017). In addition, NF-κB also regulates several other key cellular processes including cell survival (Hodge et al., 2016, Ye & Rape, 2009). The viability of host cells is essential for productive growth of intracellular pathogens. Therefore, the activity of NF-κB needs to be tightly regulated. In line with this notion, several *L. pneumophila* effectors including LegK1 and LnaB have been shown to activate NF-κB. LegK1 is a kinase that phosphorylates IκBα and p100, leading to the degradation of IκBα and the maturation of p100, respectively (Ge et al., 2009). The mechanism of action of LnaB in NF-κB activation is not well understood (Losick et al., 2010). The inhibition of NF-κB activation imposed by MavC contradicts

with the requirement of NF-κB activation at later stages of infection. Therefore, the inhibition of NF-κB activation imposed by MavC may need to be reversed. Our results show that the reversal is achieved by the effector MvcA, the structural homolog of MavC, at about 5 hours post infection. MvcA specifically removes Ub from UBE2N-Ub induced by MavC, liberating UBE2N to catalyze K63-linked polyubiquitin chains and perform its role in NF-κB activation.

Besides NF-κB activation, UBE2N plays critical roles in several other signaling events known to be important for the life cycle of *L. pneumophila*, including the autophagy and vesicle trafficking pathways. Eukaryotic cells use the autophagy pathway to sequester cytosolic proteins and organelles into autophagosomes, which fuse with lysosomes to promote cargo degradation (Kuballa, Nolte et al., 2012, Xie & Klionsky, 2007). Intracellular bacterial pathogens can also be targeted for lysosomal degradation by a branch of the autophagy machinery termed xenophagy (Levine, 2005, Lum, Bauer et al., 2005). K63-linked polyubiquitination on ULK1 and Beclin1 is required for the initiation of autophagy. Furthermore, K63-linked polyubiquitin chains on autophagic substrates are essential for their recognition by the autophagy receptor p62 (Grumati & Dikic, 2018, Shaid, Brandts et al., 2013). *L. pneumophila* extensively modulates the host vesicle trafficking pathways. UBE2N regulates subcellular trafficking, especially the endocytosis pathway by mediating ubiquitination of various plasma membrane proteins and components of the endocytic machinery (Erpapazoglou, Walker et al., 2014, Ikeda & Dikic, 2008). For example, the loss of UBE2N-dependent K63-linked polyubiquitination in *C. elegans* blocks the degradation of maternal membrane proteins, causing their recycling to the cell surface (Hodge et al., 2016, Sato, Konuma et al., 2014). In this study, we only examined the impact of MavC and MvcA on the activity of UBE2N in NF-κB activation, it is possible that modulation of UBE2N by MavC and MvcA also interferes with xenophagy or vesicle trafficking to benefit the bacterium.

Given the importance of UBE2N in multiple important pathways, it is not surprising that UBE2N is subjected to precise regulation via several different posttranslational modifications. Although the enzymes involved are not clear, UBE2N is ISGylated at Lys92, which abolishes the conjugation of ubiquitin to its catalytic cysteine residue and the formation of K63-linked polyubiquitin chains (Zou et al., 2005). UBE2N is deamidated by the *Shigella flexneri* effector OspI at Gln₁₀₀, which abolishes its interaction with TRAF6 and specifically dampens the diacylglycerol-CBM (CARD-BCL10-MALT1) complex-TRAF6-NF-κB signaling pathway

(Sanada et al., 2012, Song & Luo, 2019). Whether other types of modification occur on UBE2N by endogenous enzymes or infectious agents is worth of investigation.

MavC and MvcA are 50% identical in their primary sequences, and are highly similar in structures (Valleau et al., 2018). Each of these proteins are composed of the insertion domain and the core domain. The core domain highly resembles the canonical ubiquitin deamidases such as type 3 secretion system (T3SS) effectors CHBP and Cif from *Burkholderia pseudomallei* and *Yersinia pseudotuberculosis*, respectively (Crow et al., 2012, Cui et al., 2010). MavC and MvcA likely are evolved from canonical ubiquitin deamidases by acquiring the insertion domain, which involves in interacting with the substrate UBE2N (Valleau et al., 2018). The acquisition of the insertion domain enables MavC and MvcA to recognize UBE2N and UBE2N-Ub, respectively. In line with this notion, the MvcA insertion domain truncation mutant loses its activity to deubiquitinate UBE2N-Ub but remains the ubiquitin deamidase activity. Whether the MavC insertion domain truncation mutant behaves similarly has not been studied. Given the similarity between MavC and MvcA, these two proteins likely are evolved from the same ancestor then diverged at one point to confer opposing biochemical activities in regulating the activity of UBE2N. Although the exact source is unknown, the evolutionary pressure that led to the acquisition of the deubiquitinase activity of MvcA likely came from host cells in which the inhibitory effects of MavC needs to be relieved. The identification of the eukaryotic sources of the insertion domains would pave the way for the study the evolution of these proteins. In addition, future study is also needed to elucidate the potential evolutionary relationships among CHBP/Cif, MavC and MvcA, and the potential corresponding proteins in eukaryotes. Finally, whether the insertion domain can be modified to recognize other E2 enzymes beyond UBE2N is also equally intriguing to pursue.

The study of MavC and MvcA provides an example of balanced regulation of the activity of UBE2N and the host NF- κ B activation by bacterial effectors, which is a common phenomenon in the modulation of host function by *L. pneumophila*. For example, *L. pneumophila* effector SidM AMPylates the small GTPase Rab1 (Muller et al., 2010), SidD deAMPylates Rab1 (Tan & Luo, 2011a). AnkX phosphorylcholinates Rab1, a modification that is reversed by Lem3 dephosphorylcholinates (Tan et al., 2011). The activity of SidE family such as SdeA is regulated by SidJ which functions as a calmodulin-dependent glutamylase that specifically modifies SdeA at Glu₈₆₀, one of the catalytic residues of its mono-ADP-ribosyltransferase activity. The glutamylation on SdeA imposed by SidJ completely abolishes its activity to modify ubiquitin and

protein substrates (Black, Osinski et al., 2019, Gan el al., in press). The activity of those *L. pneumophila* effectors demonstrates that modulation of a specific cellular activity often is tightly regulated to ensure host cell homeostasis. Such balanced regulation can be either achieved by forward and reverse modifications on a host protein, or through the regulation of one effector by another effector. Furthermore, it is worth noting that MavC and MvcA is the only effector pairs known to confer opposite biochemical activities with structurally similar domains. The N-terminal region of SidM resembles that of nucleotidyl transferases, while the catalytic domain of SidD is similar to members of metal-dependent protein phosphatases (Chen, Tascon et al., 2013, Muller et al., 2010). AnkX has an atypical Fic domain comprised of two sub-domains, of which the second carries a canonical Fic motif. Lem3 does not contain any predictable Fic domain, whether Lem3 shares any structural similarity to AnkX remains unknown (Campanacci, Mukherjee et al., 2013). Clearly, balanced regulation of host activity can be achieved by either same/similar domains or unrelated domains.

Given the high level similarity, the fact that MavC and MvcA are not functionally redundant is against the common notion for structural homologs. The opposite activities carried by these two proteins expand our understanding of the function and importance of structural homologs, and will inspire more discoveries on structural homologs with similar functional implications.

CHAPTER 5. MATERIALS AND METHODS

Media, bacteria strains, plasmid constructions and cell lines

The bacterial strains, plasmids and primers used in this study were listed in Table 3. *L. pneumophila* strains used in this study were derivatives of the Philadelphia 1 strain Lp02(Berger & Isberg, 1993) and were grown and maintained on CYE plates or in ACES buffered yeast extract (AYE) broth as previously described(Berger & Isberg, 1993). The *mavC*, *mvcA*, *lpg2149* and *mavC mvcA* in-frame deletion strains were constructed as described(Luo & Isberg, 2004). *mavC*, *mvcA* and *lpg2149* genes and their mutants were cloned into pZL507 (Xu, Shen et al., 2010) for complementation. The *E. coli* strains XL1-Blue was used for expression and purification of all the recombinant proteins used in this study. *E. coli* strains were grown in LB. Genes for protein purifications were cloned into pQE30 (QIAGEN) for expression. For ectopic expression of proteins in mammalian cells, genes were inserted into the 4xFlag CMV vector(Qiu et al., 2016) or the 3xHA CDNA3.1 vector(Sheedlo et al., 2015). HEK293, 293T cells were cultured in Dulbecco's modified minimal Eagle's medium (DMEM) supplemented with 10% Fetal Bovine Serum (FBS). Raw264.7 and U937 cells were cultured in Roswell Park Memorial Institute 1640 (RPMI 1640) medium supplemented with 10% FBS. All cell lines were regularly checked for potential mycoplasma contamination by the universal mycoplasma detection kit from ATCC (cat# 30-1012K).

Purification of proteins for biochemical experiments

Ten mL overnight *E. coli* cultures were transferred to 400 mL LB medium supplemented with 100 µg/mL of ampicillin and the cultures were grown to OD₆₀₀ of 0.6~0.8 prior to the induction with 0.2 mM isopropyl-β-D-thiogalactopyranoside (IPTG). Cultures were further incubated at 18°C for overnight. Bacteria were collected by centrifugation at 4,000g for 10 min, and were lysed by sonication in 30 mL PBS. Bacteria lysates were centrifuged twice at 18,000g at 4°C for 30 min to remove insoluble fractions and unbroken cells. Supernatant containing recombinant proteins were incubated with 1 mL Ni²⁺-NTA beads (Qiagen) at 4 °C for 2 h with agitation. Ni²⁺-NTA beads with bound proteins were washed with PBS buffer containing 20 mM imidazole for 3 times, 30x of the column volume each time. Proteins were eluted with PBS

containing 300 mM imidazole. Proteins were dialyzed in buffer containing 25 mM Tris-HCl (pH 7.5), 150 mM NaCl and 1 mM Dithiothreitol (DTT) for 16-18 h.

Transfection, infection, immunoprecipitation

Lipofectamine 3000 (Thermo Fisher Scientific) was used to transfect HEK293 and 293T cells grown to about 70% confluence. Different plasmids were transfected into 293T cells respectively. Transfected cells were collected and lysed with the Radioimmunoprecipitation assay buffer (RIPA buffer, Thermo Fisher Scientific) at 16-18 h post transfection. Or infected with indicated bacterial strains. When needed, immunoprecipitation was performed with lysates of transfected cells with HA-specific antibody coated agarose beads (Sigma cat#A2095) at 4°C for 4 h. Beads were washed with pre-cold RIPA buffer or respective reaction buffers for 3 times. All samples were resolved by SDS-PAGE gels and followed by immunoblotting analysis with the specific antibodies.

For all *L. pneumophila* infection experiments, *L. pneumophila* strains were grown to the post-exponential phase ($OD_{600}=3.0-3.6$) in AYE broth. Complementation strains were induced with 0.2 mM IPTG for 3 h at 37°C before infection. Raw 264.7 and U937 cells were infected with *L. pneumophila* strains correspondingly. Cells were collected and lysed with 0.2% Saponin on ice for 30 min. Cell lysates were resolved by SDS-PAGE and followed by immunoblotting analysis with the specific antibodies respectively. *L. pneumophila* bacteria lysates were resolved by SDS-PAGE followed by immunoblotting with the MavC and MvcA specific antibodies to examine the expression of MavC and MvcA, and isocitrate dehydrogenase (ICDH) was probed as loading control with antibodies previously described(Xu et al., 2010). For intracellular growth in Raw 264.7 cells, infection was performed at an MOI of 0.05 and the total bacterial counts were determined at 24-h intervals as described(Luo & Isberg, 2004). For immunostaining, Raw264.7 cells were challenged by *L. pneumophila* at an MOI of 1 for 2 h. Fc II plasmid and 4xFlag-MavC transfected HEK293 cells were challenged at an MOI of 1 for 2 h, then cells were washed by PBS for 3 times and infected for additional 10 h. To detect deamidated ubiquitin in cells, U937 cells were infected with relevant *L. pneumophila* strains for 6 h at an MOI of 10.

***In vitro* ubiquitination assays**

For canonical ubiquitination dropout assays, 5 µg His₆-3xHA-ubiquitin, 0.2 µg E1, 1 µg UBE2N, 1 µg UBE2V2, 1 µg MavC, 2 mM ATP and 5 mM Mg²⁺ were added into a 25 µL reaction containing 50 mM Tris-HCl (pH 7.5) and 1 mM DTT. When needed, a specific component was withdrawn from the reaction. The reactions were performed at 37°C for 2 h.

For non-canonical MavC-mediated ubiquitination reaction, 5 µg His₆-3xHA-ubiquitin or His₆-ubiquitin, 0.5 µg UBE2N, 0.05 µg MavC and 5 mM Mn²⁺ were included in a 25 µL reaction system containing 50 mM Tris-HCl (pH 7.5) and 1 mM DTT. Reaction was allowed to proceed for 1 h at 37°C. When needed, 50 µg native or boiled lysates of *E. coli*, yeast or 293T cells were added into reactions. For obtaining native lysates, *E. coli*, yeast cells were lysed by sonication, HEK293T cells were lysed by RIPA buffer without EDTA. Boiled lysates were prepared by treating cells at 100°C for 5 min. Concentrations of lysates were measured by the Bradford assay.

For ubiquitin derivatives ubiquitination assays, 5 µg His-tagged wild type or ubiquitin mutants was incubated with 0.5 µg UBE2N, 0.05 µg MavC or MavC_{C74A} in 25 µL reactions, each containing 50 mM Tris-HCl (pH 7.5), 5 mM Mn²⁺ and 1 mM DTT at 37 °C for 1 h. All ubiquitin derivatives were obtained from Boston Biochem.

K63 poly-ubiquitin chain synthesis assay

Ten µg His₆-3xHA-ubiquitin, 0.5 µg UBE2N were pretreated with 0.05 µg MavC or MavC_{C74A} in 25 µL reaction system containing 50 mM Tris-HCl (pH 7.5), and 1 mM DTT at 37 °C for 4 h. After pretreatment, reactions were supplemented with 0.5 µg E1, 0.5 µg UBE2V2, 2.5 µg TRAF6, 2 mM ATP and 5 mM Mg²⁺, and incubated at 37 °C for additional 10 min.

Ubiquitin cleavage assay

Five µg K₆₃-, K₄₈-type diubiquitin or UBE2N-Ub was incubated with 1 µg MvcA or MvcAC_{83A} in a 25 µL reaction mixture containing 50 mM Tris-HCl (pH 7.5) and 1 mM DTT. The reactions were allowed to proceed for 30 min at 37°C. To measure the activity of Lpg2149, serially diluted His₆-Lpg2149 was added to 25 µl reactions that contain 0.12 µg MvcA and 16 µg UBE2N-Ub. The reactions were allowed to proceed at 37°C for 10 min prior to detection.

Antibodies and Immunoblotting

Purified His6-MavC, His6-MvcA and His6-Lpg2149 were used to raise rabbit specific antibodies using a standard protocol (Pocono Rabbit Farm & Laboratory). The antibodies were affinity purified as described(Luo & Isberg, 2004). For immunoblotting, samples resolved by SDS-PAGE were transferred onto 0.2 µm nitrocellulose membranes (Pall Life Sciences cat#66485). Membranes were blocked with 5% non-fat milk, incubated with the appropriate primary antibodies: anti-Flag (Sigma, Cat# F1804), 1: 2000; anti-HA (Roche, cat# 11867423001), 1:5,000; anti-ICDH(Xu et al., 2010), 1:10,000; anti-tubulin (DSHB, E7) 1:10,000; anti-I_Bα (Thermo Fisher Scientific, cat#MA5-15132), 1:1,000; anti-His (Sigma, cat# H1029), 1:10,000; anti-p65 (Cell signaling, cat#8242S), 1:500 anti-UBE2N (Cell signaling, cat# 6999S, Thermo Fisher Scientific, cat# 37-1100), 1:1,000; anti-Flag (Sigma, Cat# F1804), 1: 2000; anti-actin (Sigma, cat#A2103), 1:5,000, anti-Ub K63 (Millipore, cat#05-1308), 1:1,000, anti-Ub (Santa Cruz cat#sc-8017), 1:1,000, anti-p-I_Bα (Cell Signaling, cat#9246S), 1:1000, anti-UBE2K (Cell Signaling, cat#8226S), 1:1000, anti-UBE2S (Cell Signaling, cat#11878S), 1:1000, anti-UBE2E2 (Abcam, cat#Ab177485), 1:1000. Membranes were then incubated with an appropriate IRDye infrared secondary antibody and scanned using an Odyssey infrared imaging system (Li-Cor's Biosciences).

Liquid chromatography-tandem mass spectrometry analysis

Protein bands corresponding to MavC treated ubiquitin were excised from SDS-PAGE and digested with trypsin as described elsewhere(Shevchenko, Tomas et al., 2006). These experiments were performed at Pacific Northwest National Laboratory (PNNL). The digested peptides were analyzed in C18 reversed phase column connected to a UPLC (ACQUITY, Waters) by separating with a gradient acetonitrile/0.1% formic acid (solvent B) vs. 0.1% formic acid in water (solvent A): 1% B to 8% B over 5 min and 8% B to 40% B over 95 min at 300 nL/min. Eluting peptides were directly analyzed in an Orbitrap mass spectrometer (Q-Exactive Plus, Thermo Fisher Scientific), by targeting the top 12 most intense ions to HCD fragmentation with a normalized collision energy of 30.

Samples for protein identification obtained by immunoprecipitation and crosslinking products between ubiquitin and UBE2N were analyzed at the Biological Mass Spectrometry of the Chemistry Department at Indiana University, Bloomington. Protein mixture was reduced and alkylated, followed by addition of trypsin at a 1:100 (w/w) ratio. After digestion overnight at 37°C,

the resulting peptides were desalted by Zip-tip and injected into an Easy-nLC 100 HPLC system coupled to an Orbitrap Fusion Lumos mass spectrometer (Thermo Scientific, Bremen, Germany). Peptide samples were loaded onto a house-made C18 trap column ($75\text{ }\mu\text{m} \times 20\text{ mm}$, $3\text{ }\mu\text{m}$, $100\text{ }\text{\AA}$) in 0.1% formic acid. The peptides were separated using an Acclaim PepMapTM RSLC C18 analytical column ($75\text{ }\mu\text{m} \times 150\text{ mm}$, $2\text{ }\mu\text{m}$, $100\text{ }\text{\AA}$) using an acetonitrile-based gradient (Solvent A: 0% acetonitrile, 0.1% formic acid; Solvent B: 80% acetonitrile, 0.1% formic acid) at a flow rate of 300 nL/min. A 30 min gradient was as follows: 0-0.5 min, 2-6% B; 0.5-24 min, 6-40% B; 24-26 min, 40-100% B; 26-30 min, 100% B, followed by re-equilibration to 2% B. The electrospray ionization was carried out with a nanoESI source at a 260°C capillary temperature and 1.8 kV spray voltage. The mass spectrometer was operated in data-dependent acquisition mode with mass range 400 to 1600 m/z. The precursor ions were selected for tandem mass (MS/MS) analysis in Orbitrap with 3 sec cycle time using HCD at 28% collision energy. Intensity threshold was set at 4e5. The dynamic exclusion was set with a repeat count of 1 and exclusion duration of 30 s. The resulting data was searched in Protein Prospector (<http://prospector.ucsf.edu/prospector/mshome.htm>) against the 6xHis-3HA-UB-Q40E and 6xHis-UBE2N sequences. Carbamidomethylation of cysteine residues was set as a fixed modification. Protein N-terminal acetylation, oxidation of methionine, protein N-terminal methionine loss, and pyroglutamine formation were set as variable modifications. A total of three variable modifications were allowed. Trypsin digestion specificity with one missed cleavage was allowed. The mass tolerance for precursor and fragment ions was set to 10 ppm for both. The crosslinked peptide search option was selected in Protein Prospector, with the crosslinking reagent designated as “EDC” (1-ethyl-3-(3-dimethylaminopropyl)carbodiimide hydrochloride). EDC-style cross linking involves the formation of a zero-length isopeptide bond between an amine group and a carboxylic acid, as would be expected for ubiquitin conjugation. Peptide and protein identification cut-off scores were set to 15 and 22, respectively. All putative cross-linked spectra were manually inspected. In both case, data were analyzed manually by de novo sequencing or StavroX v.3.6.0.1(Gotze, Pettelkau et al., 2012) using default parameters.

To detect deamidated ubiquitin from cells, cells were lysed in 50 μL of a buffer containing 50 mM NH₄HCO₃, 8 M urea and 5 mM dithiothreitol and incubated for 30 min at 37°C . After this incubation period samples were diluted 8-fold with 50 mM NH₄HCO₃ and CaCl₂ was added to a final concentration of 1 mM from a 1 M stock solution. The digestion was carried out overnight at

37°C with 2 µg of sequencing-grade trypsin (Promega). The samples were desalted using 1-mL C18 cartridges (50 mg, Stracta, Phenomenex) under the manufacturer recommendations. The samples were dried in a vacuum centrifuge, resuspended in water and quantified by the bicinchoninic acid assay (Thermo Fisher Scientific). A total of 500 ng of digested peptides were loaded in a trap C18 column and the separation was carried out in a C18 column (70 cm x 360 µm ODx75 µm ID silica tubing, Polymicro, packed with 3-µm Jupiter C18 stationary phase, Phenomenex). Peptides were eluted at a flow rate of 300 nL/min with a gradient of acetonitrile (ACN) in water, both containing 0.1% formic acid: 1-8% ACN solvent in 2 min, 8-12% ACN in 18 min, 12-30% ACN in 55 min, 30-45% ACN in 22 min, 45-95% ACN in 3 min, hold for 5 min in 95% ACN and 99-1% ACN in 10 min. Eluting peptides were analyzed in an Orbitrap mass spectrometer (Velos, Thermo Fisher Scientific) by targeting specific of peptides to fragmentation (PRM – parallel-reaction monitoring). The normalized collision energy was set to 30 in the HCD cell and spectra were collected with a m/z range of 50-2000 and resolution of 15,000 at 400 m/z. Collected spectra were analyzed using Xcalibur v2.2 (Thermo Fisher Scientific). Extracted-ion chromatograms were plotted using a tolerance of ±10 mDa and smoothed with 11 points using the Gaussian function. Quantification was done by comparing peak areas and significantly differences in ubiquitin deamidation profiles were determined by T-test assuming two tails and equal variance between samples.

***In vitro* deamidation of ubiquitin and native PAGE**

Ten µg ubiquitin was incubated with 1 µg MvcA or MvcA mutants in 50 µL reaction in a buffer containing 50 mM Tris-HCl (pH 7.5) at 37 °C for 2 h. 20 µL reaction mixtures were mixed with 5 µL 5x native gel loading buffer (pH 8.8), and loaded onto 10% native gels, gels were run in a buffer containing 375 mM Tris-Glycine (pH 8.8). Protein bands were visualized by Coomassie Brilliant blue staining.

Immunostaining

Cells were seeded at 2x10⁵ per well. Cells were infected with corresponding strains at an MOI of 1. 2 h post infection, cells were washed with PBS. Raw 264.7 cells were fixed by 4% formaldehyde solution for 15 min at room temperature, and permeabilization by 0.2% triton solution for 5 min at room temp, and blocked with 4% goat serum for 30 min at 37 °C. HEK293

cells were further incubated for another 10 h, then fixed and permeabilized by 100% pre-cold methanol. Bacteria were stained with the anti-rat *L. pneumophila* serum at a dilution of 1:10,000 for 1 h, p65 was stained with the p65 specific antibody (Cell signaling, cat#8242S) at a dilution of 1:500, Flag was stained with the Flag specific antibody (Sigma, Cat# F1804) at a dilution of 500 for 4 h, nucleus was stained with Hoechst. After further staining with secondary antibodies conjugated to Alexa 594 or Alexa 488 (Thermo Fisher Scientific), samples were inspected under an IX-81 Olympus fluorescence microscope. For quantitation, at least 300 cells were scored.

NF-κB luciferase reporter assay

HEK293T were grown to 70% confluence in 24 well plate, and transfected with 75 ng NF-κB reporter plasmids(Li, Liu et al., 2017) and 150 ng 4xFlag CMV empty vector, 4xFlag-MavC or 4xFlag-MavC_{C74A} vectors. For NF-κB epistasis analysis, 150 ng corresponding plasmids were used. 75 ng plasmids that directs the expression of Renilla luciferase in pRL-SV40 (Promega) was co-transfected as internal controls. At 16-18 h post transfection, cells with treated with 20 ng/mL TNF-α or 50 nM PMA for 4 h. Then cells were collected and lysed for NF-κB luciferase reporter assay following the manufacturer's protocols (Promega, cat#E1910).

Crystallization, data collection and structural determination

Crystallization screens were performed at Fujian Normal University by Dr. Hongxin Guan and his colleagues using the hanging drop vapor diffusion method at 16°C, with drops containing 0.5 µl of the protein solution mixed with 0.5 µl of reservoir solution. Diffraction-quality of MvcA-UBE2N-Ub (MvcAc_{83A}, UBE2N_{K94A}) crystals were obtained in 0.2 M sodium thiocyanate, 20% polyethylene glycol 3,350. MvcAc_{83A}, crystals were obtained in 30%(v/v) Jeffamine M-600 pH 7.0, 100mM HEPES/Sodium hydroxide pH 7.0. Crystals were harvested and flash frozen in liquid nitrogen with the 20% glycerol as a cryoprotectant. Complete X-ray diffraction datasets were collected at BL-17U1 beamline of Shanghai Synchrotron Radiation Facility (SSRF). Diffraction images were processed with the HKL-2000 program(Otwinowski & Minor, 1997). Crystal structures of the ternary complex were solved by molecular replacement (MR) using Phaser-MR to obtain the model of MvcA in complex with UBE2N (MvcA: 6K11, UBE2N:1JAT), and then using IPCAS (CCP4) to obtain the entire complex model(McCoy, 2007, Valleau et al., 2018, VanDemark, Hofmann et al., 2001, Yao et al., 2009). Model building and crystallographic

refinement were carried out in Coot v0.8.2 and PHENIX v1.10.1(Adams, Afonine et al., 2010, Emsley, Lohkamp et al., 2010). The interactions were analyzed with PyMol (<http://www.pymol.org/>) and PDBsum. The figures were generated in PyMol. Detailed data collection and refinement statistics were listed in Table 1 and Table S1, respectively(Adams et al., 2010).

Preparation and purification of UBE2N-Ub

A reaction containing MavC₁₋₄₆₂ (1 μ M), UBE2N (25 μ M), and ubiquitin (100 μ M) in reaction buffer (50 mM Tris pH 7.4, 100 mM NaCl, 1 mM DTT) was incubated at 37°C for 3 h. The reaction was concentrated to 1 mL and loaded onto a size-exclusion chromatography column, and eluted with the above reaction buffer. Fractions containing pure UBE2N-Ub were pooled, concentrated, flash-frozen in liquid nitrogen, and stored at -80°C until usage.

Data quantitation and statistical analyses

Student's *t*-test was used to compare the mean levels between two groups each with at least three independent samples.

REFERENCES

- Abu-Zant A, Jones S, Asare R, Suttles J, Price C, Graham J, Kwaik YA (2007) Anti-apoptotic signalling by the Dot/Icm secretion system of *L. pneumophila*. *Cellular microbiology* 9: 246-64
- Adams PD, Afonine PV, Bunkoczi G, Chen VB, Davis IW, Echols N, Headd JJ, Hung LW, Kapral GJ, Grosse-Kunstleve RW, McCoy AJ, Moriarty NW, Oeffner R, Read RJ, Richardson DC, Richardson JS, Terwilliger TC, Zwart PH (2010) PHENIX: a comprehensive Python-based system for macromolecular structure solution. *Acta crystallographica Section D, Biological crystallography* 66: 213-21
- Akturk A, Wasilko DJ, Wu X, Liu Y, Zhang Y, Qiu J, Luo ZQ, Reiter KH, Brzovic PS, Klevit RE, Mao Y (2018) Mechanism of phosphoribosyl-ubiquitination mediated by a single Legionella effector. *Nature* 557: 729-733
- Al-Quadan T, Price CT, Abu Kwaik Y (2012) Exploitation of evolutionarily conserved amoeba and mammalian processes by Legionella. *Trends in microbiology* 20: 299-306
- Ashida H, Kim M, Sasakawa C (2014) Exploitation of the host ubiquitin system by human bacterial pathogens. *Nature reviews Microbiology* 12: 399-413
- Bardill JP, Miller JL, Vogel JP (2005) IcmS-dependent translocation of SdeA into macrophages by the Legionella pneumophila type IV secretion system. *Molecular microbiology* 56: 90-103
- Bartfeld S, Engels C, Bauer B, Aurass P, Flieger A, Bruggemann H, Meyer TF (2009) Temporal resolution of two-tracked NF-kappaB activation by Legionella pneumophila. *Cellular microbiology* 11: 1638-51
- Belyi Y, Niggeweg R, Opitz B, Vogelgesang M, Hippenstiel S, Wilm M, Aktories K (2006) Legionella pneumophila glucosyltransferase inhibits host elongation factor 1A. *Proceedings of the National Academy of Sciences of the United States of America* 103: 16953-8
- Berger KH, Isberg RR (1993) Two distinct defects in intracellular growth complemented by a single genetic locus in Legionella pneumophila. *Molecular microbiology* 7: 7-19
- Bhogaraju S, Kalayil S, Liu Y, Bonn F, Colby T, Matic I, Dikic I (2016) Phosphoribosylation of Ubiquitin Promotes Serine Ubiquitination and Impairs Conventional Ubiquitination. *Cell* 167: 1636-1649.e13
- Branigan E, Plechanovova A, Jaffray EG, Naismith JH, Hay RT (2015) Structural basis for the RING-catalyzed synthesis of K63-linked ubiquitin chains. *Nature structural & molecular biology* 22: 597-602
- Brombacher E, Urwyler S, Ragaz C, Weber SS, Kami K, Overduin M, Hilbi H (2009) Rab1 guanine nucleotide exchange factor SidM is a major phosphatidylinositol 4-phosphate-binding effector protein of Legionella pneumophila. *J Biol Chem* 284: 4846-56

Burns KE, Cerdá-Maira FA, Wang T, Li H, Bishai WR, Darwin KH (2010) "Depupylation" of prokaryotic ubiquitin-like protein from mycobacterial proteasome substrates. *Molecular cell* 39: 821-7

Burstein D, Amaro F, Zusman T, Lifshitz Z, Cohen O, Gilbert JA, Pupko T, Shuman HA, Segal G (2016) Genomic analysis of 38 Legionella species identifies large and diverse effector repertoires. *Nat Genet* 48: 167-75

Burstein D, Zusman T, Degtyar E, Viner R, Segal G, Pupko T (2009) Genome-scale identification of Legionella pneumophila effectors using a machine learning approach. *PLoS pathogens* 5: e1000508

Campanacci V, Mukherjee S, Roy CR, Cherfils J (2013) Structure of the Legionella effector AnkX reveals the mechanism of phosphocholine transfer by the FIC domain. *The EMBO journal* 32: 1469-77

Chen J, de Felipe KS, Clarke M, Lu H, Anderson OR, Segal G, Shuman HA (2004) Legionella effectors that promote nonlytic release from protozoa. *Science* 303: 1358-1361

Chen Y, Tascon I, Neunuebel MR, Pallara C, Brady J, Kinch LN, Fernandez-Recio J, Rojas AL, Machner MP, Hierro A (2013) Structural basis for Rab1 de-AMPylation by the Legionella pneumophila effector SidD. *PLoS pathogens* 9: e1003382

Chen ZJ (2005) Ubiquitin signalling in the NF- κ B pathway. *Nature cell biology* 7: 758-65

Choy A, Dancourt J, Mugo B, O'Connor TJ, Isberg RR, Melia TJ, Roy CR (2012) The Legionella effector RavZ inhibits host autophagy through irreversible Atg8 deconjugation. *Science (New York, NY)* 338: 1072-6

Christensen DE, Brzovic PS, Klevit RE (2007) E2-BRCA1 RING interactions dictate synthesis of mono- or specific polyubiquitin chain linkages. *Nature structural & molecular biology* 14: 941-8

Cianciotto NP, Fields BS (1992) Legionella pneumophila mip gene potentiates intracellular infection of protozoa and human macrophages. *Proceedings of the National Academy of Sciences of the United States of America* 89: 5188-91

Clague MJ, Heride C, Urbe S (2015) The demographics of the ubiquitin system. *Trends in cell biology* 25: 417-26

Crow A, Hughes RK, Taieb F, Oswald E, Banfield MJ (2012) The molecular basis of ubiquitin-like protein NEDD8 deamidation by the bacterial effector protein Cif. *Proceedings of the National Academy of Sciences of the United States of America* 109: E1830-8

Cui J, Yao Q, Li S, Ding X, Lu Q, Mao H, Liu L, Zheng N, Chen S, Shao F (2010) Glutamine deamidation and dysfunction of ubiquitin/NEDD8 induced by a bacterial effector family. *Science (New York, NY)* 329: 1215-8

de Felipe KS, Pampou S, Jovanovic OS, Pericone CD, Ye SF, Kalachikov S, Shuman HA (2005) Evidence for acquisition of Legionella type IV secretion substrates via interdomain horizontal gene transfer. *J Bacteriol* 187: 7716-26

De Leon JA, Qiu J, Nicolai CJ, Counihan JL, Barry KC, Xu L, Lawrence RE, Castellano BM, Zoncu R, Nomura DK, Luo ZQ, Vance RE (2017) Positive and Negative Regulation of the Master Metabolic Regulator mTORC1 by Two Families of Legionella pneumophila Effectors. *Cell reports* 21: 2031-2038

Deng L, Wang C, Spencer E, Yang L, Braun A, You J, Slaughter C, Pickart C, Chen ZJ (2000) Activation of the IkappaB kinase complex by TRAF6 requires a dimeric ubiquitin-conjugating enzyme complex and a unique polyubiquitin chain. *Cell* 103: 351-61

Di Paolo G, De Camilli P (2006) Phosphoinositides in cell regulation and membrane dynamics. *Nature* 443: 651-657

Diacovich L, Gorvel JP (2010) Bacterial manipulation of innate immunity to promote infection. *Nature reviews Microbiology* 8: 117-28

Dong N, Niu M, Hu L, Yao Q, Zhou R, Shao F (2016) Modulation of membrane phosphoinositide dynamics by the phosphatidylinositide 4-kinase activity of the Legionella LepB effector. *Nat Microbiol* 2: 16236

Dong Y, Mu Y, Xie Y, Zhang Y, Han Y, Zhou Y, Wang W, Liu Z, Wu M, Wang H, Pan M, Xu N, Xu CQ, Yang M, Fan S, Deng H, Tan T, Liu X, Liu L, Li J et al. (2018) Structural basis of ubiquitin modification by the Legionella effector SdeA. *Nature* 557: 674-678

Dorer MS, Kirton D, Bader JS, Isberg RR (2006) RNA interference analysis of Legionella in Drosophila cells: exploitation of early secretory apparatus dynamics. *PLoS pathogens* 2: e34

Eckert RL, Kaartinen MT, Nurminskaya M, Belkin AM, Colak G, Johnson GV, Mehta K (2014) Transglutaminase regulation of cell function. *Physiological reviews* 94: 383-417

Eddins MJ, Carlile CM, Gomez KM, Pickart CM, Wolberger C (2006) Mms2-Ubc13 covalently bound to ubiquitin reveals the structural basis of linkage-specific polyubiquitin chain formation. *Nature structural & molecular biology* 13: 915-20

Emsley P, Lohkamp B, Scott WG, Cowtan K (2010) Features and development of Coot. *Acta Crystallogr D Biol Crystallogr* 66: 486-501

Ensminger AW, Isberg RR (2010) E3 ubiquitin ligase activity and targeting of BAT3 by multiple Legionella pneumophila translocated substrates. *Infection and immunity* 78: 3905-19

Erpapazoglou Z, Walker O, Haguenauer-Tsapis R (2014) Versatile roles of k63-linked ubiquitin chains in trafficking. *Cells* 3: 1027-88

Escoll P, Rolando M, Gomez-Valero L, Buchrieser C (2013) From amoeba to macrophages: exploring the molecular mechanisms of *Legionella pneumophila* infection in both hosts. Current topics in microbiology and immunology 376: 1-34

Fiesel FC, Moussaud-Lamodiere EL, Ando M, Springer W (2014) A specific subset of E2 ubiquitin-conjugating enzymes regulate Parkin activation and mitophagy differently. Journal of cell science 127: 3488-504

Finley D, Ulrich HD, Sommer T, Kaiser P (2012) The ubiquitin-proteasome system of *Saccharomyces cerevisiae*. Genetics 192: 319-60

Fletcher AJ, Christensen DE, Nelson C, Tan CP, Schaller T, Lehner PJ, Sundquist WI, Towers GJ (2015) TRIM5alpha requires Ube2W to anchor Lys63-linked ubiquitin chains and restrict reverse transcription. The EMBO journal 34: 2078-95

Fraser DW, Tsai TR, Orenstein W, Parkin WE, Beecham HJ, Sharrar RG, Harris J, Mallison GF, Martin SM, McDade JE, Shepard CC, Brachman PS (1977) Legionnaires' disease: description of an epidemic of pneumonia. The New England journal of medicine 297: 1189-97

Gan N, Nakayasu ES, Hollenbeck PJ, Luo ZQ (2019a) *Legionella pneumophila* inhibits immune signalling via MavC-mediated transglutaminase-induced ubiquitination of UBE2N. Nature microbiology 4: 134-143

Gan N, Nakayasu ES, Hollenbeck PJ, Luo ZQ (2019b) *Legionella pneumophila* inhibits immune signalling via MavC-mediated transglutaminase-induced ubiquitination of UBE2N. Nature microbiology 4: 134-143

Gaspar AH, Machner MP (2014) VipD is a Rab5-activated phospholipase A1 that protects *Legionella pneumophila* from endosomal fusion. Proc Natl Acad Sci U S A 111: 4560-5

Ge J, Xu H, Li T, Zhou Y, Zhang Z, Li S, Liu L, Shao F (2009) A *Legionella* type IV effector activates the NF-kappaB pathway by phosphorylating the IkappaB family of inhibitors. Proceedings of the National Academy of Sciences of the United States of America 106: 13725-30

Ghosh S, O'Connor TJ (2017) Beyond Paralogs: The Multiple Layers of Redundancy in Bacterial Pathogenesis. Front Cell Infect Microbiol 7: 467

Gladkova C, Maslen SL, Skehel JM, Komander D (2018) Mechanism of parkin activation by PINK1. Nature 559: 410-414

Goldknopf IL, French MF, Musso R, Busch H (1977) Presence of protein A24 in rat liver nucleosomes. Proceedings of the National Academy of Sciences of the United States of America 74: 5492-5

Goldstein G, Scheid M, Hammerling U, Schlesinger DH, Niall HD, Boyse EA (1975) Isolation of a polypeptide that has lymphocyte-differentiating properties and is probably represented universally in living cells. Proceedings of the National Academy of Sciences of the United States of America 72: 11-5

Goody PR, Heller K, Oesterlin LK, Muller MP, Itzen A, Goody RS (2012) Reversible phosphocholination of Rab proteins by *Legionella pneumophila* effector proteins. *Embo J* 31: 1774-1784

Gotze M, Pettelkau J, Schaks S, Bosse K, Ihling CH, Krauth F, Fritzsche R, Kuhn U, Sinz A (2012) StavroX--a software for analyzing crosslinked products in protein interaction studies. *Journal of the American Society for Mass Spectrometry* 23: 76-87

Grumati P, Dikic I (2018) Ubiquitin signaling and autophagy. *The Journal of biological chemistry* 293: 5404-5413

Havey JC, Roy CR (2015) Toxicity and SidJ-Mediated Suppression of Toxicity Require Distinct Regions in the SidE Family of *Legionella pneumophila* Effectors. *Infection and immunity* 83: 3506-14

Herhaus L, Dikic I (2015) Expanding the ubiquitin code through post-translational modification. *EMBO reports* 16: 1071-83

Hershko A, Ciechanover A (1998) The ubiquitin system. *Annual review of biochemistry* 67: 425-79

Hershko A, Ciechanover A, Heller H, Haas AL, Rose IA (1980) Proposed role of ATP in protein breakdown: conjugation of protein with multiple chains of the polypeptide of ATP-dependent proteolysis. *Proceedings of the National Academy of Sciences of the United States of America* 77: 1783-6

Hershko A, Heller H, Elias S, Ciechanover A (1983) Components of ubiquitin-protein ligase system. Resolution, affinity purification, and role in protein breakdown. *The Journal of biological chemistry* 258: 8206-14

Hodge CD, Spyrapoulos L, Glover JN (2016) Ubc13: the Lys63 ubiquitin chain building machine. *Oncotarget* 7: 64471-64504

Hofmann RM, Pickart CM (1999) Noncanonical MMS2-encoded ubiquitin-conjugating enzyme functions in assembly of novel polyubiquitin chains for DNA repair. *Cell* 96: 645-53

Horenkamp FA, Mukherjee S, Alix E, Schauder CM, Hubber AM, Roy CR, Reinisch KM (2014) *Legionella pneumophila* Subversion of Host Vesicular Transport by SidC Effector Proteins. *Traffic* 15: 488-499

Horwitz MA (1983) Formation of a novel phagosome by the Legionnaires' disease bacterium (*Legionella pneumophila*) in human monocytes. *The Journal of experimental medicine* 158: 1319-31

Hsu F, Luo X, Qiu J, Teng YB, Jin J, Smolka MB, Luo ZQ, Mao Y (2014) The *Legionella* effector SidC defines a unique family of ubiquitin ligases important for bacterial phagosomal remodeling. *Proceedings of the National Academy of Sciences of the United States of America* 111: 10538-43

- Hsu F, Zhu W, Brennan L, Tao L, Luo ZQ, Mao Y (2012) Structural basis for substrate recognition by a unique Legionella phosphoinositide phosphatase. *Proc Natl Acad Sci U S A* 109: 13567-72
- Huang L, Boyd D, Amyot WM, Hempstead AD, Luo ZQ, O'Connor TJ, Chen C, Machner M, Montminy T, Isberg RR (2011) The E Block motif is associated with Legionella pneumophila translocated substrates. *Cellular microbiology* 13: 227-45
- Hubber A, Arasaki K, Nakatsu F, Hardiman C, Lambright D, De Camilli P, Nagai H, Roy CR (2014) The machinery at endoplasmic reticulum-plasma membrane contact sites contributes to spatial regulation of multiple Legionella effector proteins. *PLoS Pathog* 10: e1004222
- Hunt LT, Dayhoff MO (1977) Amino-terminal sequence identity of ubiquitin and the nonhistone component of nuclear protein A24. *Biochemical and biophysical research communications* 74: 650-5
- Ikeda F, Dikic I (2008) Atypical ubiquitin chains: new molecular signals. 'Protein Modifications: Beyond the Usual Suspects' review series. *EMBO reports* 9: 536-42
- Ingmondson A, Delprato A, Lambright DG, Roy CR (2007) Legionella pneumophila proteins that regulate Rab1 membrane cycling. *Nature* 450: 365-U1
- Isberg RR, O'Connor TJ, Heidtman M (2009) The Legionella pneumophila replication vacuole: making a cosy niche inside host cells. *Nature reviews Microbiology* 7: 13-24
- Jeong KC, Sexton JA, Vogel JP (2015) Spatiotemporal regulation of a Legionella pneumophila T4SS substrate by the metaeffector SidJ. *PLoS pathogens* 11: e1004695
- Jiang X, Chen ZJ (2011) The role of ubiquitylation in immune defence and pathogen evasion. *Nature reviews Immunology* 12: 35-48
- Jin J, Li X, Gygi SP, Harper JW (2007) Dual E1 activation systems for ubiquitin differentially regulate E2 enzyme charging. *Nature* 447: 1135-8
- Kalayil S, Bhogaraju S, Bonn F, Shin D, Liu Y, Gan N, Basquin J, Grumati P, Luo ZQ, Dikic I (2018) Insights into catalysis and function of phosphoribosyl-linked serine ubiquitination. *Nature* 557: 734-738
- Keillor JW, Clouthier CM, Apperley KY, Akbar A, Mulani A (2014) Acyl transfer mechanisms of tissue transglutaminase. *Bioorganic chemistry* 57: 186-97
- Kieser KJ, Kagan JC (2017) Multi-receptor detection of individual bacterial products by the innate immune system. *Nature reviews Immunology* 17: 376-390
- Kiraly R, Thangaraju K, Nagy Z, Collighan R, Nemes Z, Griffin M, Fesus L (2016) Isopeptidase activity of human transglutaminase 2: disconnection from transamidation and characterization by kinetic parameters. *Amino acids* 48: 31-40

- Kitada T, Asakawa S, Hattori N, Matsumine H, Yamamura Y, Minoshima S, Yokochi M, Mizuno Y, Shimizu N (1998) Mutations in the parkin gene cause autosomal recessive juvenile parkinsonism. *Nature* 392: 605-8
- Klock C, Khosla C (2012) Regulation of the activities of the mammalian transglutaminase family of enzymes. *Protein science : a publication of the Protein Society* 21: 1781-91
- Komander D (2009) The emerging complexity of protein ubiquitination. *Biochemical Society transactions* 37: 937-53
- Komander D, Clague MJ, Urbe S (2009) Breaking the chains: structure and function of the deubiquitinases. *Nature reviews Molecular cell biology* 10: 550-63
- Komander D, Rape M (2012) The ubiquitin code. *Annual review of biochemistry* 81: 203-29
- Kotewicz KM, Ramabhadran V, Sjöblom N, Vogel JP, Haenssler E, Zhang M, Behringer J, Scheck RA, Isberg RR (2017) A Single Legionella Effector Catalyzes a Multistep Ubiquitination Pathway to Rearrange Tubular Endoplasmic Reticulum for Replication. *Cell host & microbe* 21: 169-181
- Koyano F, Okatsu K, Kosako H, Tamura Y, Go E, Kimura M, Kimura Y, Tsuchiya H, Yoshihara H, Hirokawa T, Endo T, Fon EA, Trempe JF, Saeki Y, Tanaka K, Matsuda N (2014) Ubiquitin is phosphorylated by PINK1 to activate parkin. *Nature* 510: 162-6
- Ku B, Lee KH, Park WS, Yang CS, Ge J, Lee SG, Cha SS, Shao F, Heo WD, Jung JU, Oh BH (2012) VipD of *Legionella pneumophila* targets activated Rab5 and Rab22 to interfere with endosomal trafficking in macrophages. *PLoS Pathog* 8: e1003082
- Kuballa P, Nolte WM, Castoreno AB, Xavier RJ (2012) Autophagy and the immune system. *Annual review of immunology* 30: 611-46
- Kubori T, Galan JE (2003) Temporal regulation of salmonella virulence effector function by proteasome-dependent protein degradation. *Cell* 115: 333-42
- Kubori T, Hyakutake A, Nagai H (2008) Legionella translocates an E3 ubiquitin ligase that has multiple U-boxes with distinct functions. *Molecular microbiology* 67: 1307-19
- Kubori T, Kitao T, Ando H, Nagai H (2018) LotA, a Legionella deubiquitinase, has dual catalytic activity and contributes to intracellular growth. *Cellular microbiology* 20
- Kubori T, Shinzawa N, Kanuka H, Nagai H (2010) Legionella metaeffector exploits host proteasome to temporally regulate cognate effector. *PLoS pathogens* 6: e1001216
- Levine B (2005) Eating oneself and uninvited guests: autophagy-related pathways in cellular defense. *Cell* 120: 159-62
- Li Q, Verma IM (2002) NF-kappaB regulation in the immune system. *Nature reviews Immunology* 2: 725-34

Li W, Ye Y (2008) Polyubiquitin chains: functions, structures, and mechanisms. *Cellular and molecular life sciences : CMLS* 65: 2397-406

Li X, Liu Y, Wang Y, Liu J, Li X, Cao H, Gao X, Zheng SJ (2017) Negative Regulation of Hepatic Inflammation by the Soluble Resistance-Related Calcium-Binding Protein via Signal Transducer and Activator of Transcription 3. *Frontiers in immunology* 8: 709

Lifshitz Z, Burstein D, Peeri M, Zusman T, Schwartz K, Shuman HA, Pupko T, Segal G (2013) Computational modeling and experimental validation of the Legionella and Coxiella virulence-related type-IVB secretion signal. *Proceedings of the National Academy of Sciences of the United States of America* 110: E707-15

Lin DY, Diao J, Zhou D, Chen J (2011) Biochemical and structural studies of a HECT-like ubiquitin ligase from Escherichia coli O157:H7. *The Journal of biological chemistry* 286: 441-9

Lin YH, Lucas M, Evans TR, Abascal-Palacios G, Doms AG, Beauchene NA, Rojas AL, Hierro A, Machner MP (2018) RavN is a member of a previously unrecognized group of Legionella pneumophila E3 ubiquitin ligases. *PLoS pathogens* 14: e1006897

Liu X, Fitzgerald K, Kurt-Jones E, Finberg R, Knipe DM (2008) Herpesvirus tegument protein activates NF-kappaB signaling through the TRAF6 adaptor protein. *Proceedings of the National Academy of Sciences of the United States of America* 105: 11335-9

Liu Y, Luo ZQ (2007) The Legionella pneumophila effector SidJ is required for efficient recruitment of endoplasmic reticulum proteins to the bacterial phagosome. *Infection and immunity* 75: 592-603

Lomma M, Dervins-Ravault D, Rolando M, Nora T, Newton HJ, Sansom FM, Sahr T, Gomez-Valero L, Jules M, Hartland EL, Buchrieser C (2010) The Legionella pneumophila F-box protein Lpp2082 (AnkB) modulates ubiquitination of the host protein parvin B and promotes intracellular replication. *Cellular microbiology* 12: 1272-91

Lorand L, Graham RM (2003) Transglutaminases: crosslinking enzymes with pleiotropic functions. *Nature reviews Molecular cell biology* 4: 140-56

Losick VP, Haenssler E, Moy MY, Isberg RR (2010) LnaB: a Legionella pneumophila activator of NF-kappaB. *Cellular microbiology* 12: 1083-97

Losick VP, Isberg RR (2006) NF-kappaB translocation prevents host cell death after low-dose challenge by Legionella pneumophila. *The Journal of experimental medicine* 203: 2177-89

Lum JJ, Bauer DE, Kong M, Harris MH, Li C, Lindsten T, Thompson CB (2005) Growth factor regulation of autophagy and cell survival in the absence of apoptosis. *Cell* 120: 237-48

Luo X, Wasilko DJ, Liu Y, Sun J, Wu X, Luo ZQ, Mao Y (2015) Structure of the Legionella Virulence Factor, SidC Reveals a Unique PI(4)P-Specific Binding Domain Essential for Its Targeting to the Bacterial Phagosome. *PLoS pathogens* 11: e1004965

Luo ZQ, Isberg RR (2004) Multiple substrates of the *Legionella pneumophila* Dot/Icm system identified by interbacterial protein transfer. *Proceedings of the National Academy of Sciences of the United States of America* 101: 841-6

Machida YJ, Machida Y, Chen Y, Gurtan AM, Kupfer GM, D'Andrea AD, Dutta A (2006) UBE2T is the E2 in the Fanconi anemia pathway and undergoes negative autoregulation. *Molecular cell* 23: 589-96

Machner MP, Isberg RR (2006) Targeting of host Rab GTPase function by the intravacuolar pathogen *Legionella pneumophila*. *Dev Cell* 11: 47-56

Machner MP, Isberg RR (2007) A bifunctional bacterial protein links GDI displacement to Rab1 activation. *Science* 318: 974-977

Maculins T, Fiskin E, Bhogaraju S, Dikic I (2016) Bacteria-host relationship: ubiquitin ligases as weapons of invasion. *Cell research* 26: 499-510

Marston BJ, Plouffe JF, File TM, Jr., Hackman BA, Salstrom SJ, Lipman HB, Kolczak MS, Breiman RF (1997) Incidence of community-acquired pneumonia requiring hospitalization. Results of a population-based active surveillance Study in Ohio. The Community-Based Pneumonia Incidence Study Group. *Archives of internal medicine* 157: 1709-18

Matsuda N (2016) Phospho-ubiquitin: upending the PINK-Parkin-ubiquitin cascade. *Journal of biochemistry* 159: 379-85

McCoy AJ (2007) Solving structures of protein complexes by molecular replacement with Phaser. *Acta Crystallogr D* 63: 32-41

McKenna S, Spyracopoulos L, Moraes T, Pastushok L, Ptak C, Xiao W, Ellison MJ (2001) Noncovalent interaction between ubiquitin and the human DNA repair protein Mms2 is required for Ubc13-mediated polyubiquitination. *The Journal of biological chemistry* 276: 40120-6

Mesquita FS, Thomas M, Sachse M, Santos AJ, Figueira R, Holden DW (2012) The *Salmonella* deubiquitinase SseL inhibits selective autophagy of cytosolic aggregates. *PLoS pathogens* 8: e1002743

Mevissen TET, Komander D (2017) Mechanisms of Deubiquitinase Specificity and Regulation. *Annual review of biochemistry* 86: 159-192

Morreale FE, Walden H (2016) Types of Ubiquitin Ligases. *Cell* 165: 248-248.e1

Mukherjee S, Keitany G, Li Y, Wang Y, Ball HL, Goldsmith EJ, Orth K (2006) *Yersinia* YopJ acetylates and inhibits kinase activation by blocking phosphorylation. *Science (New York, NY)* 312: 1211-4

Muller MP, Peters H, Blumer J, Blankenfeldt W, Goody RS, Itzen A (2010) The *Legionella* effector protein DrrA AMPylates the membrane traffic regulator Rab1b. *Science (New York, NY)* 329: 946-9

Murata T, Delprato A, Ingundson A, Toomre DK, Lambright DG, Roy CR (2006) The *Legionella pneumophila* effector protein DrrA is a Rab1 guanine nucleotide-exchange factor. *Nat Cell Biol* 8: 971-U76

Nagai H, Kagan JC, Zhu X, Kahn RA, Roy CR (2002) A bacterial guanine nucleotide exchange factor activates ARF on *Legionella* phagosomes. *Science (New York, NY)* 295: 679-82

Neunuebel MR, Chen Y, Gaspar AH, Backlund PS, Yergey A, Machner MP (2011) De-AMPylation of the Small GTPase Rab1 by the Pathogen *Legionella pneumophila*. *Science* 333: 453-456

Newton HJ, Ang DK, van Driel IR, Hartland EL (2010) Molecular pathogenesis of infections caused by *Legionella pneumophila*. *Clinical microbiology reviews* 23: 274-98

O'Connor TJ, Adepoju Y, Boyd D, Isberg RR (2011) Minimization of the *Legionella pneumophila* genome reveals chromosomal regions involved in host range expansion. *Proceedings of the National Academy of Sciences of the United States of America* 108: 14733-40

O'Connor TJ, Boyd D, Dorer MS, Isberg RR (2012) Aggravating genetic interactions allow a solution to redundancy in a bacterial pathogen. *Science (New York, NY)* 338: 1440-4

Oesterlin LK, Goody RS, Itzen A (2012) Posttranslational modifications of Rab proteins cause effective displacement of GDP dissociation inhibitor. *P Natl Acad Sci USA* 109: 5621-5626

Otwinowski Z, Minor W (1997) Processing of X-ray diffraction data collected in oscillation mode. *Methods Enzymol* 276: 307-26

Ozcelik D, Barandun J, Schmitz N, Sutter M, Guth E, Damberger FF, Allain FH, Ban N, Weber-Ban E (2012) Structures of Pup ligase PafA and depupylylase Dop from the prokaryotic ubiquitin-like modification pathway. *Nature communications* 3: 1014

Pan X, Luhrmann A, Satoh A, Laskowski-Arce MA, Roy CR (2008) Ankyrin repeat proteins comprise a diverse family of bacterial type IV effectors. *Science* 320: 1651-4

Parameswaran KN, Cheng XF, Chen EC, Velasco PT, Wilson JH, Lorand L (1997) Hydrolysis of gamma:epsilon isopeptides by cytosolic transglutaminases and by coagulation factor XIIIa. *The Journal of biological chemistry* 272: 10311-7

Pearce MJ, Mintseris J, Ferreyra J, Gygi SP, Darwin KH (2008) Ubiquitin-like protein involved in the proteasome pathway of *Mycobacterium tuberculosis*. *Science (New York, NY)* 322: 1104-7

Pruneda JN, Bastidas RJ, Bertsoulaki E, Swatek KN, Santhanam B, Clague MJ, Valdivia RH, Urbe S, Komander D (2018) A Chlamydia effector combining deubiquitination and acetylation activities induces Golgi fragmentation. *Nature microbiology*

Qiu J, Luo ZQ (2017a) Hijacking of the Host Ubiquitin Network by *Legionella pneumophila*. *Frontiers in cellular and infection microbiology* 7: 487

Qiu J, Luo ZQ (2017b) Legionella and Coxiella effectors: strength in diversity and activity. *Nature reviews Microbiology* 15: 591-605

Qiu J, Sheedlo MJ, Yu K, Tan Y, Nakayasu ES, Das C, Liu X, Luo ZQ (2016) Ubiquitination independent of E1 and E2 enzymes by bacterial effectors. *Nature* 533: 120-4

Qiu J, Yu K, Fei X, Liu Y, Nakayasu ES, Piehowski PD, Shaw JB, Puvar K, Das C, Liu X, Luo ZQ (2017) A unique deubiquitinase that deconjugates phosphoribosyl-linked protein ubiquitination. *Cell research* 27: 865-881

Ragaz C, Pietsch H, Urwyler S, Tiaden A, Weber SS, Hilbi H (2008) The *Legionella pneumophila* phosphatidylinositol-4 phosphate-binding type IV substrate SidC recruits endoplasmic reticulum vesicles to a replication-permissive vacuole. *Cellular microbiology* 10: 2416-33

Rape M, Kirschner MW (2004) Autonomous regulation of the anaphase-promoting complex couples mitosis to S-phase entry. *Nature* 432: 588-95

Rasch J, Unal CM, Steinert M (2014) Peptidylprolyl cis-trans isomerases of *Legionella pneumophila*: virulence, moonlighting and novel therapeutic targets. *Biochemical Society transactions* 42: 1728-33

Ravid T, Hochstrasser M (2007) Autoregulation of an E2 enzyme by ubiquitin-chain assembly on its catalytic residue. *Nature cell biology* 9: 422-7

Sanada T, Kim M, Mimuro H, Suzuki M, Ogawa M, Oyama A, Ashida H, Kobayashi T, Koyama T, Nagai S, Shibata Y, Gohda J, Inoue J, Mizushima T, Sasakawa C (2012) The *Shigella flexneri* effector OspI deamidates UBC13 to dampen the inflammatory response. *Nature* 483: 623-6

Sato M, Konuma R, Sato K, Tomura K, Sato K (2014) Fertilization-induced K63-linked ubiquitylation mediates clearance of maternal membrane proteins. *Development* (Cambridge, England) 141: 1324-31

Say RF, Fuchs G (2010) Fructose 1,6-bisphosphate aldolase/phosphatase may be an ancestral gluconeogenic enzyme. *Nature* 464: 1077-81

Seeler JS, Dejean A (2017) SUMO and the robustness of cancer. *Nature reviews Cancer* 17: 184-197

Shaid S, Brandts CH, Serve H, Dikic I (2013) Ubiquitination and selective autophagy. *Cell death and differentiation* 20: 21-30

Sheedlo MJ, Qiu J, Tan Y, Paul LN, Luo ZQ, Das C (2015) Structural basis of substrate recognition by a bacterial deubiquitinase important for dynamics of phagosome ubiquitination. *Proceedings of the National Academy of Sciences of the United States of America* 112: 15090-5

Shen X, Banga S, Liu Y, Xu L, Gao P, Shamovsky I, Nudler E, Luo ZQ (2009) Targeting eEF1A by a *Legionella pneumophila* effector leads to inhibition of protein synthesis and induction of host stress response. *Cellular microbiology* 11: 911-26

- Shevchenko A, Tomas H, Havlis J, Olsen JV, Mann M (2006) In-gel digestion for mass spectrometric characterization of proteins and proteomes. *Nature protocols* 1: 2856-60
- Singh RK, Zerath S, Kleifeld O, Scheffner M, Glickman MH, Fushman D (2012) Recognition and cleavage of related to ubiquitin 1 (Rub1) and Rub1-ubiquitin chains by components of the ubiquitin-proteasome system. *Molecular & cellular proteomics : MCP* 11: 1595-611
- Skaug B, Jiang X, Chen ZJ (2009) The role of ubiquitin in NF-kappaB regulatory pathways. *Annu Rev Biochem* 78: 769-96
- Song L, Luo ZQ (2019) Post-translational regulation of ubiquitin signaling. *The Journal of cell biology*
- Stewart MD, Ritterhoff T, Klevit RE, Brzovic PS (2016) E2 enzymes: more than just middle men. *Cell research* 26: 423-40
- Swanson MS, Hammer BK (2000) Legionella pneumophila pathogenesis: a fateful journey from amoebae to macrophages. *Annual review of microbiology* 54: 567-613
- Swatek KN, Komander D (2016) Ubiquitin modifications. *Cell research* 26: 399-422
- Takada K, Hirakawa T, Yokosawa H, Okawa Y, Taguchi H, Ohkawa K (2001) Isolation of ubiquitin-E2 (ubiquitin-conjugating enzyme) complexes from erythroleukaemia cells using immunoaffinity techniques. *The Biochemical journal* 356: 199-206
- Takeuchi T, Yokosawa H (2005) ISG15 modification of Ubc13 suppresses its ubiquitin-conjugating activity. *Biochemical and biophysical research communications* 336: 9-13
- Tan Y, Arnold RJ, Luo ZQ (2011) Legionella pneumophila regulates the small GTPase Rab1 activity by reversible phosphorylation. *Proceedings of the National Academy of Sciences of the United States of America* 108: 21212-7
- Tan Y, Luo ZQ (2011a) Legionella pneumophila SidD is a deAMPyrase that modifies Rab1. *Nature* 475: 506-9
- Tan YH, Luo ZQ (2011b) Legionella pneumophila SidD is a deAMPyrase that modifies Rab1. *Nature* 475: 506-U102
- Thorslund T, Ripplinger A, Hoffmann S, Wild T, Uckelmann M, Villumsen B, Narita T, Sixma TK, Choudhary C, Bekker-Jensen S, Mailand N (2015) Histone H1 couples initiation and amplification of ubiquitin signalling after DNA damage. *Nature* 527: 389-93
- Toulabi L, Wu XC, Cheng YS, Mao YX (2013) Identification and Structural Characterization of a Legionella Phosphoinositide Phosphatase. *Journal of Biological Chemistry* 288: 24518-24527

Urbanus ML, Quaile AT, Stogios PJ, Morar M, Rao C, Di Leo R, Evdokimova E, Lam M, Oatway C, Cuff ME, Osipiuk J, Michalska K, Nocek BP, Taipale M, Savchenko A, Ensminger AW (2016) Diverse mechanisms of metaeffector activity in an intracellular bacterial pathogen, *Legionella pneumophila*. *Molecular systems biology* 12: 893

Valente EM, Abou-Sleiman PM, Caputo V, Muqit MM, Harvey K, Gispert S, Ali Z, Del Turco D, Bentivoglio AR, Healy DG, Albanese A, Nussbaum R, Gonzalez-Maldonado R, Deller T, Salvi S, Cortelli P, Gilks WP, Latchman DS, Harvey RJ, Dallapiccola B et al. (2004) Hereditary early-onset Parkinson's disease caused by mutations in PINK1. *Science (New York, NY)* 304: 1158-60

Valleau D, Quaile AT, Cui H, Xu X, Evdokimova E, Chang C, Cuff ME, Urbanus ML, Houlston S, Arrowsmith CH, Ensminger AW, Savchenko A (2018) Discovery of Ubiquitin Deamidases in the Pathogenic Arsenal of *Legionella pneumophila*. *Cell reports* 23: 568-583

Vance RE, Isberg RR, Portnoy DA (2009) Patterns of pathogenesis: discrimination of pathogenic and nonpathogenic microbes by the innate immune system. *Cell Host Microbe* 6: 10-21

VanDemark AP, Hofmann RM, Tsui C, Pickart CM, Wolberger C (2001) Molecular insights into polyubiquitin chain assembly: Crystal structure of the Mms2/Ubc13 heterodimer. *Cell* 105: 711-720

Viner R, Chetrit D, Ehrlich M, Segal G (2012) Identification of Two *Legionella pneumophila* Effectors that Manipulate Host Phospholipids Biosynthesis. *Plos Pathogens* 8

Wang Y, Shi M, Feng H, Zhu Y, Liu S, Gao A, Gao P (2018) Structural Insights into Non-canonical Ubiquitination Catalyzed by SidE. *Cell* 173: 1231-1243.e16

Wasilko DJ, Huang Q, Mao Y (2018) Insights into the ubiquitin transfer cascade catalyzed by the *Legionella* effector SidC. *eLife* 7

Wauer T, Swatek KN, Wagstaff JL, Gladkova C, Pruneda JN, Michel MA, Gersch M, Johnson CM, Freund SM, Komander D (2015) Ubiquitin Ser65 phosphorylation affects ubiquitin structure, chain assembly and hydrolysis. *The EMBO journal* 34: 307-25

Weber SS, Ragaz C, Reus K, Nyfeler Y, Hilbi H (2006) *Legionella pneumophila* exploits PI(4)P to anchor secreted effector proteins to the replicative vacuole. *PLoS Pathog* 2: e46

Wilkinson KD, Urban MK, Haas AL (1980) Ubiquitin is the ATP-dependent proteolysis factor I of rabbit reticulocytes. *The Journal of biological chemistry* 255: 7529-32

Wong K, Kozlov G, Zhang Y, Gehring K (2015) Structure of the *Legionella* Effector, lpg1496, Suggests a Role in Nucleotide Metabolism. *The Journal of biological chemistry* 290: 24727-37

Wu B, Skarina T, Yee A, Jobin MC, Dileo R, Semesi A, Fares C, Lemak A, Coombes BK, Arrowsmith CH, Singer AU, Savchenko A (2010) NleG Type 3 effectors from enterohaemorrhagic *Escherichia coli* are U-Box E3 ubiquitin ligases. *PLoS pathogens* 6: e1000960

Xie Z, Klionsky DJ (2007) Autophagosome formation: core machinery and adaptations. *Nature cell biology* 9: 1102-9

Xu L, Shen X, Bryan A, Banga S, Swanson MS, Luo ZQ (2010) Inhibition of host vacuolar H+-ATPase activity by a *Legionella pneumophila* effector. *PLoS Pathog* 6: e1000822

Yao Q, Cui J, Zhu Y, Wang G, Hu L, Long C, Cao R, Liu X, Huang N, Chen S, Liu L, Shao F (2009) A bacterial type III effector family uses the papain-like hydrolytic activity to arrest the host cell cycle. *Proceedings of the National Academy of Sciences of the United States of America* 106: 3716-21

Ye Y, Rape M (2009) Building ubiquitin chains: E2 enzymes at work. *Nature reviews Molecular cell biology* 10: 755-64

Yudina Z, Roa A, Johnson R, Biris N, de Souza Aranha Vieira DA, Tsiperson V, Reszka N, Taylor AB, Hart PJ, Demeler B, Diaz-Griffero F, Ivanov DN (2015) RING Dimerization Links Higher-Order Assembly of TRIM5alpha to Synthesis of K63-Linked Polyubiquitin. *Cell reports* 12: 788-97

Zhang H, Hu H, Greeley N, Jin J, Matthews AJ, Ohashi E, Caetano MS, Li HS, Wu X, Mandal PK, McMurray JS, Moghaddam SJ, Sun SC, Watowich SS (2014) STAT3 restrains RANK- and TLR4-mediated signalling by suppressing expression of the E2 ubiquitin-conjugating enzyme Ubc13. *Nature communications* 5: 5798

Zhou H, Wertz I, O'Rourke K, Ultsch M, Seshagiri S, Eby M, Xiao W, Dixit VM (2004) Bcl10 activates the NF-kappaB pathway through ubiquitination of NEMO. *Nature* 427: 167-71

Zhou Y, Zhu Y (2015) Diversity of bacterial manipulation of the host ubiquitin pathways. *Cellular microbiology* 17: 26-34

Zhu W, Banga S, Tan Y, Zheng C, Stephenson R, Gately J, Luo ZQ (2011) Comprehensive identification of protein substrates of the Dot/Icm type IV transporter of *Legionella pneumophila*. *PloS one* 6: e17638

Zou W, Papov V, Malakhova O, Kim KI, Dao C, Li J, Zhang DE (2005) ISG15 modification of ubiquitin E2 Ubc13 disrupts its ability to form thioester bond with ubiquitin. *Biochemical and biophysical research communications* 336: 61-8

APPENDIX

Table. 1 X-ray crystallography data collection and refinement statistics

Dataset	MvcA-UBE2N-Ub
Data collection	
Beamline	BL-17U1, SSRF
Wavelength	0.979
Resolution range*	51.17-2.45 (2.54-2.45)
Space group	<i>C</i> 2 <i>2</i> ₁
Cell dimensions	
a, b, c (Å)	104.32, 107.60, 263.84
α, β, γ (°)	90, 90, 90
Total reflections	340409(55165)
Unique reflections	52753 (7924)
Multiplicity	6.5
Completeness (%)	96.5 (99.9)
Mean I/sigma(I)	14.9(2.5)
R-merge	0.062(0.509)
R-meas	0.074(0.599)
R-pim	0.039(0.313)
CC1/2	0.999(0.928)
Refinement	
Wilson B-factor	58.47
Reflections used in refinement	52680 (5395)
Reflections used for R-free	2639 (313)
R-work	0.2062 (0.2873)
R-free	0.2102 (0.3131)
Number of non-hydrogen atoms	9776
macromolecules	9712
solvent	64
Protein residues	1214
RMS(bonds)	0.007
RMS(angles)	1.12
Ramachandran favored (%)	96.17
Ramachandran allowed (%)	2.91
Ramachandran outliers (%)	0.92
Rotamer outliers (%)	0.56
Clashscore	11.28
Average B-factor	80.26
macromolecules	80.38
solvent	62.89

*Highest resolution shell is shown in parentheses

Note: the structural work was performed by Dr. Hongxin Guan and colleagues at Fujian Normal University.

Table 2. X-ray crystallography data collection and refinement statistics

Dataset	Se-MvcA(13-395 C83A)
Data collection	
Beamline	BL-17U1, SSRF
Wavelength	0.979
Resolution range*	58.73-1.94 (2.04-1.94)
Space group	<i>P</i> 2 ₁ 22
Cell dimensions	
a, b, c (Å)	122.65, 135.23, 66.90
α, β, γ (°)	90, 90, 90
Total reflections	1094751(162336)
Unique reflections	83566 (12059)
Multiplicity	13.1
Completeness (%)	99.9 (100.0)
Mean I/sigma(I)	14.4(2.6)
R-merge	0.093(0.948)
R-meas	0.101(1.025)
R-pim	0.038(0.387)
CC1/2	0.997(0.890)
Wilson B-factor	36.66
Refinement	
Reflections used in refinement	83442 (8248)
Reflections used for R-free	4203 (388)
R-work	0.2021 (0.2500)
R-free	0.2383 (0.2819)
Number of non-hydrogen atoms	6613
macromolecules	6137
solvent	476
Protein residues	762
RMS(bonds)	0.007
RMS(angles)	0.80
Ramachandran favored (%)	98.42
Ramachandran allowed (%)	1.58
Ramachandran outliers (%)	0.00
Rotamer outliers (%)	0.59
Clashscore	4.02
Average B-factor	43.44
macromolecules	43.18
Solvent	46.79

*Highest resolution shell is shown in parentheses

Note: the structural work was performed by Dr. Hongxin Guan and colleagues at Fujian Normal University

Table. 3 Bacterial strains, plasmids and primers used in this study

Bacterial Strains	Source	Identifier
<i>L. pneumophila</i> (Philadelphia-1) LP02	(Berger & Isberg, 1993)	N/A
<i>L. pneumophila</i> LP03	(Berger & Isberg, 1993)	N/A
LP02 Δ mavC	This study	N/A
LP02 Δ mavC (pZL507)	This study	N/A
LP02 Δ mavC (pMavC)	This study	N/A
LP02 Δ mavC (pMavCC _{74A})	This study	N/A
LP02 Δ mvcA	This study	N/A
LP02 Δ mvcA (pZL507)	This study	N/A
LP02 Δ mvcA (pMvcA)	This study	N/A
LP02 Δ mvcA (pMvcAC _{83A})	This study	N/A
LP02 Δ mavC Δ mvcA	This study	N/A
LP02 Δ mavC Δ mvcA (pZL507)	This study	N/A
LP02 Δ mavC Δ mvcA (pMvcA)	This study	N/A
LP02 Δ mavC Δ mvcA (pMvcAC _{83A})	This study	N/A
LP02 Δ mavC Δ mvcA (pMavC)	This study	N/A
LP02 Δ mavC Δ mvcA (pMavC _{74A})	This study	N/A
LP02(pAM239) expressing GFP	(Dorer et al., 2006)	N/A
LP02 Δ mvcA (pMvcA _{Δmid})	This study	N/A
LP02 Δ lpg2149	This study	N/A
LP02 Δ lpg2149 (pZL507)	This study	N/A
LP02 Δ lpg2149 (Lpg2149)	This study	N/A
LP02 Δ 2ab	(O'Connor et al., 2011)	N/A
LP02 Δ 3	(O'Connor et al., 2011)	N/A
LP02 Δ 4a	(O'Connor et al., 2011)	N/A
LP02 Δ 5	(O'Connor et al., 2011)	N/A
LP02 Δ 6a	(O'Connor et al., 2011)	N/A
LP02 Δ 7a	(O'Connor et al., 2011)	N/A
<i>E.coli</i> BL21(DE3)	NEB	CAT#C2527I
<i>E.coli</i> XL1-Blue	Agilent	CAT# 200249

Plasmids	Source	Identifier
pZL507	(Xu et al., 2010)	N/A
pZL507::mvcA	This study	N/A
pZL507::mvcAC _{83A}	This study	N/A
pZL507::mavC	This study	N/A
pZL507::mavCC _{74A}	This study	N/A
pZL507::mvcA _{Δmid}	This study	N/A

Table. 3 continued

p4xFlagCMV	(Qiu et al., 2016)	N/A
p4xFlagCMV:: <i>mavC</i>	This study	N/A
p4xFlagCMV:: <i>mvcA</i>	This study	N/A
p4xFlagCMV:: <i>mvcA C83A</i>	This study	N/A
p4xFlagCMV:: <i>mavC C74A</i>	This study	N/A
p4xFlagCMV:: <i>mavC C82A</i>	This study	N/A
p4xFlagCMV:: <i>mavC C117A</i>	This study	N/A
p4xFlagCMV:: <i>mavC C226A</i>	This study	N/A
p4xFlagCMV:: <i>mavC C314A</i>	This study	N/A
p4xFlagCMV:: <i>mavC C362A</i>	This study	N/A
p4xFlagCMV:: <i>ube2n</i>	This study	N/A
pAM239:: <i>gfp</i>	Dorer et al., 2006	N/A
p3xHACDNA3.1:: <i>ub</i>	(Sheedlo et al., 2015)	N/A
p3xHACDNA3.1:: <i>ub-AA</i>	(Sheedlo et al., 2015)	N/A
pQE30	Qiagen	CAT#32915
pQE30:: <i>mavC</i>	This study	N/A
pQE30:: <i>mavC C74A</i>	This study	N/A
pQE30:: <i>ube2n</i>	This study	N/A
pQE30:: <i>ube2nK92A</i>	This study	N/A
pQE30:: <i>ube2nK94A</i>	This study	N/A
pQE30:: <i>ube2nK92AK94A</i>	This study	N/A
pQE30:: <i>ube2nC87A</i>	This study	N/A
pQE30:: <i>ube2v2</i>	This study	N/A
pQE30:: <i>ube2e3</i>	This study	N/A
pQE30:: <i>ube2k</i>	This study	N/A
pQE30:: <i>ube2s</i>	This study	N/A
pQE30:: <i>ube2t</i>	This study	N/A
pQE30:: <i>mvcA</i>	This study	N/A
pQE30:: <i>mvcA C83A</i>	This study	N/A
pQE30:: <i>nedd8</i>	This study	N/A
pET28a	Novagen	CAT#69864
pET28a:: <i>ub</i>	This study	N/A
pGEX6p-1	GE Healthcare	CAT# 28954648
pGEX6p-1:: <i>ube2n</i>	This study	N/A
pQE30-3xHA:: <i>ub</i>	This study	N/A
pQE30-3xHA:: <i>ubQ40E</i>	This study	N/A
pQE30:: <i>mvcA R140A</i>	This study	N/A
pQE30:: <i>mvcA D208A</i>	This study	N/A
pQE30:: <i>mvcA E214A</i>	This study	N/A
pQE30:: <i>mvcA E216A</i>	This study	N/A
pQE30:: <i>mvcA R322A</i>	This study	N/A
pQE30:: <i>mvcA L330A</i>	This study	N/A
pQE30:: <i>mvcA Δmid</i>	This study	N/A
pQE30:: <i>sdeA</i>	(Qiu et al., 2016)	N/A
pGEX6p-1:: <i>mvcA C83A(13-395)</i>	This study	N/A

Table. 3 continued

pGEX6p-1:: <i>mavC</i>	This study	N/A
pGEX6p-1:: <i>ube2n</i> _{K94A}	This study	N/A
pCMV5:: <i>traf6</i>	Addgene	ID#21624
pCMV-HA:: <i>myd88</i>	Addgene	ID#12287
p4xFlagCMV:: <i>bcl10</i>	This study	N/A
p4xFlagCMV:: <i>legA6</i>	This study	N/A
p4xFlagCMV:: <i>legK2</i>	This study	N/A
p4xFlagCMV:: <i>ankB</i>	This study	N/A
p4xFlagCMV:: <i>lpg2149</i>	This study	N/A
p4xFlagCMV:: <i>sdeC</i>	(Qiu et al., 2016)	N/A
p4xFlagCMV:: <i>sidJ</i>	(Qiu et al., 2017)	N/A
p4xFlagCMV:: <i>sdeA</i>	(Qiu et al., 2016)	N/A
p4xFlagCMV:: <i>yopJ</i> _{Ypt}	This study	N/A
p4xFlagCMV:: <i>cif</i> _{Ypt}	This study	N/A
pCMV4:: <i>p65</i>	Addgene	ID#21966
pCMV2:: <i>ikk</i> _β	Addgene	ID#11103
p4xFlagCMV:: <i>tak1</i>	This study	N/A
p4xFlagCMV:: <i>tab1</i>	This study	N/A
pQE30:: <i>lpg2149</i>	This study	N/A

Primers	Sequence (Restriction enzyme sites are underlined)	Note
pNG1001	cgggatccatgacaacttccaagcttg	<i>mavC</i> 5F BamHI
pNG1002	cggtcgactcaattcacgaagaac	<i>mavC</i> 3R Sall
pNG1003	cgggatccatgattgtcggtggcatt	<i>mvcA</i> 5F BamHI
pNG1004	cggtcgacttagcttggccccctttt	<i>mvcA</i> 3R Sall
pNG1005	cgggatccatggccggctgccccgcaggatcat	<i>ube2n</i> 5F BamHI
pNG1006	cggtcgacttaaatattattcatgcataatagcc	<i>ube2n</i> 3R Sall
pNG1007	cgggatccatgcagatttcgtaaaa	<i>ub</i> 5F BamHI
pNG1008	cggtcgacttaaccaccacgaagtct	<i>ub</i> 3R Sall
pNG1009	cggtcgacatccctgtccaataaaag	<i>mavC</i> up Sall knockout
pNG1010	cgggatccattaacctcactgataga	<i>mavC</i> up BamHI knockout
pNG1011	cgggatctaaatcgaatcggtttgt	<i>mavC</i> down BamHI knockout
pNG1012	cggagctcttcgtcaattcaa	<i>mavC</i> down SacI knockout
pNG1013	cggtcgactagaagaagttcaagagt	<i>mvcA</i> up Sall knockout
pNG1014	cgggatccatgtatatattataggc	<i>mvcA</i> up BamHI knockout
pNG1015	cggagatctcaataaaaacaataaaaatc	<i>mvcA</i> down BglIII knockout
pNG1016	cggagctcgatatggccaaaatgaat	<i>mvcA</i> down SacI knockout

Table. 3 continued

pNG1017	cattgctcgctttccggcgtgttgtgggttag	<i>mavC</i> C74A-1
pNG1018	ctcaacccacaaacagcggcggaaaagcgagcaatg	<i>mavC</i> C74A-2
pNG1019	tgtactgaacccactcagagtgcgtggccaagccag	<i>mvca</i> C83A-1
pNG1020	ctggcttggccaggcactctgagtgggttcagtcata	<i>mvca</i> C83A-2
pNG1021	ccaatacatgggagggttctgcgtcaattcaatcgtaatagg	<i>mvca</i> R140A-1
pNG1022	acctattaatacgtttgaaattgacgcagaagaccctcccattgtattgg	<i>mvca</i> R140A-2
pNG1023	ggcttcagaacaaaaggagcacaaagactatattcgctg	<i>mvca</i> D208A-1
pNG1024	cagcagaatatagtcgtgcctttgttctgaagagcc	<i>mvca</i> D208A-2
pNG1025	atcctcagggtttcaggcgttcagaacaaaaggatc	<i>mvca</i> E214A-1
pNG1026	gatcctttgttctgaagcgcctgaaaaacctgaggat	<i>mvca</i> E214A-2
pNG1027	attgcaaaaatcctcagggtttgcaggcttcagaacaaaag	<i>mvca</i> E216A-1
pNG1028	ctttgttctgaagcgcctgaaaacctgaggatggatttgcata	<i>mvca</i> E216A-2
pNG1029	ggcgcaaaaaaatgcgtccgcgcctgcttgaaaaaaat	<i>mvca</i> R322A-1
pNG1030	atttttcaaaagcgaggcgcggaaagcatttttgcgc	<i>mvca</i> R322A-2
pNG1031	gtaatgggtgttttcttgcgtggcgcaaaaaatgcgtccc	<i>mvca</i> L330A-1
pNG1032	ggaagcatttttgcgcacgcataatgaaaaaagacaaccattac	<i>ube2n</i> K94A-1
pNG1033	cagtgcggggaccacgcataatctaaacatattctcc	<i>ube2n</i> K94A -2
pNG1034	ggaagaatatgttttagatatttgaagatgcgtggccccagactg	<i>Ube2v2</i> 5F <i>BamHI</i>
pNG1035	cgggatccatggcggttcacaggagtt	<i>Ube2v2</i> 3R <i>SalI</i>
pNG1036	cggtcacttaattgtgtatgttgc	<i>ube2n</i> K92A-1
pNG1037	gtgcggggaccacttatctgcaaaaatctaaacatattctccaaact	<i>ube2n</i> K92A -2
pNG1038	agttgggaagaatatgttttagatatttgcagataagtggccccagcac	<i>ube2n</i> C87A-1
pNG1039	ccacttatcttcaaaaatctaaagctattctccaaactgtctacatttagga	<i>ube2n</i> C87A -2
pNG1040	tcctaattgttagacaagttggaaagaatagcttttagatatttgaagataagtgg	<i>ub</i> Q40E-1
pNG1041	atcagtctctgtcatcaggaggaattccttcct	<i>ub</i> Q40E-2
pNG1042	aggaaggaaattcctcgtatgagcagagactgat	<i>lpg2131</i> <i>BamHI</i>
pNG1043	cgggatccatggcatttataaa	<i>lpg2131</i> 3R <i>SalI</i>
		<i>lpg2137</i> 5F
pNG1044	cggtcgacttatgaaactgcagaaat	<i>lpg2137</i> 3R <i>SalI</i>
pNG1045	cgggatccatggtttattacataaaat	<i>lpg2137</i> <i>BamHI</i>
pNG1046	cggtcgacttagctggcctcgcat	<i>lpg2137</i> 3R <i>SalI</i>
pNG1047	cggtcgactcgacaagtatattgaaaa	<i>lpg2149</i> up <i>SalI</i>
pNG1048	cgggatccaaatcaaactcctcggt	<i>knockout</i>
pNG1049	cgggatcctgaaatgaggatggggc	<i>lpg2149</i> up <i>BamHI</i>
pNG1050	cggagctcatcaattaaatccagaccc	<i>lpg2149</i> down <i>BamHI</i>
pNG1051	ttctgttctaaaagtaatcagccacttcattgcgtttccg	<i>lpg2149</i> down <i>SacI</i>
pNG1052	cgaaaaagcgagcaatgaagtggctgatttacttttaggaacagaa	<i>mavC</i> C82A-1
pNG1053	cattaaatagtcatacgactgtgtctgtatcgatgtccaaaggctcg	<i>mavC</i> C82A-2
pNG1054	cgaccctggacagacatcagacacacagactcatagactatttaatg	<i>mavC</i> C117A-1
pNG1055	gaatgggtgcgttccaagcatctatgttttcttgcatttaactatctca	<i>mavC</i> C117A-2
		<i>mavC</i> C226A-1

Table. 3 continued

pNG1056	tgagatagttaaagctaaaatgaaaaacatagatgctggacagcaaccattc	<i>mavC</i> C226A-2
pNG1057	cgttcatcccgtagcaaaaacatgttctttcctggaggag	<i>mavC</i> C314A-1
pNG1058	ctcctccaggaaaagaacatgtttctgtaccgggatgaacg	<i>mavC</i> C314A-2
pNG1059	gctttatttataaagtccggcttgatcttcgcgtttcgccagg	<i>mavC</i> C362A-1
pNG1060	cctggcggaaaacgcgaaagatcaagccgaactttataaaaataaaagc	<i>mavC</i> C362A-2
pNG1061	tctgcagtgcgtgggaccacgcatctgccaaaatatctaaacatattctcccaacttg	<i>ube2n</i> K92AK94A-1
pNG1062	caagttgggaagaatatgttagatatttggcagatgcgtggccccagcactgcaga	<i>ube2n</i> K92AK94A-2
pNG1063	cggatctatgatgagtgcgaaaaagc	<i>lpg2149</i> 5F BglII
pNG1064	cggtcgacttaagagtagtcgggtgc	<i>lpg2149</i> 3R Sall
pNG1065	cgggatccatggctccaaaaccgc	<i>ube2c</i> 5F BamHI
pNG1066	cggtcgactcagggtcctggctgg	<i>ube2c</i> 3R Sall
pNG1067	cgggatccatggccaacatcgccgtg	<i>ube2k</i> 5F BamHI
pNG1068	cggtcgactcagttactcagaagcaa	<i>ube2k</i> 3R Sall
pNG1069	cgggatccatgaactccaacgtggag	<i>ube2s</i> 5F BamHI
pNG1070	cggtcgacccatcagccgcgcagcgc	<i>ube2s</i> 3R Sall
pNG1071	cgggatccatgcagagagctcacgt	<i>ube2t</i> 5F BamHI
pNG1072	cggtcgacctaaacatcaggatgaaa	<i>ube2t</i> 3R Sall
pNG1073	cgtgatcaatgatcggaccaatatcac	<i>yopJ</i> 5F BclII
pNG1074	cgtcgagttactttgagaagtgt	<i>yopJ</i> 3R XhoI
pNG1075	cgggatccatgaaagacattacccttcc	<i>cif</i> 5F BamHI
pNG1076	cggtcgacctaattacagtgagttt	<i>cif</i> 3R SalI

VITA

Ninghai Gan was born in Beijing, China. He attended the Zhejiang University (Hangzhou, China) in 2009 to study Applied Biological Sciences and obtained the Bachelor of Science degree in 2013. He joined Dr. Zhao-Qing Luo's Lab in 2014 and started his project on the modulation of the host ubiquitination machinery by *L. pneumophila* effectors. Later he identified that *L. pneumophila* effectors MavC and MvcA are able to regulate the activity of ubiquitin conjugating enzyme UBE2N by transglutaminase-mediated ubiquitination and deubiquitination. He will continue his postdoctoral training in structural biology. He also identified that *L. pneumophila* effector SidJ functions as a calmodulin-dependent glutamylase that specifically modifies SidE family effectors.

PUBLICATIONS

1. **Gan, N.**, Zhen, X, Liu Y, Xiu X, He C, Qiu J, Fujimoto GM, Nakayasu ES, Zhou B, Zhao L, Puvar K, Das C, Ouyang SY, Luo ZQ. Regulation of phosphoribosyl-ubiquitination by a calmodulin-dependent glutamylase (Nature, in press)
2. **Gan N**, Nakayasu ES, Hollenbeck PJ, Luo ZQ. Legionella pneumophila inhibits immune signalling via MavC-mediated transglutaminase-induced ubiquitination of UBE2N. *Nat Microbiol*. 2019 Jan;4(1):134-143.
3. Kalayil S, Bhogaraju S, Bonn F, Shin D, Liu Y, **Gan N**, Basquin J, Grumati P, Luo ZQ, Dikic I. Insights into catalysis and function of phosphoribosyl-linked serine ubiquitination. *Nature*. 2018 May;557(7707):734-738.
4. Yao J, Yang F, Sun X, Wang S, **Gan N**, Liu Q, Liu D, Zhang X, Niu D, Wei Y, Ma C, Luo ZQ, Sun Q, Jia D. Mechanism of inhibition of retromer transport by the bacterial effector RidL. *Proc Natl Acad Sci U S A*. 2018 Feb 13;115(7):E1446-E1454.
5. **Gan, N.**, H. Guan, Y. Huang, T. Yu, E. S. Nakayasu, K. Puvar, C. Das, S. Ouyang, Z. Q. Luo. Legionella pneumophila regulates the activity of the E2 ubiquitin conjugating enzyme UBE2N by deamidase-mediated deubiquitination (Under review with the EMBO Journal)